University of Pretoria

Faculty of Engineering, Built Environment and Information Technology

Department of Mechanical and Aeronautical Engineering

Johannes Marthinus Koorts 24053423

Master's Dissertation

Report

Entropy Minimisation and Structural Design for Industrial Heat Exchanger Optimisation

June 24, 2014

Abstract

Title : Entropy Minimisation and Structural Design for Industrial Heat Exchanger Optimisation

Author : JM Koorts

Supervisors : Prof T Bello-Ochende

Co-supervisors : Prof JP Meyer

Department : Mechanical and Aeronautical Engineering

University : University of Pretoria

Degree : Master of Engineering (Mechanical)

The mass flow rate for shell-and-tube, tube-fin and tube-in-tube industrial-type heat exchangers can be optimised by minimising entropy generation over a finite temperature difference. The purpose of the work was to apply the principles of entropy generation minimisation based on the second law of thermodynamics to determine whether the intercept between entropy generation due to heat transfer and fluid friction is a good approximation for the global minimum entropy generation, as well as to optimise a number of variables. Optimisation was achieved by applying numerical methods.

In order to yield meaningful results, the optimisation was done by setting a number of boundary conditions such as the maximum inlet steam temperature. The heat exchanger optimisation was based on a case study of the heat exchangers used at Columbus Stainless' cold products division.

The mentioned case study consisted of 27 industrial-types of heat exchangers with power ratings ranging between 100 and 800 kW. The original specification included lengths varying between 1 and 2.42 m, shell-side diameters from 0.4 to 2 m and number of tubes varying from 1 to 20. The medium mass flow rates ranged between 0.048 and 0.855 kg/s while the steam mass flow rates ranged between 0.029 and 0.236 kg/s. The medium output temperatures were between 303 and 403K

The effect of various conditions was taken into account. Apart from the conditions already mentioned, the specific material properties at their specific pressures and temperatures (such as density, viscosity, conductivity, heat transfer coefficient) were also taken into account in the calculations.

Through numeric optimisation it was possible to conclude that the main variables that affected entropy generation were the steam inlet temperature, followed by the tube-side diameter for the given sample set. These variables were thus used in all further graphs as the main variables to be changed.

These variables were manipulated and the entropy generation due to fluid friction and heat transfer were independently plotted to determine if the intercept of these two lines could be used as a good approximation of the global minimum entropy generation. It was found that the approximation is not that good, unless one uses the entropy generation due to operational heat transfer, which yielded deviations between the intercept values and the global minimum ranged between 0.21 % and 21.88 % with an average deviation of 6.52 %, which is considered to be a good approximation. The constructal design theory does thus hold well under the current operating conditions.

It was clear that the main mechanism contributing to entropy generation was the effect of fluid friction, although this was only the case at smaller tube diameters. Of the entropy generated due to fluid friction the majority was contributed due to the tube side (steam), with almost no entropy generated due to fluid friction in the shell-side (medium) of the heat exchanger.

The effect of a number of variables on entropy generation were discussed and plotted. It was seen that an increased inlet temperature resulted in most cases in less entropy generated and that larger tube diameters have a similar effect due to less entropy generated due to fluid friction.

By using the principles of entropy generation minimization the entropy generated of each heat exchanger could be reduced by between 2% and 64%, with the tube-fin heat exchangers having the largest scope for improvement in the sample set used.

By using the principals of construal design, the intercepts of the entropy generation due to heat transfer and due to fluid friction was used to determine the optimal diameter. This correlation yielded very good results (Within 1% of the global minimum entropy generation) to predict the global minimum entropy generation.

Keywords: Entropy, shell-and-tube, tube-fin, tube-in-tube, heat exchanger, heat transfer, irreversibility, model, thermodynamics, numerical, optimisation, geometric, constructal design.

Acknowledgements

I would like to thank Professor Tunde Bello-Ochende and Doctor Axel Lexmond for their guidance and many years of experience on the topic of entropy generation minimisation, which they were willing to share with me and which contributed greatly to the completion of this dissertation. I would further like to thank my loving wife for her continuous support, my family for their faith in my work and my close friends for their thoughtful insights.

Table of contents

List of figures

List of tables

Nomenclature

Latin symbols

A	Area	m^2
C	Heat capacity	*W/K*
C_p	Specific heat capacity	*W/kgK*
D	Diameter	-
f'	Friction factor	-
h	Convection heat transfer coefficient	*W/K*
hx	Heat exchanger	-
k	Conduction heat transfer coefficient	*W/mK*
L	Length	*m*
m	Mass flow rate	*kg/s*
n	Number of tubes	-
Nu	Nusselt number	-
P	Pressure	Pa
Pr	Prandtl number	-
Q	Heat transfer	*W*
r	Resistance	K/Wm^2
R	Gas constant	*J/kgK*
Re	Reynolds number	-

S	Entropy	W/K
T	Temperature	K
U	Overall heat transfer coefficient	Wm^2/K
U	Work done	W
V	Volume	m^3
v	Speed	m/s

Greek symbols

β	Volume change factor	(-)
Δ	Change	(-)
μ	Viscosity	kgm/s
ε_{tubes}	Roughness of tubes	-
Σ	Summation	-
ε_{tubes}	Roughness of tubes	-
ε	Effectiveness	-
ρ	Density	kg/m^3

Subscripts

c	Cold fluid/surface
eff	Effective
gen	Generated
h	Hot fluid/surface
HT	Heat transfer

i In

o Out

Chapter 1:

Introduction

1.1 Heat exchangers

There are many different forms of energy (electrical, chemical, nuclear, mechanical, heat, potential (height), light, pressure etc.) which can be converted into each other. For these conversion processes, equipment has been invented such as solar panels that convert light into electrical energy, nuclear reactors that convert nuclear energy into heat, turbines to convert pressure (and heat) into mechanical energy and generators to convert mechanical energy into electricity.

However, the most common type of energy conversion equipment is also the simplest one: heat exchangers transfer heat from a warm process flow to a colder one. About 80% of all energy conversion systems consist of heat exchangers [1].

Since energy conversion occurs in almost every industrial process – whether it is an oil refinery, electricity production, production in a chemical plant, platinum mining or conversion of iron ore into iron, heat exchanger optimisation is critical in achieving a highly efficient industry, saves money and reduces greenhouse emissions (less energy necessary).
There are many types of heat exchangers available, ranging in size and design. The heat exchangers used for the purpose of this report are shell-and-tube, tube-fin and tube-in-tube heat exchangers.

Figure 1: Shell-and-tube heat exchanger [2]

In shell-and-tube heat exchangers one medium flows through a number of small tubes inside located inside the heat exchanger whilst the other medium flows between the outside of the tubes and the inside of the exterior shell. Inside the heat exchanger are a number of baffles, which are used to keep the tubes in place and to reduce shell-side heat transfer. Typical examples of these heat exchangers are boilers (energy used to heat water in the tubes to above its boiling point, in order to form steam), and condensers (where a vapour, usually on the shell side, is cooled down to form a liquid).

In many industrial processes steam is usually generated by either gas or electric boilers (with the electric boilers being phased out due to the ever-increasing energy constraints worldwide, or by other processes generating excess heat that could be used instead), to heat up water to temperatures above water's boiling point.

This steam is then used as a medium to transfer energy to various areas of plants due to the ease of transporting and the subsequent energy the steam contains. The steam is used in heat exchangers to heat up other mediums or processes as is required in the industry.

Figure 2: Tube-fin heat exchanger [3]

A tube-fin heat exchanger is always operated in cross flow. It is generally used with two different mediums, with the medium in the tubes being gaseous or liquid, and the medium going through the fins being gaseous. This is why there are a number of small fins in the heat exchanger, to increase the contact area between the different mediums. A typical example of a tube-fin heat exchanger is a car's radiator, where the hot water from cooling the engine needs to be cooled down by the incoming moving air entering through the grill of the car.

Figure 3: Tube-in-tube heat exchanger [4]

In tube-in-tube heat exchangers the two mediums, being either liquids, gaseous or even solid powders, enters from two separate directions and exits on the opposite side of the heat exchanger. They are thus always operated in either counterflow or cross-flow. This type of heat exchanger is typically used in rotary kilns (where the fresh cool air is heated by coming in contact with the hot material and off gasses leaving the kiln) and distillation columns of chemicals (vapours from low temperature chemicals bubbles upwards and comes into contact with the high temperature chemicals flowing downward)

1.2 Thermodynamics

Thermodynamics is a division of natural science concerned with the relationship between energy and work to heat. It defines macroscopic variables (such as temperature, internal energy, entropy, and pressure) and explains how they are related and by what laws they change with time.

In order to improve the effectiveness of these systems we use a thermodynamic entity, entropy, to help us define the lost efficiency of heat exchangers. Entropy is the property that describes how useful a certain amount of energy is. Higher entropy of a system correlates with lower usefulness.

Energy cannot be generated or destroyed; it can only be converted [5]. Entropy on the other hand is usually produced in a process. Only in an ideal process without any losses, no entropy is generated. The more entropy is generated, the less useful the energy in a system has become. For this reason, entropy generation is a very good measure for the quality of a process.

The total irreversibility (equation 1.1) is the sum of the different types of irreversibility sources due to fluid friction and heat transfer, where S is the entropy generation, C_p is the specific heat capacity, T is the temperature, R is the ideal gas constant, f' is the friction factor, L is the tube length, D is the diameter, ρ is the density, μ is the viscosity, P is the pressure and V is the volume [6]:

$$S_{T_2} - S_{T_1} = C_p \ln\left(\frac{T_2}{T_1}\right) - \left[R \ln\left(\frac{P_2}{P_1}\right)_{gasses} + \left(\frac{\dot{m}(V_2 - V_1)(P_2 - P_1)}{T_2 - T_1}\right)_{liquids}\right] \quad (1.1)$$

Entropy is thus used to quantify the lost energy and efficiency in processes and is also referred to as the second law of thermodynamics. One cannot use the second law of thermodynamics without understanding the first law of thermodynamics, since the two build onto each other and are interlinked. The first law of thermodynamics states that energy cannot be created or destroyed and can only change in form.

The previous definition for the first law of thermodynamics can be summarised by the equation 1.2, where ΔU is the change in internal energy, ΔQ is the net heat supplied to the system by its surroundings and ΔW is the net work done by the system on its surroundings [7]:

$$\Delta U = \Delta Q - \Delta W \quad (1.2)$$

Thus by using the second law of thermodynamics and understanding and applying the basic rules of the first law of thermodynamics it is possible for us to quantify the amount of lost energy generated by any system.

Nowhere is this drive for more efficient systems more evident than in the modern-day industrial-type heat transfer devices such as the shell-and-tube heat exchangers, tube-fin heat exchangers and tube-in-tube heat exchangers.

1.2.1. Background on modern-day focus

In the early 1900s the main areas of research were focused on the costs associated with the creation of new technologies, because these were seen as the main obstacles in the starting of new companies and the launching of new products.

As the world population and thus demand increased in the mid-1900s, the emphasis shifted to the production of larger volumes of products to accommodate the growing markets [8].

The culture shifted a bit in the 1980s to focus more on quality as consumer-driven aspects started to take form all over the world, with quality management systems such as ISO 9000

emerging in 1987 [9]. This was not the first time that the emphasis moved towards quality, although it was the first instance where a global standard was recognised almost universally and today certifies more than a million companies [10].

It is only recently, since the 1990s, that the need for more efficient systems has grown due to stringent market constraints, increasing international competition and big players evolving on every front. These factors as well as the ever-increasing cost of power contributed to the research focus shifting towards creating more efficient systems, thus resulting in the field of entropy generation [8].

1.2.2. Background on the discovery entropy

As stated earlier, entropy generation minimisation is the application of the first and second law of thermodynamics to finite systems in order to minimise irreversibilities. The first law of thermodynamics was first defined by Rudolf Julius Clausius, a German physicist and mathematician in 1850, 28 years after Fourier discovered conduction and 149 years after Newton discovered convection [11]. The first law of thermodynamics was defined as:

> *In all cases in which work is produced by the agency of heat, a quantity of heat is consumed which is proportional to the work done; and conversely, by the expenditure of an equal quantity of work, an equal quantity of heat is produced [6],*

The first law of thermodynamics thus states plainly that energy cannot be created nor destroyed and can only change its form.

Although the first law of thermodynamics worked with the constant internal energy, it did not explain why a preferred direction of progress occurred in natural processes. This was originally overcome by the concept of reversibility by Nicolas Léonard Sadi Carnot, a French military engineer, in 1824. Although his explanation focused more on caloric heat rather than entropy, he paved the way for Rudolf Julius Clausius to redefine the second law in 1854, just after defining the first law in 1950 as:

> *Heat can never change from a colder to a warmer body without some change, connected therewith, occurring at the same time [6],*

This second law of thermodynamics defines the concept of entropy by simply stating that there is an amount of the system's thermal energy per unit temperature which is unavailable for useful work, which is also referred to as irreversibilities. These irreversibilities occur due to a number of reasons such as temperate changes, pressure changes and volume changes. Clausius named the phenomenon entropy due to the Greek words "en tropein" meaning content transformation.

1.3 Constructal design

In thermodynamics there are two main laws which are first principles, the first law is about the conservation of energy and the second law is about the tendency of all mediums to flow from high temperature or pressure to a low temperature or pressure. Although these two laws define the thermodynamics of systems relatively well, they say nothing about the shape and structure of them.

Where thermodynamics state that a medium should flow from high to low, the constructual law says that they should flow in configurations that flow more and more easily over time. Similarly, constructual design is the process of designing a system where a medium flows more easily and thus will have less entropy generated.

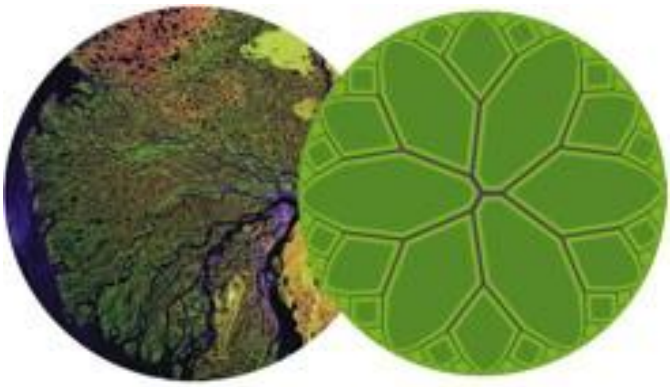

Figure 4: The flow of a river delta (left), a constructed flow design (right) [12]

The constructual law states that we can see design in nature as flow, and can thus we can design devices for human use based on the same principles. In Figure 4 we can see how

mankind has created a flow design pattern based on a river delta that has changed its own flow to flow easier as the time passed on [12].

1.4 Problem statement

In Columbus Stainless there are 27 industrial type heat exchangers that are operating in four different areas that form part of a larger continuous process. Due to the ever stringent focus on lean manufacturing the question was brought up whether these heat exchangers were running optimally and whether a better original design could have reduced operating costs (running more efficiently). An entropy generation analysis could reveal areas of concern which might lead to various potential areas of optimisation.

1.5 Research objectives

The objectives in the research of this dissertation is to develop a dynamic model, which takes temperature and pressure changes into account for each simulation, which in turn influences all the thermodynamic variables, as well as to optimise heat exchangers bases on the principles of entropy generation minimisation. It is also the objective of this dissertation to prove or disprove that by minimising entropy generation for the different contributing factors of the global entropy generation independently (which in this case is pressure drop and temperature losses), one can obtain local minimum at their intercept that is reasonably close to the global minimum.

The secondary objectives in the research of the dissertation are to determine which heat exchanger group is the most efficient as well as to determine the geometric effect of heat exchangers on entropy generation, specifically the length-to-diameter ratio.

1.6 Scope of study

The scope of this dissertation is to model 27 heat exchangers present in the steam system of Columbus Stainless' Cold Products. The heat exchangers will be shell-and tube, tube-fin and tube-in-tube heat exchangers and are limited to steam powered heat exchangers.

The flow is limited to fully developed turbulent flow, which is assumed to only occur at Reynolds numbers larger than 10,000, with the mediums to be heated limited to low viscous watery solutions (acids, alkalis, water and air). It is assumed that all the gasses behave ideal and that there are no losses due to the surroundings or due to fouling inside the heat exchangers.

The inlet steam temperature will range between 403 and 473K, whilst the inlet medium temperature will range between 298 and 333K. The mass flow rates will vary between 50% below and above the current operating conditions, which depending on the heat exchanger ranges between 0.02 and 1.28kg/s of steam, and 1.47 and 35.34kg/s of medium to be heated.

The shell-side and tube-side pressure will also vary between 50% below and above the current operating conditions, which depending on the heat exchanger ranges between 400 and 1500kPa for the tube-side, and 150 and 1500kPa for the shell-side.

The current total energy transfer of the heat exchangers remains constant in order to perform a similar duty compared to the current installation.

The entropy generation and heat transfer equations will be combined with mathematical programming using MATLAB in order optimise a number of design parameters and input variables.

1.7 Structure of dissertation

A summary of the basic report structure and layout can be seen below:

Chapter 2 Literature Study

This chapter briefly explains the background of the set-up of various heat exchangers used as a case study for this dissertation. Section **Error! Reference source not found.**2.2, looks at previous work on minimise entropy generation with tube-fin, tube-in-tube and shell-and-tube heat exchangers. Similarly, section 2.3 gives some background on work on constructal design theory of tube-fin, tube-in-tube and shell-and-tube heat exchangers. Finally, section 2.4 gives a background of various literature sources that could be used to validate the model.

Chapter 3 Background on Equipment

The case study which is under investigation is explained. Section 3.1, focuses on the physical set-up of the system in order to understand how the various parts of the processes fit into each other. Section 3.2 gives information regarding the heat exchangers, defining the original geometric dimensions as well as the mediums used in the processes and energy requirements of each heat exchanger.

Chapter 4 Model Development

The mathematical steps taken in order to obtain the dissertation's objectives and required to optimise the various heat exchangers are given in this section. Section 4.1 gives a brief introduction, followed by section 4.2, which explains the thermodynamic equations. Section 4.3, focuses on the heat transfer equations used in the modelling.

Chapter 5 Validation

In this chapter, the developed work is compared with research done by other scholars to ensure the validity of the model in question.

Chapter 6 Results

The chapter gives an overview of some of the results obtained during the study, with the rest in appendix D. The current system setup is explained in section 6.2. The choice of the main variable is discussed in section 6.3. Section 6.4 shows the relationship between entropy generation due to fluid friction and due to temperature losses relative to the total entropy generated. Section 6.5 and 6.6 then shows us how many variables and the response of the individual heat exchangers reacts respectively, by changing the main variable (as determined in section 6.3). Section 6.7 shows us information regarding the optimised results obtained from the study.

Chapter 7 Conclusion

A summary of the finding of the dissertation is given in this chapter with some concluding remarks.

Chapter 2:

Literature Study

2.1 Introduction

Entropy generation has become a well-recognised name in optimisation due to the drive for more efficient systems. This has resulted in much research being done in the last three decades on the topic. It is the purpose of this dissertation to analyse the various factors that contribute to the generation of entropy in a number of different heat exchangers to finally obtain the optimal values to benefit the system as a whole.

To create a model to predict entropy generation, some information regarding entropy generation models needs to be obtained. This can be found in Section 2.2 The information required to better understand the application of constructal design in heat exchangers, is found in Section 2.3 In order to properly validate the model, various results on the topic will be discussed and compared in Section 2.4.

Various models regarding entropy generation in heat exchangers can be found in the Appendix section of the report.

2.2 Entropy generation in heat exchangers

This chapter gives a brief overview of work done to optimise the entropy production of heat exchangers and related equipment relative to flow characteristics. The chapter starts off by looking at the work done specifically on shell-and-tube heat exchangers, tube-fin heat exchangers and tube-in-tube heat exchangers, focusing on irreversibilities due to heat transfer and pressure losses.

Work was done in order to explain the various trends and backgrounds on basic entropy generation minimisation techniques. Emphasis was made on the fact that one can not only rely solely on thermodynamics. [13]

In the paper, Bejan notes that the entropy generation due to fluid friction and heat transfer oppose each other in many cases, such as a change in tube diameter. The author writes how various heat exchanger types were optimised by keeping various design variables constant such as area and volume, and varying other variables such as flow rate and inlet temperatures.

The need for many of the modern day computational fluid dynamic packages to include local entropy generation rates is also discussed [13]. The author finishes by giving a number of examples of the application of this technique, such as to optimise convective mass transfer [14][15], reacting flows, radiative heat transfer [16][17], convection through porous media [15][18][19], and conduction through non-homogeneous and anisotropic media.

As previously stated, many researchers turned their attention towards the increase of the heat transfer surface area to improve the effectiveness of their heat exchangers. Much work was done on the topic. The effect of different mediums inside the tubes of a typical shell-and-tube heat exchanger on low Reynolds numbers below 1450 was evaluated as one of these works. They used copper, aluminium and mild steel chips as porous media and found that by inserting the metal shards into the heat exchanger the overall efficiency can be increased and thus the entropy generation could be reduced. They showed that copper had the greatest effect, followed by aluminium and then by normal mild steel. They also saw that in the same order, the pressure

drop also increased but that the overall entropy generation was still less. They accounted it to the fact that the dominant factor was by far that contributed to entropy generation in their case was the entropy generated due to heat transfer, and the effect of increased pressure drop could not counter the reduction in entropy generated due to heat transfer [19] [20][26].

A number of scholars have used the principles of entropy generation minimisation and developed their own specific dimensionless numbers to define the amount of entropy generated. One such case was used to do scaling on the entropy generation number by using the ratio of the heat transfer rate to the inlet temperature of cold fluid. By using this modified indicator, the total entropy generation due to heat transfer and fluid friction was reduced. It was once again noted that the effect of heat transfer effectiveness contributes a lot more than the effect of pumping power for the predescribed data set [20].

Due to the coupling effect of fluid friction and heat transfer on entropy generation, the attempt to optimise the one parameter would almost always reduce the efficiency of the other [13][21]. For this reason some scholars have used entropy generation to successfully optimise heat exchanger geometry in regions where the two opposing contributors together generated the least amount of entropy. One such case optimised the cross sectional area of the tubes inside heat exchangers [21]. It was found that for adiabatic flow, circular cross-sections minimise flow resistance and thus reduced entropy generation the most. In contrast it was showed that in flows where heat transfer irreversibilities dominates (low flow rates, high heat transfer rates and large available cross-sectional areas), channels with rectangular shapes with large aspect ratios proved to be the most effective due to an increased heat transfer area and thus resulted in the least amount of entropy generation. Another case was the optimisation of length, width, height and number of heat exchanger channels. This is different from the optimisation of the cross-flow area alone, as it includes more specific design parameters [22].

Some scholars take the route of improving heat exchangers relative to dimensionless variables other then the Bejan Number, such as the dimensionless area and dimensionless mass velocity [23]. One such case is presented but uses a balanced cross-flow heat exchanger which is not common in industry, and use complex relations to predict entropy generation [23].

A lot of research has also been done on the systems surrounding heat exchangers such as the heat pipe to and from various heat exchangers. The same principles of thermodynamics and heat transfer were combined to determine the amount of entropy generated, such as frictional losses, pressure drops and temperature differences between the hot and cold reservoirs. They reproved the well know fact that the entropy increases with pipe length and heat load [24]. Similar work have been done on tube dimensions between heat exchangers, but changed the geometry from circular to square. It was found that there exists a certain length where the entropy generation rate is at a minimum. It was further also seen that above a certain length the entropy generation rate per unit length remained the constant [25].

There are also research done on phase flow specifically two phase, and phase change within heat exchanger which is typically found during the condensation process wear the steam releases enough energy to condense back to a liquid form. In a study it was showed that tubes for designed for enhanced heat transfer is a viable solution at low flow rates, whereas at higher mass flow rates still require smooth tubes to reduce the total entropy generation in heat exchanger where two-phase flow is present. This was mainly due to frictional losses associated with the obstructions in tubes designed to increase mass flow rate increasing too much at higher flow rates [26].

The effect of fouling has also been investigated. In these studies the fouling thickness as well as the surface temperatures was taken as the main variables. It was shown that entropy generation due to fluid friction increased whereas entropy generation due to heat transfer decreased with an increase in fouling thickness. Although entropy generation due to friction was lower than the entropy generation due to heat transfer by a factor of 100, it was reduced to within 25% at a fouling thickness of 25mm for the given scenario, and thus played a significant role in entropy generation. It was also shown that the effect of fouling plays a larger role in smaller tubes compared to larger tubes [27].

Some scholars also choose the route of deriving the entropy generation correlations from experimental results, and not from simulations. One of these used experimental results to determine the optimal heat exchanger length, heat transfer and pressure drop for a tube-plate heat exchanger. Although it was concluded that from a thermodynamic view of point, larger number of passages with smaller pin height in the given frontal area of heat exchanger are more

preferred than less heat exchanger passages with larger pin height, this was found to not always be possible due to the amount of heat transfer required [28].

Section 2.2 gives a brief background on the application of entropy generation minimisation to various systems in and around the heat exchanger environment. It is clear that the only main contributors that were considered were entropy generation due to heat transfer and entropy generation due to fluid friction. It is also clear that a lot of work has gone into better understanding the optimal structure (length, width, depth, cross sectional area and form of heat exchanger and adjacent tubes) of the heat exchangers, as well as the optimal fluid properties (viscosity, temperatures, fouling in tubes and phase changes). It is also clear that in mot instances the effect of heat transfer at larger lower flow rates and larger diameters are much more dominant than the effect of fluid friction.

2.3 Constructal design in heat exchangers

This chapter gives a brief overview of work done to implement constructal design theory to heat exchangers, together with some feedback of its application. The main sections are flow geometry, inlet geometry as well as overall heat exchanger cost.

An application of constructal design in heat exchangers internal flow patterns was done. The relationship between heat exchanger effectiveness and number of transfer units were evaluated. The various flow patterns considered were constructal dichotomous trees covering uniformly a rectangular area, tree on a disk-shaped area, trees on a square shaped area. These can also be seen in Figure 5.

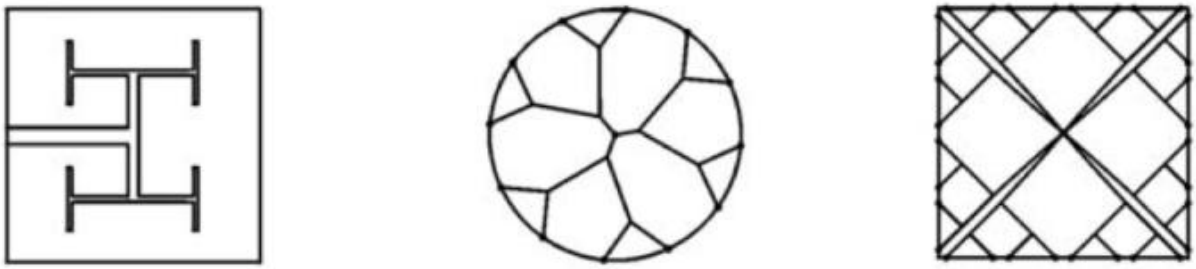

Figure 5: Flow patterns considered: Constructal dichotomous trees covering uniformly a rectangular area (left), tree on a disk-shaped area (middle), trees on a square shaped area (right) [29]

The main objectives in optimising the architecture of the heat exchanger were to increase the heat transfer and reduce the total pumping power. By changing the complexity the effect on the heat exchanger performance were evaluated. It was seen that the effect of complexity can be quite substantial, with a parallel flow of tree-shaped streams distributed over an area, and almost negligible in a square design [29].

A similar approach has been used in tube-finned heat exchangers operating in cross-flow arrangement as well. By keeping the heat transfer area constant and varying the plate, tube and fin arrangement, the overall entropy generated could be reduced by up to 20%. The maximum effectiveness was also investigated for the given arrangements [30].

Similarly, the flow architecture of conjugate cooling channels in forced convection with internal heat generation for an array of circular cooling channels with different flow orientations were evaluated. There were three scenarios that were evaluated, an array of channels with parallel flow, an array of channels in which the flow in every second row is in a counter direction and flows in all the arrays of channels are in counterflow relative to each other, as can be seen in Figure 6.

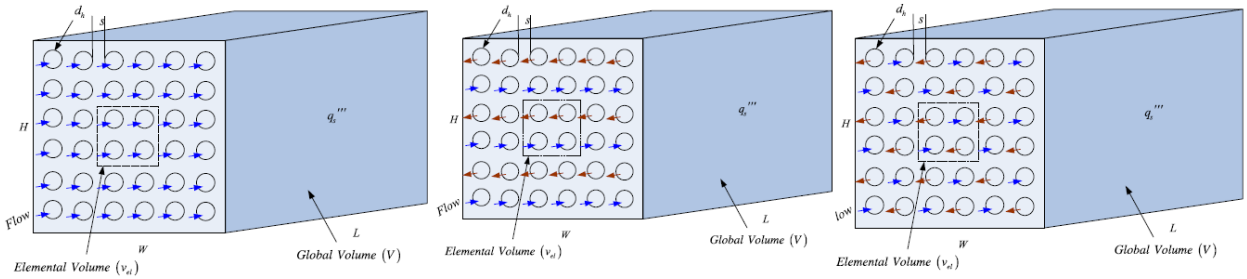

Figure 6: The three flow orientations that were studied: array of channels with parallel flow (left), array of channels in which the flow in every second row is in a counter direction (middle) and flows in all the arrays of channels are in counterflow relative to each other (right) [31]

It was found that the thermal resistances were very sensitive to flow orientation. Due to this, the array of channels in which the flow in every second row is in a counter direction and the flows in all the arrays of channels are in counterflow relative to each other, performed similarly and generated less thermal resistances than the array of channels with parallel flow. It was also possible to optimise the optimal channel diameter and spacing between channels [31].

The tube geometry was also evaluated and optimised with constructal design theory. the channel's hydraulic volume was first obtained, followed by the optimal geometry and then optimal channel spacing.

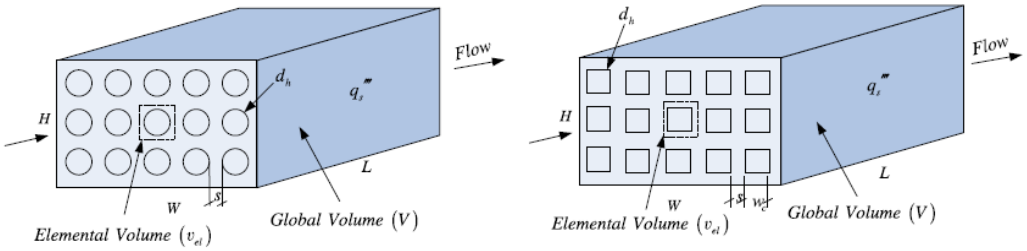

Figure 7: The two tube geometries that were studied: circular (left) and square (right) [32]

It was found that the square channel performed better under the predetermined conditions than the circular channels. It also showed that channel porosity is directly related to pressure drop. It was also showed that the global optimal hydraulic diameter and channel spacing decreased as the pressure difference increases for fixed global volume constraint [32].

Similarly, the search for optimal flow patterns in tube-plate heat exchangers has been evaluated. In a study it was found that by applying the principles of constructal design theory, it was possible to determine the optimal tube size with only two tubes, and the optimal tube spacing with only three tubes. This is different from the conventional approach of using many tubes to do the simulations [33].

The geometry of the tubes and fins has also been investigated. The main constraints were the total volume and the volume of the fin or tube material relative to the cavity. The best results were obtained with the largest material volume with the smallest cavity volume, although this resulted in expensive manufacturing costs. It was also found that there exists an optimal length over width ratio in T-fins [34].

Much work has been done on inlet design of heat exchangers [35]. A tube-tube heat exchanger inlet and outlet was optimised in order to reduce the maldistribution in flow associated with the conventional design. The determining factors that was taken into account to improve the flow distribution was pressure drop and heat transfer. After comparing various different inlet designs an optimal design was found where the inlet had a conventional pyramid distributor and the outlet had an optimised apec distributor. According to the author, this inlet design gave reasonably low pressure drops whilst having a very good heat transfer and thus flow distribution [36].

Similar to Section 2.2, some scholars have started doing research on the surrounding systems present around most heat exchangers, such as the insulation of the heat pipes transporting steam to and from the heat exchangers. The three factors generally considered to have the largest effect are heat insulation, mechanical strength and insulation weight. Two opposing forces, strength and thermal resistances, were optimised to find an area of optimal practical usage [37].

Constructal theory has been successfully implemented to minimize the overall cost of a shell-and-tube heat exchanger. In a study it was assumed that the main costs contributing to the financial evaluation of a new heat exchanger were the capital cost and the pumping cost. By applying the theory of constructal design the overall assumed costs could have been reduced by up to 50% of the original assumed cost. During this process the heat transfer coefficient was also improved [38].

Constructal theory has thus been used widely in heat exchanger optimisation to improve various geometries to generate less entropy and finally reduce overall heat exchanger cost. It is clear that the road to future advances with the constructal law is very wide [39].

2.4 Validation of entropy generation in heat exchangers

In order to validate the model in question, it was needed to compare the results from the model with ones that was experimentally obtained. There are a number of prerequisites that need to be met before a literature source can be used as an adequate validation process. These include having experimental data, giving enough system information to adequately remodel the setup to use as a comparison and results that compare with literature.

The largest obstacle regarding proper data to correlate the model with, arised with the absence of experimental test work in many of the literature sources, either due to not being required or due to being too difficult to reasonably obtain [24][26][28][31][32][33].

Some scholars have used sensitivity analysis to try and indicate the accuracy of various results due to the lack of experimental results [22]. The lack of detail background on the systems also resulted in difficulties to adequately model results that could be compared to experiments in literature.

Even with all the constraints there are a number of sources that includes experimental results and gives adequate system information that could be used to compare results [28][30][40].

Chapter 3:

Background on

Equipment

3.1 Introduction

The system which will be analysed is modelled after an actual plant (Columbus Stainless) and includes four separate areas (VPP, AP1, AP2 and VBA) each with different types of heat exchanger, which all use steam as an energy transfer medium to heat up various liquids, gases, alkalis and acids. There are three main types of heat exchangers included in the model:

- Tube-in-tube
- Tube-fin
- Shell-and-tube

These different types are operated in a cross-flow, a counterflow or a concurrent flow arrangement.

3.2 Heat exchanger information

A summary of each heat exchanger type can be seen in Table 1 and in Table 2.

Table 1: Heat exchanger types summary

Heat Exchanger Properties				
Area	HX nr	Equipment	Heat Exchanger	Type
VPP	1	Entry drier	Tube-fin	Single-pass tube-fin with both fluids unmixed
	2	Pickling Spray #1	Tube-in-tube	Tube-in-tube, both fluids unmixed
	3	Pickling Spray #2	Tube-in-tube	Tube-in-tube, both fluids unmixed
	4	Hot rinse	Tube-fin	Single-pass tube-fin with both fluids unmixed
	5	Exit drier	Tube-fin	Single-pass tube-fin with both fluids unmixed
AP1	6	Quench drier	Tube-fin	Single-pass tube-fin with both fluids unmixed
	7	Pickler #1	Tube-in-tube	Tube-in-tube, both fluids unmixed
	8	Pickler #2	Tube-in-tube	Tube-in-tube, both fluids unmixed
	9	Pickle drier	Tube-fin	Single-pass tube-fin with both fluids unmixed
AP2	10	Pre-degreaser	Shell-and-tube	Single shell, multiple of 2 tubes, mixed flow
	11	Secondary degreaser	Shell-and-tube	Single shell, multiple of 2 tubes, mixed flow
	12	Final degreaser	Shell-and-tube	Single shell, multiple of 2 tubes, mixed flow
	13	Degreaser drier	Tube-fin	Single-pass tube-fin with both fluids unmixed
	14	Quench drier	Tube-fin	Single-pass tube-fin with both fluids unmixed
	15	Neoylite #1	Tube-in-tube	Tube-in-tube, both fluids unmixed
	16	Neoylite #2	Tube-in-tube	Tube-in-tube, both fluids unmixed
	17	SSO_4 vessel	Tube-in-tube	Tube-in-tube, both fluids unmixed
	18	Pickling Section #1	Tube-in-tube	Tube-in-tube, both fluids unmixed
	19	Pickling Section #2	Tube-in-tube	Tube-in-tube, both fluids unmixed
	20	Hot rinse	Tube-in-tube	Tube-in-tube, both fluids unmixed
	21	Pickle drier	Tube-fin	Single-pass tube-fin with both fluids unmixed
	22	Tension leveller drier	Tube-fin	Single-pass tube-fin with both fluids unmixed
	23	SP3 mill drier	Tube-fin	Single-pass tube-fin with both fluids unmixed
VBA	24	Pre-degreaser	Shell-and-tube	Single shell, multiple of 2 tubes, mixed flow
	25	Secondary degreaser	Shell-and-tube	Single shell, multiple of 2 tubes, mixed flow
	26	Final degreaser	Shell-and-tube	Single shell, multiple of 2 tubes, mixed flow
	27	Degreaser drier	Tube-fin	Single-pass tube-fin with both fluids unmixed

The number of tubes in each heat exchanger was not known and a value was calculated based on calculations in equation 4.28.

Table 2: Heat exchanger types summary

Heat Exchanger Properties									
Area	HX number	Equipment	D_{ts-act} (m)	D_{ts} (m)	n	D_{ss} (m)	L_{ts} (m)	L_{ss} (m)	Power Rating (kW)
VPP	1	Entry drier	0.006283	0.02	33	1.30	1.00	1.00	500
	2	Pickling Spray #1	0.006283	0.02	7	0.40	2.00	2.00	400
	3	Pickling Spray #2	0.006283	0.02	7	0.40	2.00	2.00	400
	4	Hot rinse	0.006283	0.02	15	1.30	2.00	2.00	260
	5	Exit drier	0.006283	0.02	33	1.30	1.00	1.00	500
AP1	6	Quench drier	0.006283	0.02	29	1.30	1.00	1.00	250
	7	Pickler #1	0.006283	0.02	8	0.40	2.42	2.42	650
	8	Pickler #2	0.006283	0.02	8	0.40	2.42	2.42	650
	9	Pickle drier	0.006283	0.02	29	1.30	1.00	1.00	250
AP2	10	Pre-degreaser	0.000314	0.02	22	2.00	2.00	2.00	800
	11	Secondary degreaser	0.000314	0.02	20	2.00	2.00	2.00	450
	12	Final degreaser	0.000314	0.02	15	2.00	2.00	2.00	100
	13	Degreaser drier	0.006283	0.02	30	1.30	1.00	1.00	300
	14	Quench drier	0.006283	0.02	30	1.30	1.00	1.00	300
	15	Neoylite #1	0.006283	0.02	10	0.40	2.00	2.00	700
	16	Neoylite #2	0.006283	0.02	10	0.40	2.00	2.00	700
	17	SSO_4 vessel	0.000314	0.02	7	0.40	2.00	2.00	100
	18	Pickling Section #1	0.006283	0.02	8	0.40	2.42	2.00	525
	19	Pickling Section #2	0.006283	0.02	8	0.40	2.42	2.00	525
	20	Hot rinse	0.006283	0.02	6	0.40	2.00	2.00	150
	21	Pickle drier	0.006283	0.02	30	1.30	1.00	1.00	300
	22	Tension leveller drier	0.006283	0.02	30	1.30	1.00	1.00	300
	23	SP3 mill drier	0.006283	0.02	30	1.30	1.00	1.00	300
VBA	24	Pre-degreaser	0.000314	0.02	22	2.00	2.00	2.00	800
	25	Secondary degreaser	0.000314	0.02	20	2.00	2.00	2.00	450
	26	Final degreaser	0.000314	0.02	15	2.00	2.00	2.00	100
	27	Degreaser drier	0.006283	0.02	30	1.30	1.00	1.00	300

Chapter 4:

Model

Development

4.1 Introduction

A model to predict entropy generation in heat exchangers is necessary to predict optimal performance and compare results. That model will be described in this chapter. Firstly, the entropy generation is determined for each individual case, taking into account heat transfer and fluid friction as the only contributors. From equation 1.1 thus follows the equation [23]:

$$S_{gen} = (S_{gen})_{Heat\ Transfer} + (S_{gen})_{Fluid\ Friction} \tag{4.1}$$

Section 4.2 will discuss the first term on the right hand side (Entropy generation due to heat transfer), whilst section 4.3 will discuss the second term on the right hand side (Entropy generation due to fluid friction). The heat transfer mathematics associated with the model will then be discussed during section 4.4 and 4.5. The chapter ends with a summary of assumptions and limits applicable to the model in section 4.6.

4.2. Entropy generation due to heat transfer

The first term on the right hand side of equation 4.1, entropy generation due to heat transfer, can be defined as [41]:

$$dS_{gen} = C\frac{dT}{T} \tag{4.2}$$

$$\Delta S_{gen} = C\ ln\left(\frac{T_o}{T_i}\right) \tag{4.3}$$

In the above equations, C is the heat capacity of the fluid (W/K), and is obtained by multiplying the specific heat capacity (J/kgK) with the mass flow rate (kg/s) of the various streams. Equation 4.3 can then be broken down into separate divisions to incorporate the hot and cold fluid respectively [41]:

$$\Delta S_{gen} = C_h \ln\frac{T_{h,0}}{T_{h,i}} + C_c \ln\frac{T_{c,0}}{T_{c,i}} \tag{4.4}$$

4.3. Entropy generation due to fluid friction

Below we can see the fundamental thermodynamic relation:

$$TdS = dH - VdP \tag{4.5}$$

The first law of thermodynamics state in a control volume:

$$\therefore dH = \delta Q - \delta W \tag{4.6}$$

In the equations above, T is the temperature (K), dS is the change in entropy (W/K), dH is the change in internal energy (W), V is the volume (m^3), dP is the change in pressure (Pa), dQ is the heat supplied to the system by its surroundings (W), dW is the work done by the system on its surroundings (W).

For entropy generation due to fluid friction we make two assumptions:

- The process is adiabatic (thus δQ=0)
- No haft work is done by process (thus δW=0)

This means that δH is equal to 0. This reduces the equation 4.5 and equation 4.6 when combined into:

$$\therefore TdS = -VdP \tag{4.7}$$

4.3.1. Gasses

All the heat exchangers use steam as the heating medium and many of these processes heat up air and other gasses. Assuming the gasses behave ideal, one can see the ideal gas law:

$$PV = \dot{m}RT \tag{4.8}$$

$$\therefore V = \frac{\dot{m}RT}{P} \tag{4.9}$$

- In the equations above,

Inserting the volume term in equation 4.9 into the entropy term in equation 4.7 yields:

$$TdS = -\frac{\dot{m}RT}{P}dP \tag{4.10}$$

$$\therefore dS = -\frac{\dot{m}R}{P}dP \tag{4.11}$$

$$\therefore dS = -\dot{m}R\, ln\left(\frac{P_o}{P_i}\right) \tag{4.12}$$

$$\therefore \Delta S_{gen} = -\dot{m}R\, ln\left(\frac{P_o}{P_i}\right) \tag{4.13}$$

With m being the mass flow rate (kg/s) and R being the universal gas constant (J/kgk).

For gasses, the entropy generation due to fluid friction is thus represented as [41]:

$$\therefore \Delta S_{gen} = -\dot{m}R\, ln\left(\frac{P_o}{P_i}\right) \tag{4.14}$$

By rewriting equation 4.14 for both streams, it can be rewritten as:

$$\Delta S_{gen} = -R\left(\dot{m}ln\left(\frac{P_o}{P_i}\right)\right)_h - R\left(\dot{m}ln\left(\frac{P_o}{P_i}\right)\right)_c \tag{4.15}$$

4.3.2. Liquids

From equation 4.7 it can be seen that the entropy generation due to fluid friction for liquids can be given by:

$$\Delta S = -V_{avg}\frac{\Delta P}{T_{avg}} \tag{4.16}$$

Due to the relative low volume expansion of most liquids with a change in temperature, this function is almost neglectable.

The combined equation 4.4, 4.15 and 4.16 into equation 4.1, the entropy generation equation for heat transfer as well as fluid friction can be seen below for heat exchangers heating gasses (equation 4.13) and liquids (equation 4.14) respectively:

$$\Delta S_{gen} = C_h\, ln\frac{T_{h,0}}{T_{h,i}} + C_c\, ln\frac{T_{c,0}}{T_{c,i}} - \left[R\left(\dot{m}ln\left(\frac{P_o}{P_i}\right)\right)_h + R\left(\dot{m}ln\left(\frac{P_o}{P_i}\right)\right)_c\right] \tag{4.17}$$

$$\Delta S_{gen} = C_h \ln\frac{T_{h,0}}{T_{h,i}} + C_c \ln\frac{T_{c,0}}{T_{c,i}} - \left[R\left(\dot{m}ln\left(\frac{P_o}{P_i}\right)\right)_h + \left(V_{avg}\frac{\Delta P}{T_{avg}}\right)_c\right] \tag{4.18}$$

4.4. Pressure drop relationships

In order to determine the effect of pressure on the system, it was important to predict the pressure drop associated with a specific scenario. The pressure difference caused by frictional losses can be written as [42]:

$$\Delta P = \frac{f' L}{D} \frac{\rho v^2}{2} \tag{4.19}$$

Where f' is the friction factor, L is the effective tube length, ρ is the density of the fluid, u is the speed of the fluid, and D is the tube or shell effective diameter. Since the inlet pressure in all circumstances is know, the outlet pressure was thus calculated as:

$$P_o = P_i - \Delta P \tag{4.20}$$

$$P_o = P_i - \frac{f' L}{D} \frac{\rho v^2}{2} \tag{4.21}$$

The friction factor correlation for turbulent flow can be seen in equation 4.22:

$$f' = \left(\left(-1.8 \log \left(\left(\frac{\frac{\varepsilon_{tubes}}{D}}{3.7} \right)^{1.11} + \frac{6.9}{Re} \right) \right)^{-1} \right)^2 \tag{4.22}$$

In the above equation, ε_{tubes} represents the roughness of the tubes. For steel pipes in turbulent flow it is assumed to be 4.6×10^{-5}. For the purpose of this dissertation, it is assumed that the effect of bends in tubes is not important and is thus not taken into account.

4.5. Heat flux calculations

4.5.1. Heat flux calculations

In all cases there was a specific mass flow rate (m) which was heated from one temperature to another. Since all the material properties were known, the theoretical actual energy required could be calculated using information of the medium to be heated and the following equation:

$$Q = m_c C_{p_c} \Delta T_c \tag{4.23}$$

Since the energy required to heat the cold fluid needs to be similar to what is lost from the hot fluid, and knowing all the inlet temperatures are 453K, one can use this information to determine the outlet temperature of the steam in each individual case as such:

$$T_o = T_i - \frac{Q}{m_c C_{p_c}} \tag{4.24}$$

4.5.2. Estimation of necessary heat transfer area

The sum of all the resistances can be seen as [7]:

$$r = \frac{1}{R_1} + \frac{1}{R_2} + \frac{1}{R_3} + \frac{1}{R_4} + \frac{1}{R_5} \tag{4.25}$$

With:

- R_1 Resistances due to heat transfer on the tube-side
- R_2 Resistances due to fouling on the tube-side
- R_3 Resistances due to tube diameter, length and thickness
- R_4 Resistances due to heat transfer on the shell-side
- R_5 Resistances due to fouling on the shell-side

Assuming no fouling, equation 4.25 is reduced to:

$$r = \frac{1}{R_1} + \frac{1}{R_3} + \frac{1}{R_4} = \frac{1}{h_{eff_i} A_i} + \frac{Ln\left(\frac{D_o}{D_i}\right)}{2\pi kL \times n} + \frac{1}{h_{eff_o} A_o} \tag{4.26}$$

In equation 4.26, L and n are the tube lengths and number of tubes respectively. D_o and D_i are the outer and inner diameters of the tube side's shell and similarly A_i and A_o are the inner and outer surface areas of the of the tube side's shell and thus the effective heat transfer areas inside and outside the tube side's shell. Also, k is the conduction heat transfer coefficient of the tube side steel and $h_{eff,i}$ and $h_{eff,o}$ are the effective convection heat transfer coefficient for gasses and liquids.

But the total heat exchanger resistances are also equal to the inverse of overall heat transfer coefficient (U) multiplied by the effective heat transfer area (A_{ht}) [7]:

$$r = \frac{1}{UA_{ht}} \tag{4.27}$$

Similarly to equation 4.23, the equation for $U \times A_{ht}$ can also be written as:

$$Q = UA_{ht}\Delta T \tag{4.28}$$

$$\therefore UA_{ht} = \frac{\Delta T}{Q} \tag{4.29}$$

Since we by now know the actual heat transfer (Q) and the inlet and outlet temperatures of all the streams (ΔT), we can calculate the value of the overall heat transfer coefficient multiplied by the affective heat transfer area.

That means that by combining equation 4.21, 4.22 and 4.24 one abstains the following equation:

$$\frac{Q}{\Delta T} = \frac{1}{h_{eff} A_i} + \frac{Ln\left(\frac{D_o}{D_i}\right)}{2\pi kL \times n} + \frac{1}{h_{eff} A_o} \tag{4.30}$$

We also know that the effective heat transfer area can be depicted as:

$$A_{ht} = \frac{2\pi D_i L \times n}{2} \tag{4.31}$$

Thus by inserting equation 4.26 into equation 4.25, we can obtain the following equation:

$$\frac{Q}{\Delta T} = \frac{1}{h_{eff_i}\pi D_i \times n} + \frac{Ln\left(\frac{D_o}{D_i}\right)}{2\pi k L \times n} + \frac{1}{h_{eff_o}\pi D_o \times n} \tag{4.32}$$

We can now manipulate equation 4.27 to give us an equation for determining how many tubes (n) are required to generate the required amount of energy (Q) to overcome the temperature differences (ΔT) required by each specific application.

$$n = \left[\frac{1}{h_{eff_i}\pi D_i} + \frac{Ln\left(\frac{D_o}{D_i}\right)}{2\pi k L} + \frac{1}{h_{eff_o}\pi D_o}\right] \times \frac{\Delta T}{Q} \tag{4.33}$$

4.5.3. Calculation of effective convection heat transfer coefficient

The effective convection heat transfer coefficient is medium specific, varying with temperature as well as flow rate, and can be defined as [7]:

$$h_{eff} = \frac{kNu}{D} \tag{4.34}$$

In equation 4.29, the tube side inner and outer diameter is once again used. The Nusselt number (Nu) for flow in turbulent tubes can be estimated as [7]:

$$Nu = 0.037 Re^{0.8} Pr^{1/3} \tag{4.35}$$

The Nusselt number (Nu) is thus a function of the Prandtl number which is medium and temperature specific, and the Reynolds which is given for turbulent flow by [7]:

$$Re = \frac{Dv\rho}{\mu} \tag{4.36}$$

The Reynolds number (Re) is a function of the flow rate and viscosity and diameter, but in this case the diameter is the diameter of flow and is thus the inner tube side diameter for the steam and the inner shell side diameter for the medium.

4.5.4. Efficiencies of various heat exchangers

The efficiencies of the heat exchangers are calculated by comparing the actual energy transferred with the maximum energy transferred [23]:

$$Q_{act} = m_c C_{p_c} \Delta T_c \tag{4.37}$$

$$Q_{max} = C_{min}(T_{h_i} - T_{c_i})` \tag{4.38}$$

With C_{min} being the smallest heat capacity (Specific heat capacity times mass flow rate). The efficiency is then calculated as follows [23].

$$\varepsilon = \frac{Q_{act}}{Q_{max}} \tag{4.39}$$

4.2. Constructal design equations

4.2.1. Introduction

If our hypothesis is correct, and the intercept between the heat transfer and fluid friction will be a close approximation of the global minimum entropy generated, we should be able use this information as an optimisation tool. By setting the entropy generation due to heat transfer equal to the entropy generation due to fluid friction, we will be able to determine an optimal tube side diameter.

$$\Delta S_{gen_{friction}} = \Delta S_{gen_{heat\ transfer}} - S_{gen_{design\ mismatch}} \tag{4.40}$$

4.2.2. Entropy generation due to friction

The tube-side diameter has a very strong influence on the pressure drop associated with the heat exchangers. When combining the entropy generation due to friction for gasses (equation 4.14) with the outlet pressure equation (equation 4.21), one can obtain the entropy generation due to fluid friction for gasses in terms of the tube side diameter. 4.31

$$\Delta S_{gen} = -\dot{m}R\ ln\left(1 - \frac{f'L}{P_i D}\frac{\rho u^2}{2}\right) \tag{4.41}$$

Breaking down the linear velocity, we use the effective area to calculate the effective diameter:

$$\pi\frac{D_{eff}^2}{4} = \frac{\pi D^2}{4} \times n \tag{4.42}$$

$$D_{eff} = \sqrt{D^2 n} \tag{4.43}$$

Thus the flow rate can be rewritten as:

$$u = \frac{4\dot{m}}{\rho\pi \times D_{eff}^2} = \frac{4\dot{m}}{\rho\pi \times D^2 n} \tag{4.44}$$

This results in the entropy generation, broken down to its basic unites to be displayed as:

$$\Delta S_{gen} = -\dot{m}R\, ln\left(1 - \frac{8f'L\dot{m}^2}{P_i\pi^2\rho\times nD^5}\right) \tag{4.45}$$

Similarly for gasses, if one combines the entropy generation due to friction for liquids (equation 4.16) with the outlet pressure equation (equation 4.21), one can obtain the entropy generation due to fluid friction for liquids in terms of the tube side diameter.

$$\Delta S_{gen} = -V_{avg}\frac{8f'L\dot{m}^2}{T_{avg}\pi^2\rho\times nD^5} \tag{4.46}$$

Due to the fact that the output temperature is a function of the tube-side diameter, the average temperature needs to be assumed. Due to the entropy generation due to fluid friction for fluids being a lot smaller than those for gasses, the assumption should have a minimal effect on the overall result.

4.2.3. Entropy generation due to heat transfer

Similarly to the previous section, the tube side diameter has a very strong effect on the forced heat transfer coefficient by increasing the linear velocity of the fluid, and thus effects the outlet temperatures. From equation 4.4 we can see that the entropy generation due to heat transfer is given by:

$$\Delta S_{gen} = C_h \ln \frac{T_{h,0}}{T_{h,i}} + C_c \ln \frac{T_{c,0}}{T_{c,i}} \tag{4.47}$$

The entropy generation due to heat transfer is a strong function of the inlet and outlet temperatures. Rewriting equation 4.30 gives us the generalised equation to determine the outlet temperature:

$$T_2 = T_1 + \frac{Q}{h_{eff} A} \tag{4.48}$$

But, by combining equation 4.34-4.36, we can obtain the equation for the effective heat transfer coefficient:

$$h_{eff} = \frac{k 0.037 \left(\frac{Dv\rho}{\mu}\right)^{0.8} Pr^{1/3}}{D} = \frac{0.037 k Pr^{1/3} v^{0.8} \rho^{0.8}}{D^{0.2} \mu^{0.8}} \tag{4.49}$$

By inserting equation 4.49 into equation 4.48, the true equation for the outlet temperature can thus be determined:

$$T_2 = T_1 + \frac{Q D^{0.2} \mu^{0.8}}{A 0.037 k Pr^{1/3} v^{0.8} \rho^{0.8}} \tag{4.50}$$

$$\therefore T_2 = T_1 + \frac{Q \mu^{0.8} D^{0.8}}{0.14 n^{0.2} L k Pr^{1/3} \dot{m}^{0.8}} \tag{4.51}$$

Now we can combine this (Equation 4.50) into the original entropy generation due to heat transfer equation (Equation 4.47), to yield:

$$\Delta S_{gen} = C_h \ln \left(1 - \frac{Q \mu^{0.8} D^{0.8}}{0.14 n^{0.2} L k Pr^{1/3} \dot{m}^{0.8}}\right)_h + C_c \ln \left(1 + \frac{Q \mu^{0.8} D^{0.8}}{0.14 n^{0.2} L k Pr^{1/3} \dot{m}^{0.8}}\right)_c \tag{4.52}$$

4.2.4. Entropy generation due to design mismatch

In this dissertation, we want to optimise the entropy generation out of a design point of view, not entropy generated due incorrect heat exchangers usage. For this reason we want to distinguish between entropy generation mechanisms namely, due to choosing the incorrect design for the duty (Operational conditions), and actual entropy generation due to design.

The design mismatch entropy thus generated due to the heat exchanger not used optimal. This would mean that for cross-flow, parallel-flow and counter flow arrangements, the medium should be able achieve the same outlet temperature (or even slightly higher in the case of cross-flow and counter-flow), than the steam heating it.

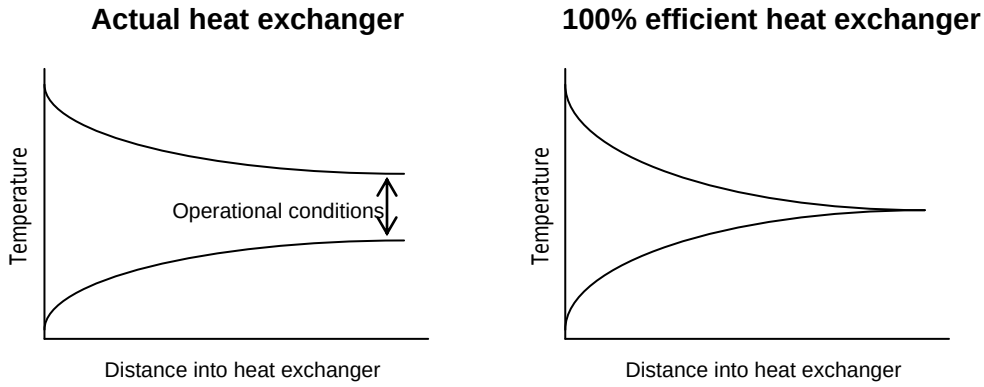

Figure 8: Indication of the entropy generation due to operational conditions (left) and the entropy generation due to design mismatch (right)

This is done in order to indicate the inherent entropy due to the heat exchanger design, and thus separate it from the entropy generated due to operational conditions. This is quite easily done by increasing the overall heat transfer coefficient to infinity.

The equation defining design mismatch can thus be defined by combining equation 4.38 for the maximum allowable energy transferred, with equation 4.24 that predicts the outlet temperature:

$$T_o = \frac{C_{min}\left(T_{h_i} - T_{c_i}\right)}{mC_p} + T_i \tag{4.53}$$

The minimum entropy thus generated will be defined as combining equation 4.53 with the overall entropy generation equation due to heat transfer (Equation 4.45):

$$\Delta S_{gen} = C_h \ln\left(\frac{C_{min}\left(T_{h_i} - T_{c_i}\right)}{C_h T_{h,i}} + 1\right) + C_C \ln\left(\frac{C_{min}\left(T_{h_i} - T_{c_i}\right)}{C_c T_{c,i}} + 1\right) \quad (4.54)$$

4.2.5. Determining the optimal diameter

If our hypothesis is correct, the optimal diameter could be found where the intercept of the entropy generation due to heat transfer and fluid fiction occurs. To do this these values must be equal in size. We thus we can insert equation 4.45, 4.46, 4.52 and 4.54 into equation 4.40 to yield the balanced equation for entropy generation for liquids and gasses:

$$-\left[\dot{m}R\ ln\left(1-\frac{8f'L\dot{m}^2}{P_i\pi^2\rho\times n^{1.5}D^5}\right)\right]_h-\left[V_{avg}\frac{8f'L\dot{m}^2}{T_{avg}\pi^2\rho\times n^{1.5}D^5}\right]_c=C_h\ln\left(1-\frac{Q\mu^{0.8}D^{0.8}}{0.14n^{0.2}LkPr^{1/3}\dot{m}^{0.8}}\right)_h+$$
$$C_c\ln\ln\left(1+\frac{Q\mu^{0.8}D^{0.8}}{0.14n^{0.2}LkPr^{1/3}\dot{m}^{0.8}}\right)_c-C_h\ln\left(\frac{C_{min}\left(T_{h_i}-T_{c_i}\right)}{C_hT_{h,i}}+1\right)-C_C\ln\left(\frac{C_{min}\left(T_{h_i}-T_{c_i}\right)}{C_cT_{c,i}}+1\right) \quad (4.55)$$

Similarly for gasses only:

$$-\left[\dot{m}R\ ln\left(1-\frac{8f'L\dot{m}^2}{P_i\pi^2\rho\times n^{1.5}D^5}\right)\right]_h-\left[\dot{m}R\ ln\left(1-\frac{8f'L\dot{m}^2}{P_i\pi^2\rho\times n^{1.5}D^5}\right)\right]_c=C_h\ln\left(1-\frac{Q\mu^{0.8}D^{0.8}}{0.14n^{0.2}LkPr^{1/3}\dot{m}^{0.8}}\right)_h+$$
$$C_c\ln\ln\left(1+\frac{Q\mu^{0.8}D^{0.8}}{0.14n^{0.2}LkPr^{1/3}\dot{m}^{0.8}}\right)_c-C_h\ln\left(\frac{C_{min}\left(T_{h_i}-T_{c_i}\right)}{C_hT_{h,i}}+1\right)-C_C\ln\left(\frac{C_{min}\left(T_{h_i}-T_{c_i}\right)}{C_cT_{c,i}}+1\right) \quad (4.56)$$

Solving this equation implicitly, we can obtain the diameter where the entropy generation due to heat transfer and entropy generation due to fluid friction are identical. If our hypothesis is correct this will yield a result very close to the global minimum entropy generation.

$$\Delta S_{gen_{friction}}=\Delta S_{gen_{heat\ transfer}}-S_{gen_{design\ mismatch}} \quad (4.40)$$

$$\Delta S_{gen}=-\dot{m}R\ ln\left(1-\frac{8f'L\dot{m}^2}{P_i\pi^2\rho\times n^{1.5}D^5}\right) \quad (4.45)$$

$$\Delta S_{gen}=-V_{avg}\frac{8f'L\dot{m}^2}{T_{avg}\pi^2\rho\times n^{1.5}D^5} \quad (4.46)$$

$$\Delta S_{gen}=C_h\ln\left(1-\frac{Q\mu^{0.8}D^{0.8}}{0.14n^{0.2}LkPr^{1/3}\dot{m}^{0.8}}\right)_h+C_c\ln\ln\left(1+\frac{Q\mu^{0.8}D^{0.8}}{0.14n^{0.2}LkPr^{1/3}\dot{m}^{0.8}}\right)_c \quad (4.52)$$

$$\Delta S_{gen}=C_h\ln\left(\frac{C_{min}\left(T_{h_i}-T_{c_i}\right)}{C_hT_{h,i}}+1\right)+C_C\ln\left(\frac{C_{min}\left(T_{h_i}-T_{c_i}\right)}{C_cT_{c,i}}+1\right) \quad (4.54)$$

4.3. Summary of assumptions

4.3.1. Assumptions

A summary of all the key assumptions can be seen below:

- Total energy transfer of the heat exchangers remains constant
- All flow is fully developed
- There are no losses to the surroundings
- There is no entropy generation due to fouling
- All gasses act like ideal gasses
- The roughness of the tubes are 4.6×10^{-5}
- The effect of bends on the friction factor and pressure drop is neglectable

4.3.2. Limits on results

For the results section, the following limits were used in order to giver representable and useable results:

- The inlet steam temperature needs to be at least 10K more than the outlet medium temperature
- The outlet pressures needs to be more than 101.3kPa

If any of the simulations yielded results outside these limits they were excluded from the graphs and figures.

Chapter 5:

Validation

5.1 Introduction

In order to prove the integrity and validity of the model and to prove that the model holds for all conditions required for this dissertation, it needs to be validated against experimental data or results obtained from other scholars.

The procedure of this validation process is to simulate a similar set-up to what was used by other scholar's experiments. By looking at these comparisons it will be clear that the model developed in this dissertation holds for all conditions applicable to this desertion.

Unfortunately, one cannot measure entropy generation directly, however, once the change in temperature and pressure is known, one can quite easily calculate entropy generation. Pressure and temperature differences are quite complex to calculate but there are a lot of experimental results on them. Section 5.2 will be giving a brief background on the methodology that the researcher (to which the work will be compared to) used in obtaining their results, together with a summary of both fluid and design variables used in their calculations.

Section 5.3, 5.4 and 5.5 will be showing how the model derived in this dissertation correlates to the model designed by the researchers, based on calculations predicting various temperatures, pressures and heat transfer coefficients. Section 5.6 will then show so practical analytical examples of entropy generation calculations.

5.2 Background on comparison to be used

Faizal and Ahmed did work on tube-plate heat exchangers operated in parallel flow [40], with both mediums being water (hot and cold). Its reaction to the various mechanisms of heat transfer when varying the mass flow rate of the hot water was observed. The following table shows us the main information regarding the fluid that was used by them to do their analysis:

Table 3: Medium variables used by Faizal and Ahmed to do their entropy analysis [40]

Medium variables		
Variable	Fluid 1_{ts}	Fluid 2_{ss}
Inlet temperature, T_i (K)	322	299
Mass flow rate, m (kg/s)	0.18-0.63	0.16
Density, ρ (kg/m^3)	990.44	992.78
Constant pressure specific heat, Cp (J/kg K)	4188	4195
Kinematic viscosity, μ (m^2/s)	1.492E-05	1.398E-05
Entrance pressure, P_i (kPa)	100	100
Fouling resistance, r (m^2K/W)	0.00	0.00
Prandtl number, Pr (-)	5.54	7.53

By using the variables above they attempted determine how the streams would behave in the heat exchanger with geometric and operational variables as seen in Table 4:

Table 4: Heat exchanger geometric properties used by Faizal and Ahmed to do their analysis [40]

Optimised design variables					
Plate height (m)	Plate width (m)	Number of hot channels	Number of cold channels	A_{HT} (m^2)	Spacing (m)
0.273	0.213	9	10	1.16298	0.012

With the information in Table 3 and Table 4 it is possible to do a complete reconstruction of their results with the model designed in this dissertation, in order to determine the accuracy of this model. Due to the lack of experimental results on entropy generation, it was decided to compare this model with the main variables contributing to entropy generation.

5.3. Effect of temperature on varying mass flow rate

Using the design and fluid variables shown in Table 3 and Table 4, the effect varying the hot water mass flow rate on the inlet and outlet temperatures of the various streams can be seen. The results obtained by Faizal and Ahmed were compared by those calculated in the model derived in this dissertation [40].

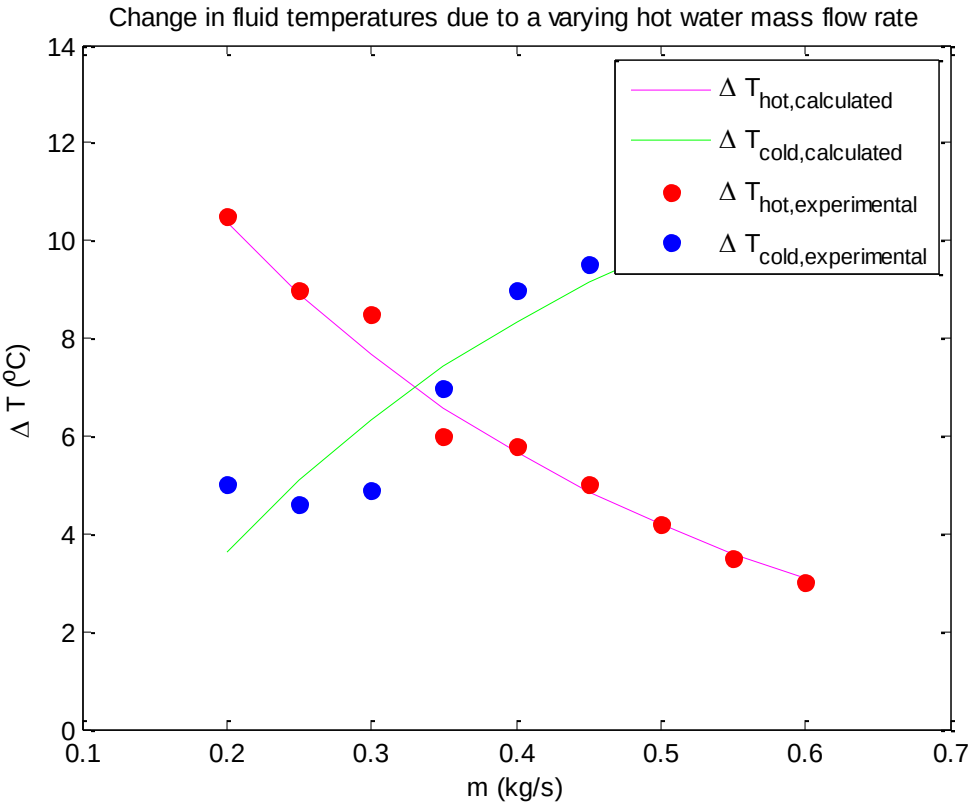

Figure 9: Change in fluid temperatures due to a varying hot water mass flow rate [40]

It is clear that there is an inverse correlation between the temperature differences of the hot and cold streams. With an increased mass flow rate the hot water loose the least amount of temperature whereas the cold water increase the most. This is due to the effect forced convection has on the effective heat transfer rate which is increases with larger flow rates as seen in equation 4.29 to 4.31 (Also shown below).

$$h_{eff} = \frac{kNu}{D} \tag{5.1}$$

This is due to the Nusselt number being directly related to the Reynolds number which is a function of mass flow rate.

In Figure 10, one can see that there is not a large change in the difference in outlet temperatures when varying the mass flow rate of the hot water. Initially the temperature differences increases, where after it decreases slightly again up to a point where it seems as if it will be planning out. Once again there exists a good correlation between the calculated (from equation 4.24) and experimental values [40].

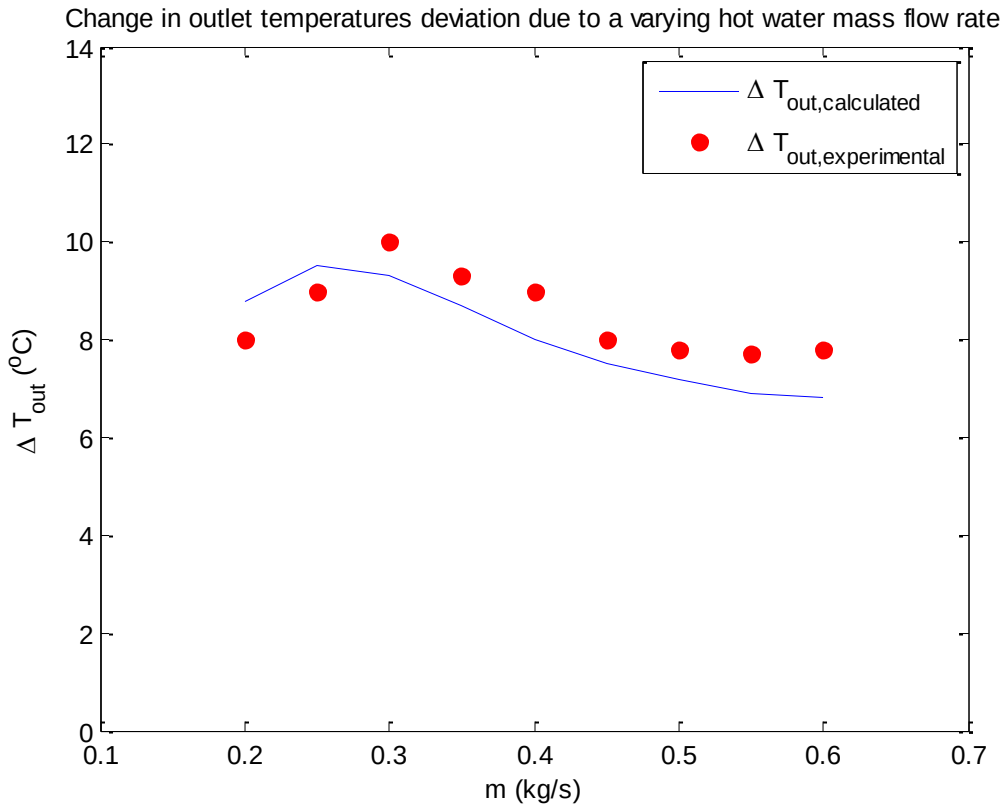

Figure 10: Change in outlet temperatures deviation due to a varying hot water mass flow rate [40]

5.4. Effect of pressure on varying mass flow rate

One can clearly see the dependency of pressure with regards to mass flow rate. This is due to the correlation found in literature (equation 4.19), which is also shown here below in equation 5.2.

$$\Delta P = \frac{f' L}{D} \frac{\rho u^2}{2} \tag{5.2}$$

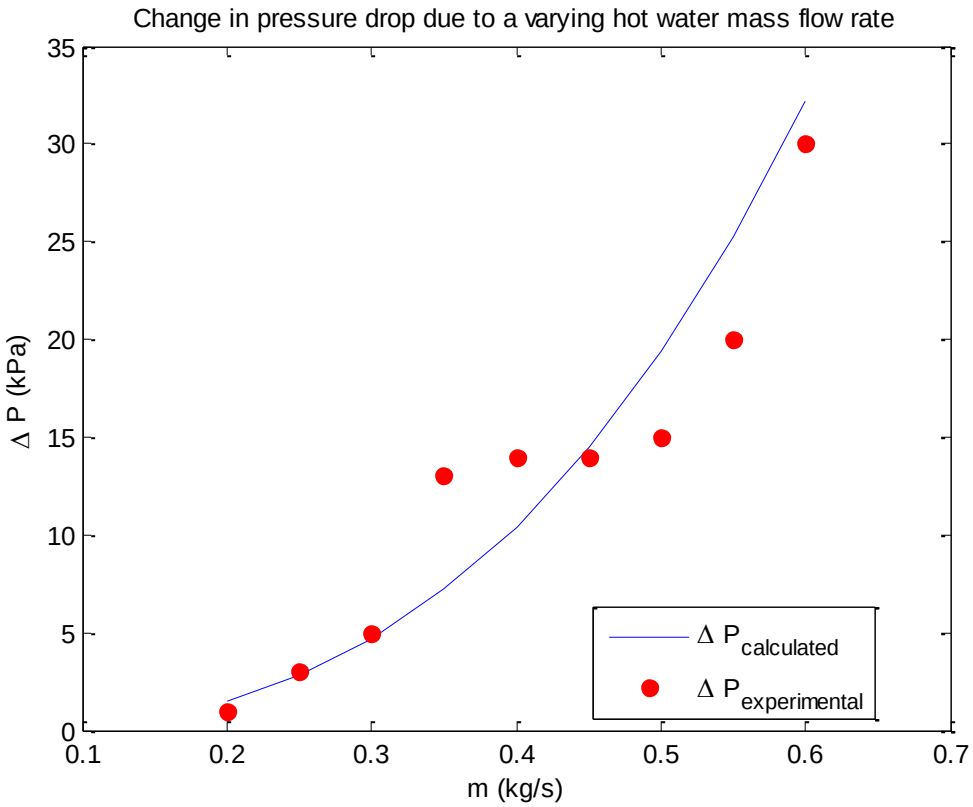

Figure 11: Change in pressure drop due to a varying hot water mass flow rate [40]

Once again it is seen that the experimental values have a good correlation with the theoretical values calculated with the model that is developed in this dissertation.

5.5. Effect of overall heat transfer coefficient on varying mass flow rate

In Figure 12, one can once again see that there is a good correlation between the results of the experiments of Faizal and Ahmed and the model developed in this dissertation.

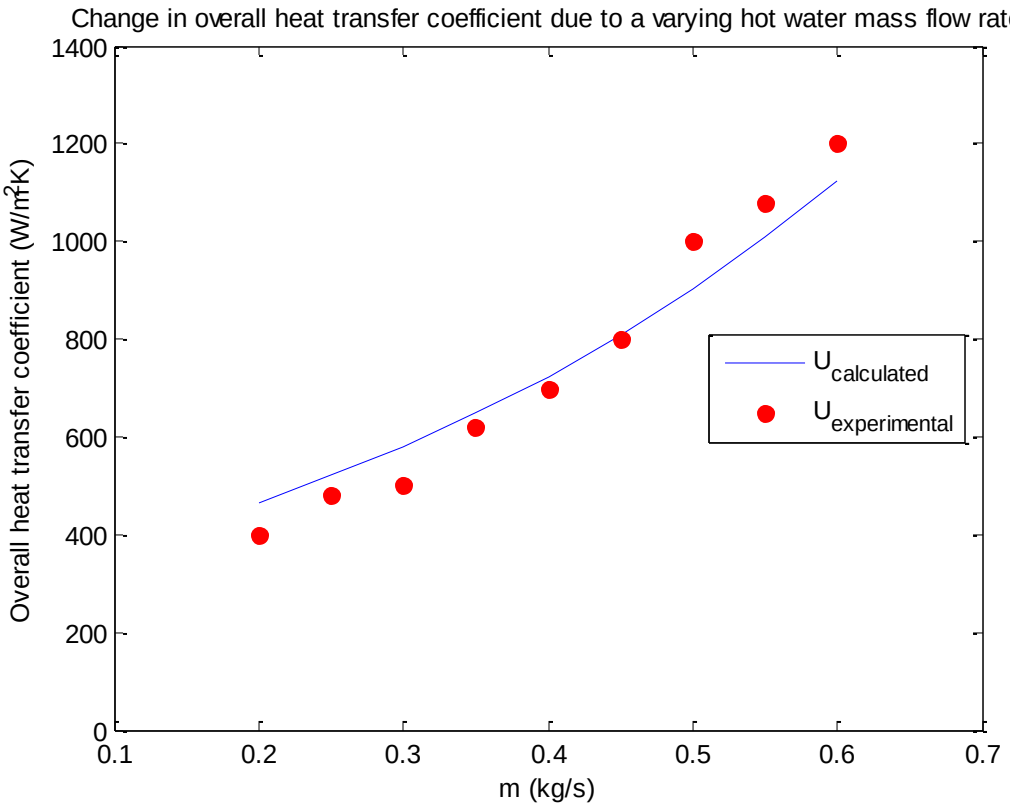

Figure 12: Change in overall heat transfer coefficient due to a varying hot water mass flow rate [40]

It is clear that there is an upward trend when comparing the hot water mass flow rate to the overall heat transfer coefficient. This is once again due to equation 4.29 to 4.31 and also shown in this chapter in equation 5.1, where the dependency of the overall heat transfer coefficient to the mass flow rate is emphasised.

5.6. Application of entropy generation calculations

Now that it has been proven that the calculations of the variables that entropy generation depends on is correct, we are going to apply these variables to some real case examples. Take two streams exchanging heat with each other as is the case in a typical heat exchanger. Stream 1 (Hot stream), is a gas that is used to heat stream 2 (Cold stream), a liquid water. The details of the two streams can be seen in Table 5:

Table 5: Working example of the application of the entropy equitation

Working Example		
Variable	Hot	Cold
Medium	Steam	Water
R (J/kgK)	461.5	NA
C_p (J/kgK)	2500	4200
ρ (kg/m^3)	4.1	990
m (kg/s)	0.3	0.36
V (m^3/s)	0.07317	0.00036
T_1 (K)	453	303
T_2 (K)	433	313
Q (W)	15,000	15,000
P_1 (kPa)	800	300
P_2 (kPa)	500	200

For the hot stream, equation 4.17 is reduced to:

$$\Delta S_{gen} = C_h \, ln \frac{T_{h,o}}{T_{h,i}} - R \left(\dot{m} ln \left(\frac{P_o}{P_i} \right) \right)_h \tag{5.3}$$

By inserting the variables from Table 5 of the hot stream we obtain:

$$\Delta S_{gen} = 2500 \times ln \left(\frac{433}{533} \right) - 461.5 \times 0.3 \times ln \left(\frac{500}{800} \right) = 31.2 W/K \tag{5.4}$$

Now we do exactly the same with the cold stream, where we reduce equation 4.18 to:

$$\Delta S_{gen} = C_c \ln \frac{T_{c,0}}{T_{c,i}} - \left(V_{avg} \frac{\Delta P}{T_{avg}}\right)_c \quad (5.5)$$

By inserting the variables from Table 5 of the cold stream we obtain:

$$\Delta S_{gen} = 4200\, ln\left(\frac{313}{303}\right) - 0.00036 \times \frac{(200-300)}{\frac{(313-303)}{2}} = 49.1 W/K \quad (5.6)$$

The total entropy generated in the two streams is thus:

$$\Delta S_{gen\_tot} = 31.2 + 49.1 = 80.3 W/K \quad (5.7)$$

The same example was used by the Matlab model, and by comparing the results with the ones from the Matlab program the following results were obtained:

Table 6: Model Accuracy

Model Accuracy			
Section	Hot	Cold	Total
$S_{gen\ Model}$ (W/K)	31.2062	49.0953	80.3015
$S_{gen\ Manual\ Calculation}$ (W/K)	31.2	49.1	80.3
Difference (%)	0.02%	0.01%	0.00%

From Table 6, it is clear that the model is accurate to 1 decimal, which proves that the entropy generation calculations, based on the change in pressure and temperature, is programmed correctly.

To summarise Chapter 5, Section 5.2 to 5.5 proves that the main variables contributing to entropy generation is calculated correctly (and was validated against actual experimental data), whilst section 5.6 proves that if the model is using the correct change in temperatures and pressures, it will predict the entropy generation correctly.

Chapter 6:

Results

6.1 Introduction

The model to calculate entropy generation, derived in Chapter 3 and 4, and validated in Chapter 5, can be expressed for the three types of heat exchangers.

Section 6.2 gives a summary of the entropy generation of all the heat exchangers, as well as a split in the processes which cause the entropy generation. In section 6.3 we will then discuss the reasoning behind the choice of the main variables used in depicting the results from this dissertation. Section 6.4 gives us a summation of the findings with regard to the correlation between the global minimum entropy generation relative to the intercept between the entropy generated due to friction and heat independently. Section 6.5 and 6.6 discusses the relationship between different variables as well as the effect of different heat exchangers. The chapter ends with section 6.7 which gives a summary of optimised results and findings.

6.2. Entropy generation at current operating conditions

In Figure 13, one can see the current entropy generated due to fluid friction as well as due to heat transfer by each piece of equipment. It is clear that the dominant mechanism is entropy generation due to fluid friction under the current operating conditions.

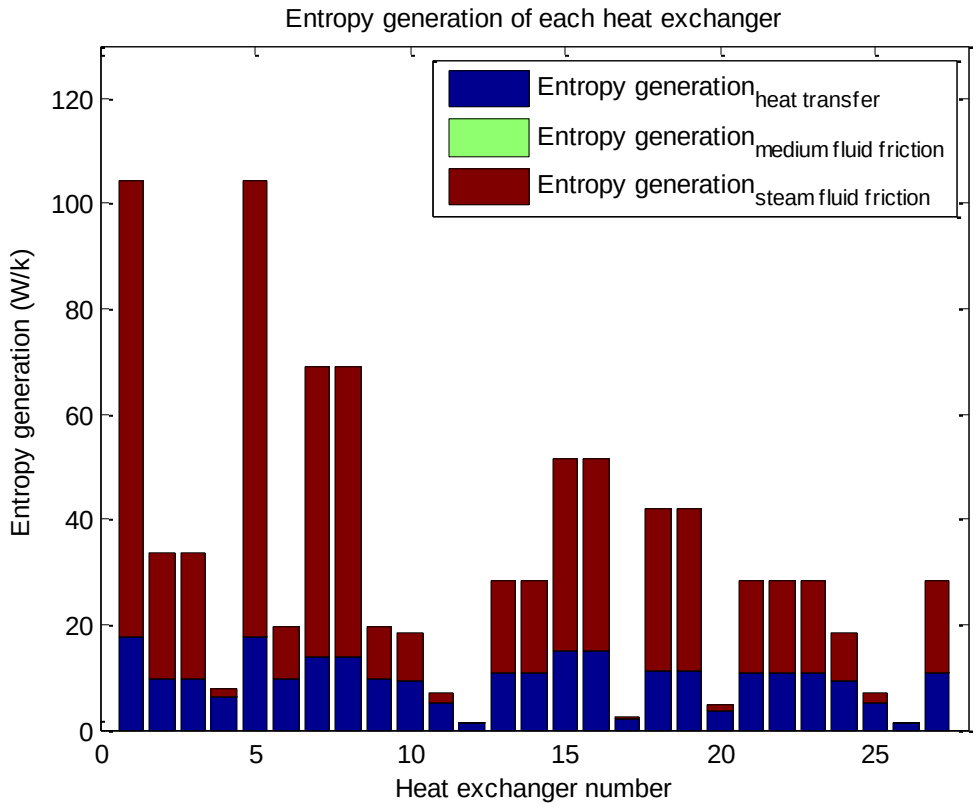

Figure 13: Entropy generation of each heat exchanger

When comparing the various heat exchangers it is clear that entropy generation due to fluid friction is more dominant in the tube-fin heat exchangers than the other heat exchangers under the current operating conditions.

6.3. Sensitivity Analysis

To determine the main variable that will be used to present the results it is important to know which variable has the largest impact on the total entropy generated. Below we can see the effect of changing a single variable and keeping all other variables constant, on entropy generation. All the variables were changed by 10%, apart from temperature that was varied by 30K from the original temperatures.

For the presentation of their effects a tube-fin heat exchanger (heat exchanger 2) was chosen. In Figure 14 one can see the effect of varying a number of variables without compensating with other variables in order to keep the heat rating constant.

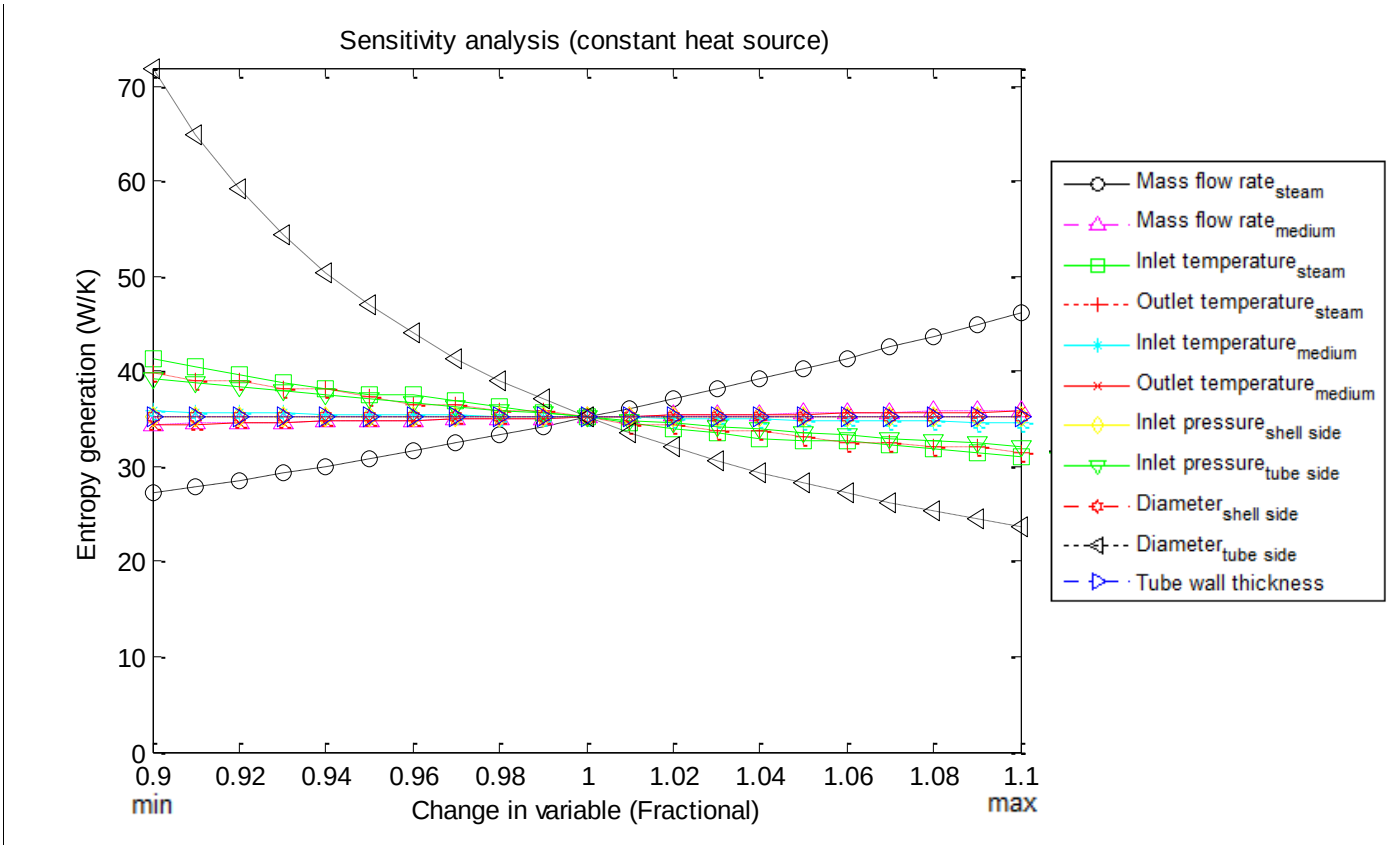

Figure 14: Sensitivity analysis of a tube-fin heat exchanger (constant heat source)

From Figure 14 it is clear that the variables affecting entropy generation was mostly the tube-side diameter, as by reducing it to less than 90% yielded results that fell outside the limits as per section 4.5.2.

A similar graph to Figure 14 was created, but in this case the other variables were manipulated to keep the amount of heat transfer constant as explained in Section 4.4 and 4.5, in order to keep the heat exchanger power rating the same (Thus using a variable heat source).

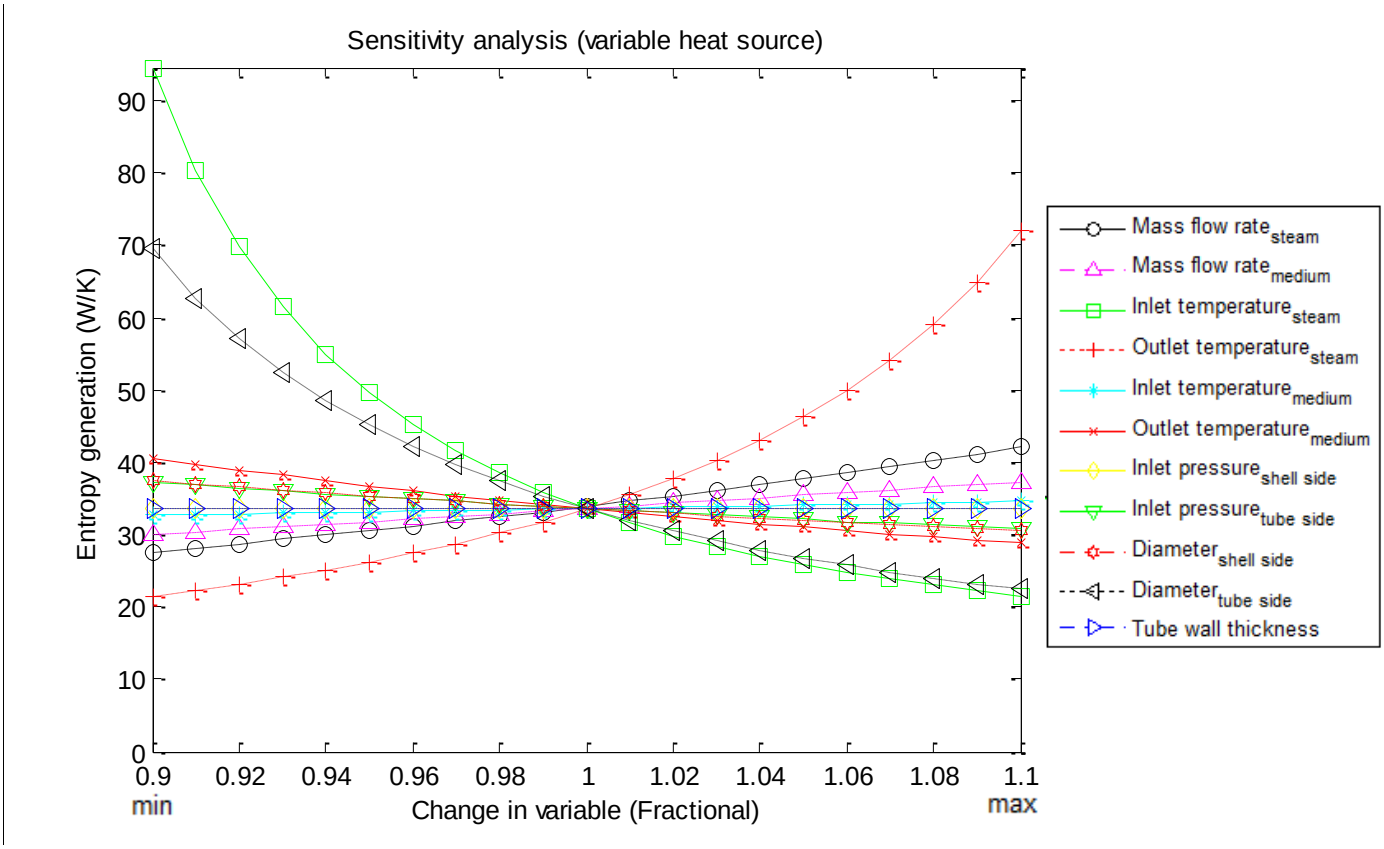

Figure 15: Sensitivity analysis of a tube-fin heat exchanger (variable heat source)

From Figure 15 it is clear the factor influencing the entropy generation the most was again due to the tube side diameter and inlet and outlet steam temperature, as by varying any of them slightly resulted in the largest changes in entropy generation.

In this case reducing the inlet steam temperature reduced the temperature difference in equation 4.18. To compensate for this effect the mass flow rate needs to be increased to

transfer the same amount of energy. This effect becomes very large and very soon results in so much mass to be transferred that entropy generation increases uncontrollably.

This effect is further emphasised in Table 7 where the average result of varying the different variables are tabulated. This table includes the average effect of varying the variables on all 27 heat exchangers.

In Table 7, the maximum allowable values obtainable (that yields usable results within the boundary limits), can be seen.

Table 7: Average effect of variables on entropy generation with a variable heat source

Sensitivity Analysis		
Variable	Change in Variable	Average Change in Entropy generation (%)
Steam inlet temperature (K)	30K	103.60%
Steam outlet temperature (K)	30K	72.83%
Diameter tube-side (m)	10%	58.82%
Mass flow rate of steam (kg/s)	10%	19.69%
Medium outlet temperature (K)	30K	15.01%
Mass flow rate of medium (kg/s)	10%	10.49%
Diameter shell side (m)	10%	9.01%
Pressure tube-side (kPa)	10%	7.93%
Medium inlet temperature (K)	30K	0.42%
Tube side wall thickness (m)	10%	0.08%
Pressure shell-side (kPa)	10%	0.03%

Due to this being similar to the approach that will be used in the modelling during the course of this section, the two variables that will thus be used in presenting the results are inlet steam temperature and tube-side diameter.

6.4. Cause for large entropy generation sensitivity to inlet steam temperature and tube-side diameter

In this section, we will be breaking down the main factors contributing to entropy generation as identified in section 6.3, in order to understand why they play such an important role. Based on Figure 14, Figure 15 and Table 7, it was seen that they main factors contributing to entropy generation was inlet steam temperatures and tube-side diameter. In Figure 16, one can once again see the effect of the inlet steam temperature and varying diameters on entropy generation (For heat exchanger number 2).

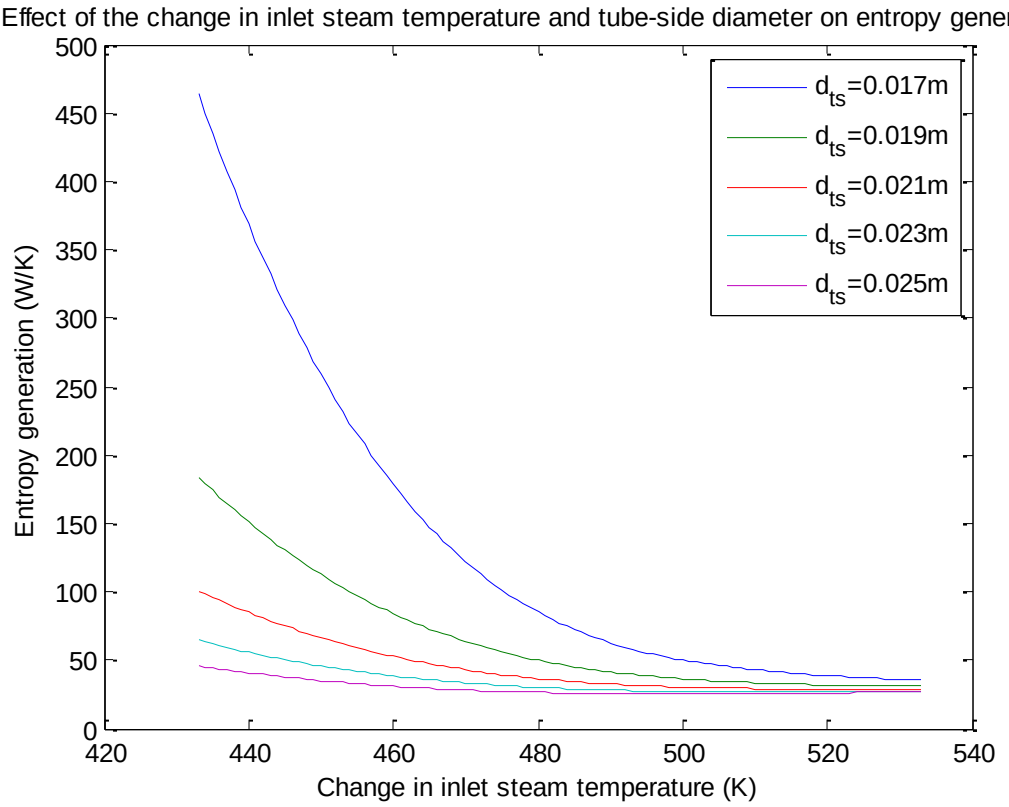

Figure 16: Effect of the change in inlet steam temperature and tube-side diameter on entropy generation

It is apparent that entropy generation decreases with an increase in tube diameter. It also decreases as inlet steam temperature increases, up to a point where the increase in entropy

generation due to heat transfer starts to increase (Seen in the larger diameter pipes above 500K). The entropy generation decreasing due to a higher steam inlet temperature is as a result of a lower steam mass flow rate associated with the increased temperature (to keep the heat transfer to the medium constant). Referring back to equation 4.13 and 4.14, entropy generation due to fluid friction is proportional to mass flow rate to the third, and entropy generation due to heat transfer directly proportional. As stated before, the increased temperature allows for less volume of medium required (As per equation 4.19), this in turn translates to a lower linear flow rate.

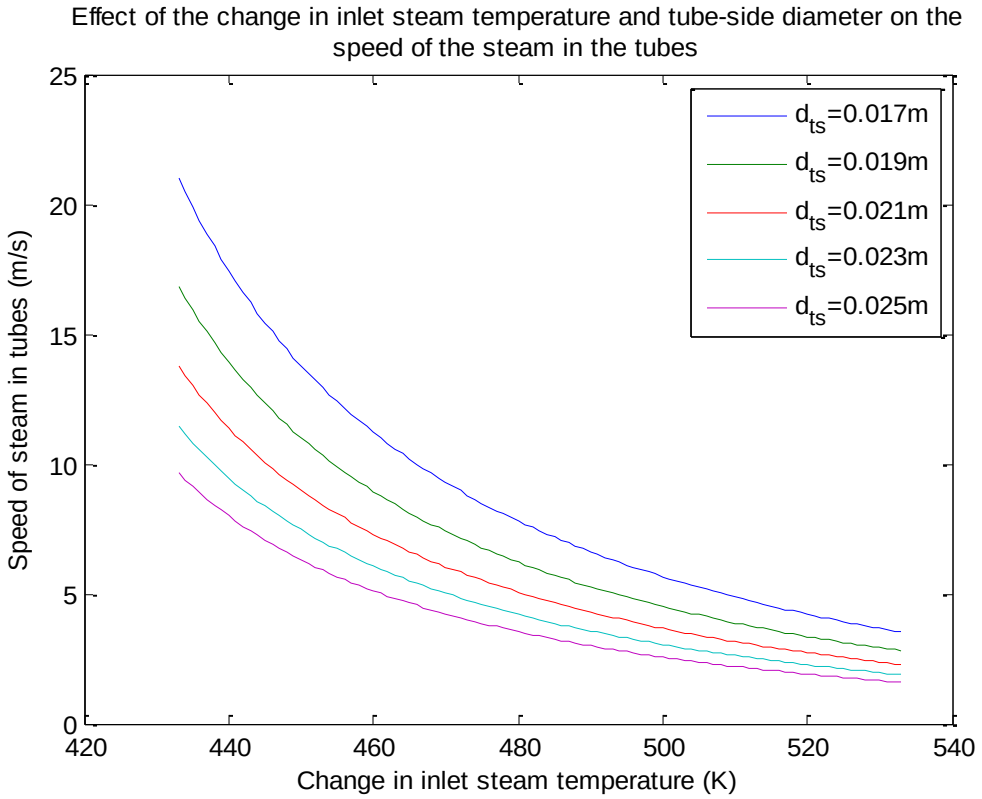

Figure 17: Effect of the change in inlet steam temperature and tube-side diameter on the speed of the steam in the tubes

The change in tube diameter is offset by the increase in number of tubes (done in order to keep the total heat transfer the same, as seen in equation 4.28), which offsets the linear speed the slightly for the different tube diameters. The lower flow rates associated with an increased steam temperature also results in a lower Reynolds and Nusselt numbers (The latter seen in Figure 18).

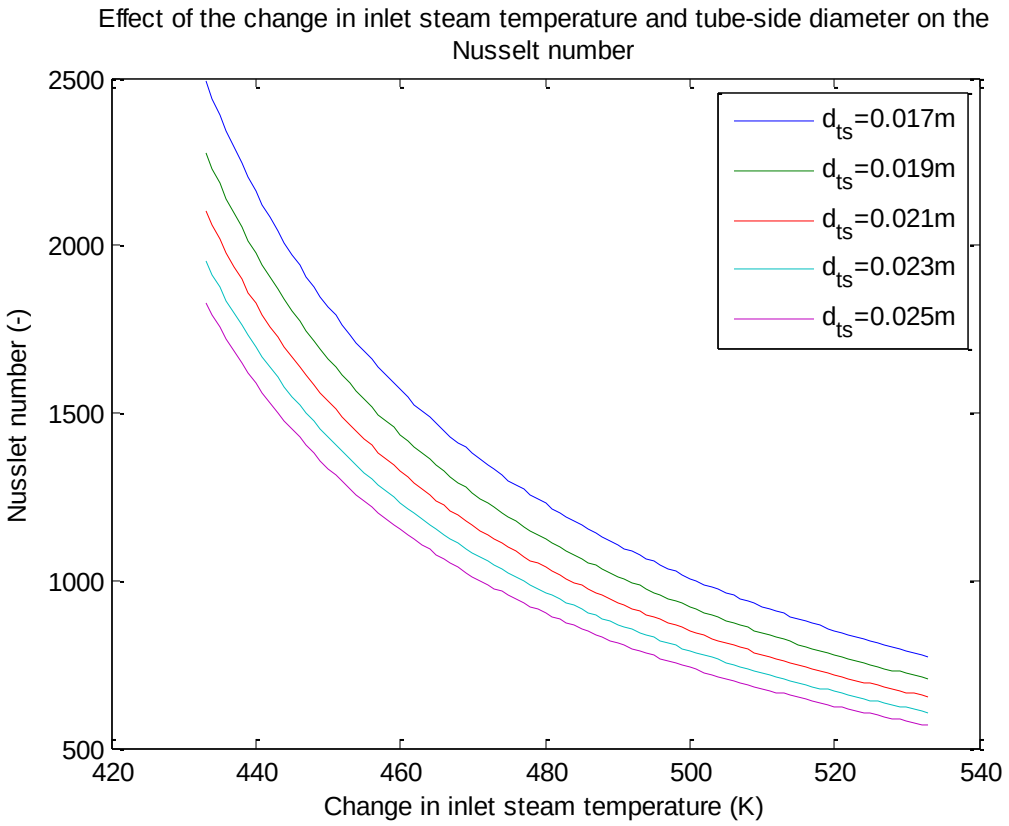

Figure 18: Effect of the change in inlet steam temperature and tube-side diameter on the Nusselt number

The decrease in Nusselt number seen at lower mass flow rates and smaller tube diameters increases, decreases the effective heat which in turn increases the overall heat transfer coefficient due to its inverse correlation as seen in Figure 19.

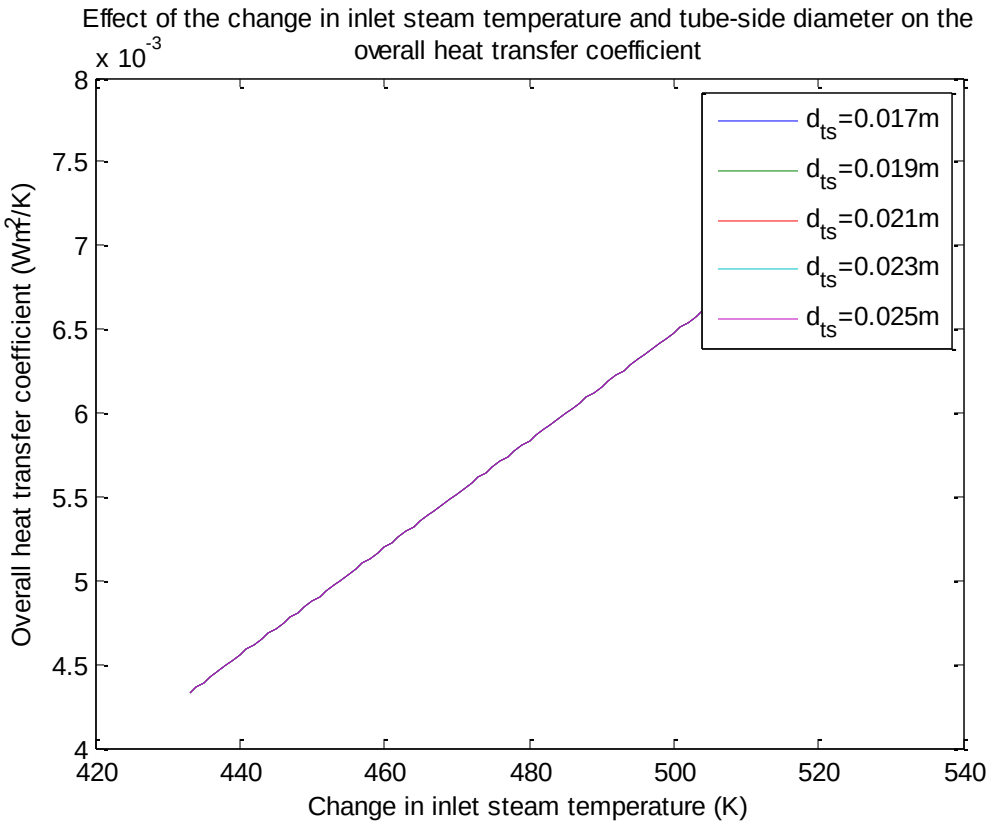

Figure 19: Effect of the change in inlet steam temperature and tube-side diameter on the overall heat transfer coefficient

This exercise was repeated with all 27 heat exchangers to ensure that the same trend holds for all the heat exchangers in the sample group (As seen in Figure 20). Due to the number of heat exchangers under investigation, the various heat exchangers were colour coded to improve readability:

- Tube-fin - Red
- Tube-in-tube - Green
- Shell-and-tube - Blue

All of the heat exchangers' entropy decreased as less mass flow rate was required due to the increased steam temperature as long as the dominant entropy generation mechanism was heat transfer. At higher temperatures some of the heat exchangers started exhibiting an increase in entropy generation due to entropy generation due to heat transfer becoming more dominant.

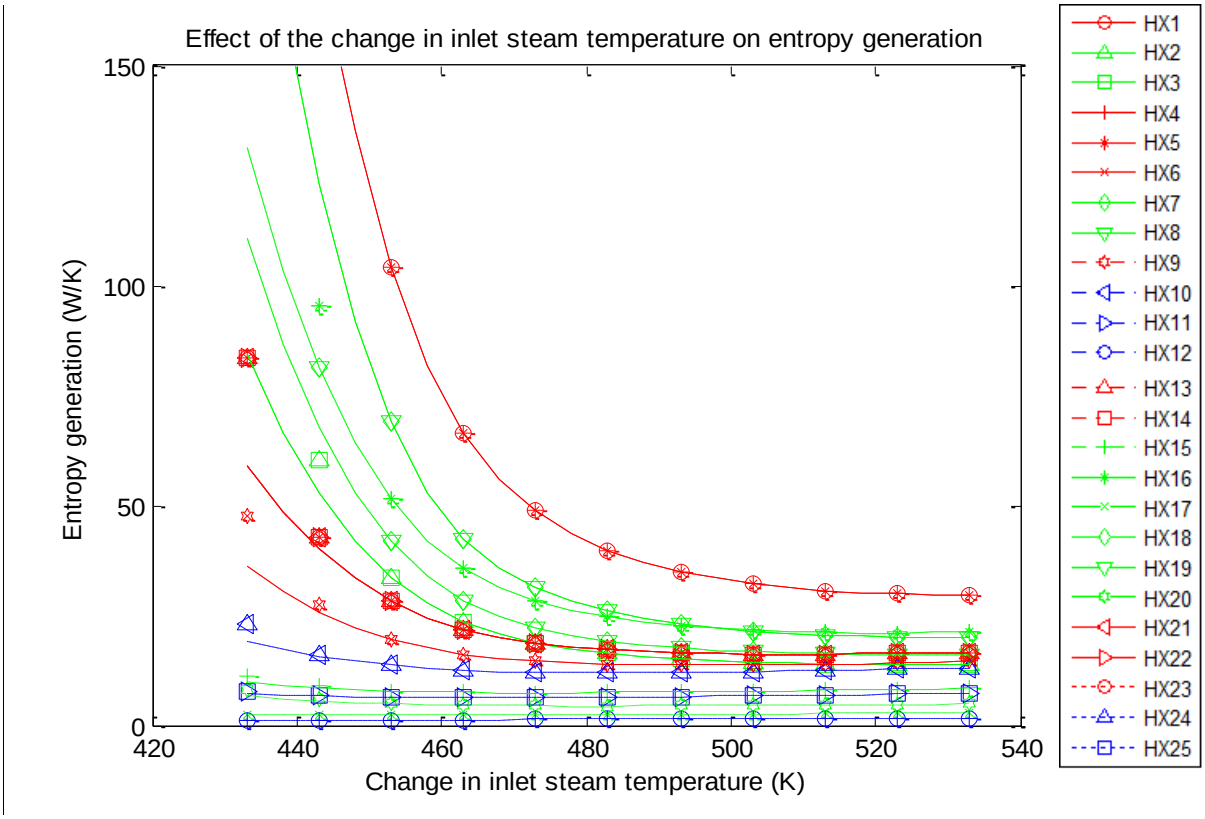

Figure 20: The effect of various tube-fin, tube-in-tube and shell-and-tube heat exchangers with varying mass flow rates on entropy generation

6.5. Use of constructal design in predicting minimum entropy generation

The tube-side diameter was changed to obtain values that affected the entropy generation due to fluid friction as well as heat transfer independently. The purpose of this section is to determine whether the different contributing mechanisms of entropy generation can be used independently to calculate a reasonably accurate global minimum entropy generation.

The diameter was reduced by 10% and increased by 50% from the design values and the results can be seen in Figure 21 to Figure 23. The three heat exchangers used are heat exchangers 6, 25 and 27 (for tube-in-fin, shell-in-tube and tube-in-fin heat exchangers).

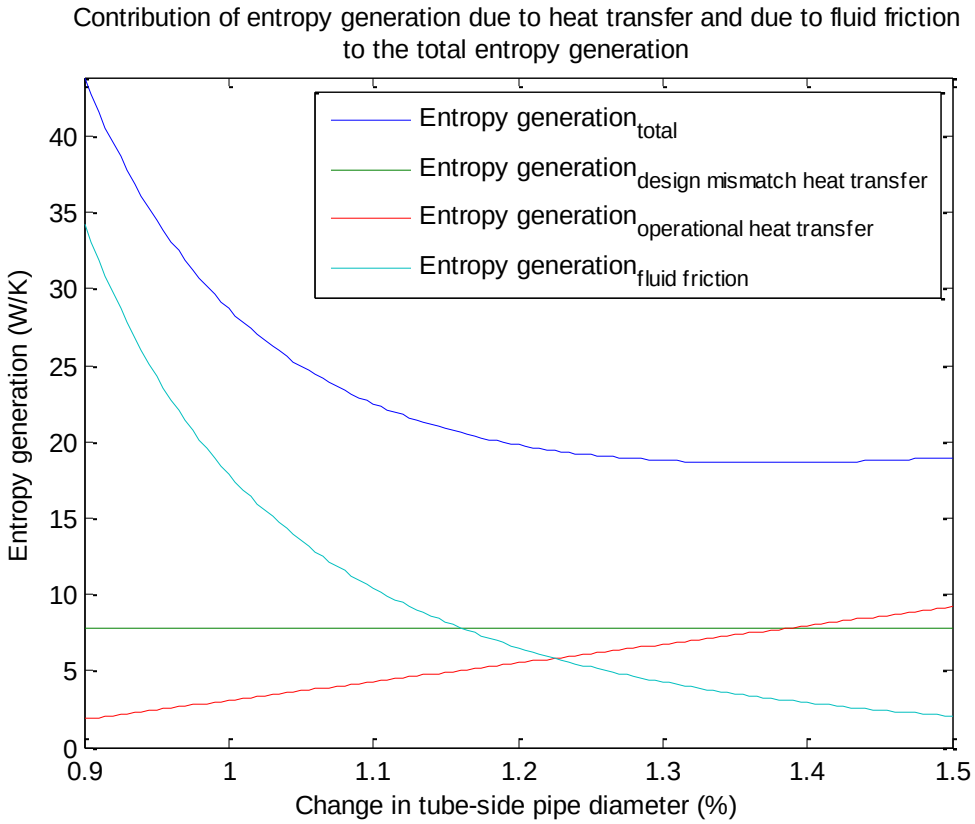

Figure 21: Contribution of entropy due to heat transfer and due to fluid friction to the total entropy generation relative to the tube side diameter in a plate-tube heat exchanger

In this case it is clear that the entropy generation due to design mismatch contributes to a sizable amount of the total entropy generation due to heat transfer. It remains constant throughout the change in tube-side diameter.

There is a definite correlation between the minimum entropy generation and the intercept between the operational heat transfer and the entropy generated between friction. The absolute minimum was found at 18.623 W/K whereas the total entropy generation at the intercept between the operational heat transfer entropy generation and entropy generation due to friction was found at 19.143 W/K. This is a deviation of 2.71 % and can thus be seen as reasonably accurate.

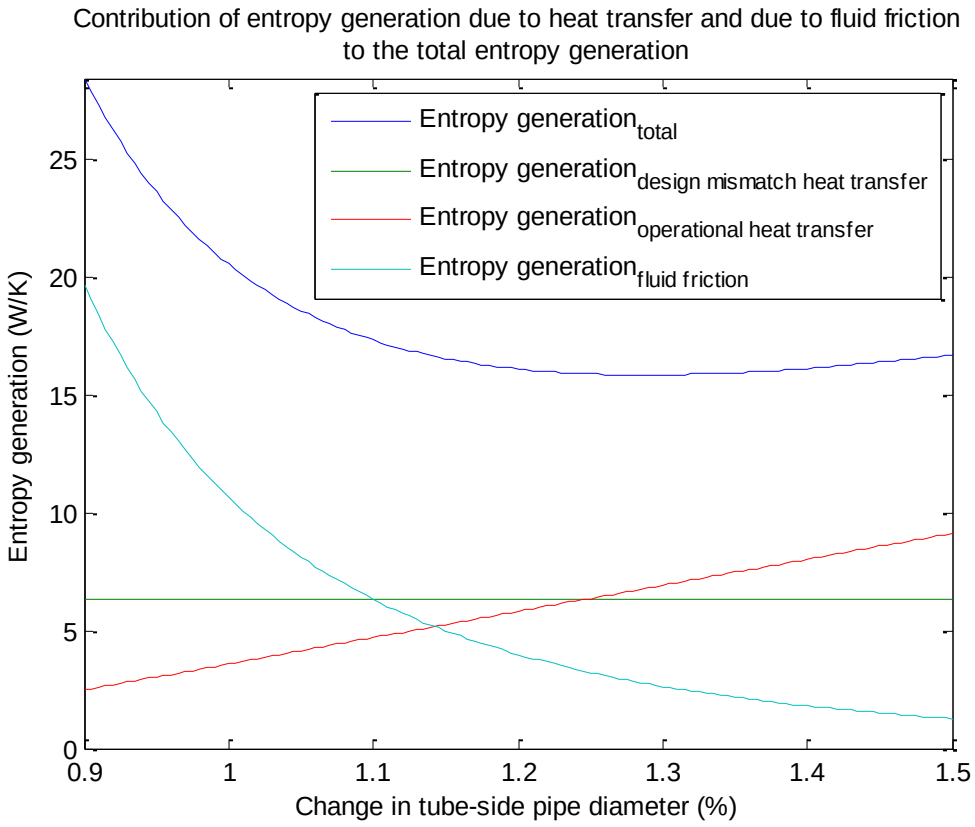

Figure 22: Contribution of entropy due to heat transfer and due to fluid friction to the total entropy generation relative to the tube side diameter in a tube-fin heat exchanger

In Figure 22 one can once again see the effect of entropy generation due to its contributing parts. We can also note that the intercept of the entropy generation due to operational heat

transfer and entropy generation due to fluid friction occurs quite close to one another. At the intercept the total entropy generation is 17.931 W/K whereas the absolute minimum obtained is 17.822 W/K, which is less than 1% deviation.

Similarly, Figure 23 shows that the absolute minimum entropy generation occurs reasonably close to the limit of the graph (8.506 W/K compared to 8.524 W/K).

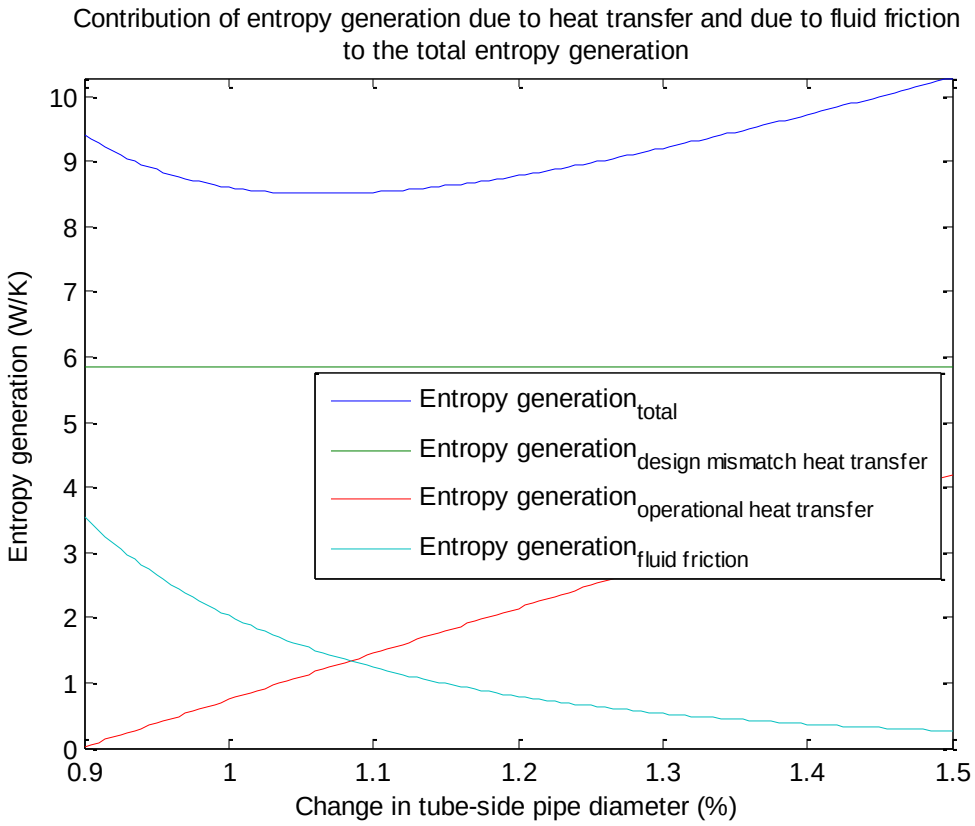

Figure 23: Contribution of entropy due to heat transfer and due to fluid friction to the total entropy generation relative to the tube side diameter in a shell-and-tube heat exchanger

Figure 21 to Figure 23 shows that the intercept of the entropy generation due to operational heat transfer and entropy generation due to fluid friction lines are a very good approximation of the global minimum of a heat exchanger.

The same exercise was repeated for all heat exchangers in the study and the results are tabulated in Table 8. For the given heat exchangers the maximum deviation using this method was 21.88 % and the average deviation for the set of heat exchangers are 6.52 %.

These correlations were used together with equation 4.55 and 4.56, to predict a tube-side diameter. As we can see in Figure 21 to Figure 23, the minimum usually occurs just to the right of where the intercept occurs. We can thus obtain the optimal tube-side diameter by multiplying the diameter obtained with 1.15. These results of the predicted optimal and actual optimal diameters as well as entropy generation can be seen on the next page.

Table 8: Summary of absolute entropy generation minimum and entropy generation intercept

Summary of Optimisation									
HX	Entropy Generated (J/kgK)				Entropy Deviation (%)		Diameter (m)		
	Normal	Minimum	Intercept	Model	Intercept	Model	Minimum	Intercept	Model
1	105.05	35.84	37.37	35.94	4.26%	0.29%	0.030	0.028	0.032
2	31.50	17.29	18.91	17.31	9.38%	0.14%	0.028	0.024	0.028
3	31.50	17.29	18.91	17.31	9.38%	0.14%	0.028	0.024	0.028
4	9.21	9.21	9.54	9.22	3.64%	0.12%	0.020	0.018	0.021
5	105.05	35.84	37.37	35.94	4.26%	0.29%	0.030	0.028	0.032
6	20.52	15.83	16.53	15.84	4.38%	0.07%	0.026	0.023	0.026
7	67.60	27.20	30.46	27.35	11.96%	0.52%	0.030	0.025	0.029
8	67.60	27.20	30.46	27.35	11.96%	0.52%	0.030	0.025	0.029
9	20.52	15.83	16.53	15.84	4.38%	0.07%	0.026	0.023	0.026
10	21.71	17.82	17.93	17.83	0.61%	0.06%	0.025	0.024	0.028
11	8.60	8.51	8.52	8.51	0.21%	0.04%	0.021	0.022	0.025
12	1.45	1.31	1.38	1.32	5.19%	0.91%	0.018	0.019	0.022
13	28.71	18.62	19.14	18.65	2.77%	0.17%	0.027	0.025	0.029
14	28.71	18.62	19.14	18.65	2.77%	0.17%	0.027	0.025	0.029
15	49.84	27.78	30.40	27.82	9.42%	0.14%	0.028	0.024	0.028
16	49.84	27.78	30.40	27.82	9.42%	0.14%	0.028	0.024	0.028
17	2.19	2.03	2.03	2.03	0.00%	0.00%	0.018	0.018	0.021
18	38.95	21.31	23.47	21.34	10.14%	0.15%	0.028	0.024	0.028
19	38.95	21.31	23.47	21.34	10.14%	0.15%	0.028	0.024	0.028
20	4.27	4.24	4.27	4.24	0.80%	0.07%	0.021	0.020	0.023
21	28.71	18.62	19.14	18.65	2.77%	0.17%	0.027	0.025	0.029
22	28.71	18.62	19.14	18.65	2.77%	0.17%	0.027	0.025	0.029
23	28.71	18.62	19.14	18.65	2.77%	0.17%	0.027	0.025	0.029
24	21.71	17.82	17.93	17.83	0.61%	0.06%	0.025	0.024	0.028
25	8.60	8.51	8.52	8.51	0.21%	0.04%	0.021	0.022	0.025
26	1.45	1.31	1.38	1.32	5.19%	0.91%	0.018	0.019	0.022
27	28.71	18.62	19.14	18.65	2.77%	0.17%	0.027	0.025	0.029
					4.90%	0.22%			

As can be seen, solving the diameter implicitly from equation 4.55 and 4.56, and multiplying it with a factor of 1.15 we obtain values very close (Within 1%) to the global minimum entropy generation. All the graphs used for the results tabulated in Table 8 can be seen in the Appendix section to the report in Figure 36 to Figure 40.

6.6. Optimisation

In Figure 24 one can see the improvement in heat exchanger efficiencies by applying principles of entropy generation minimisation, and using the values derived in Section 6.5 and summarized in Table 8.

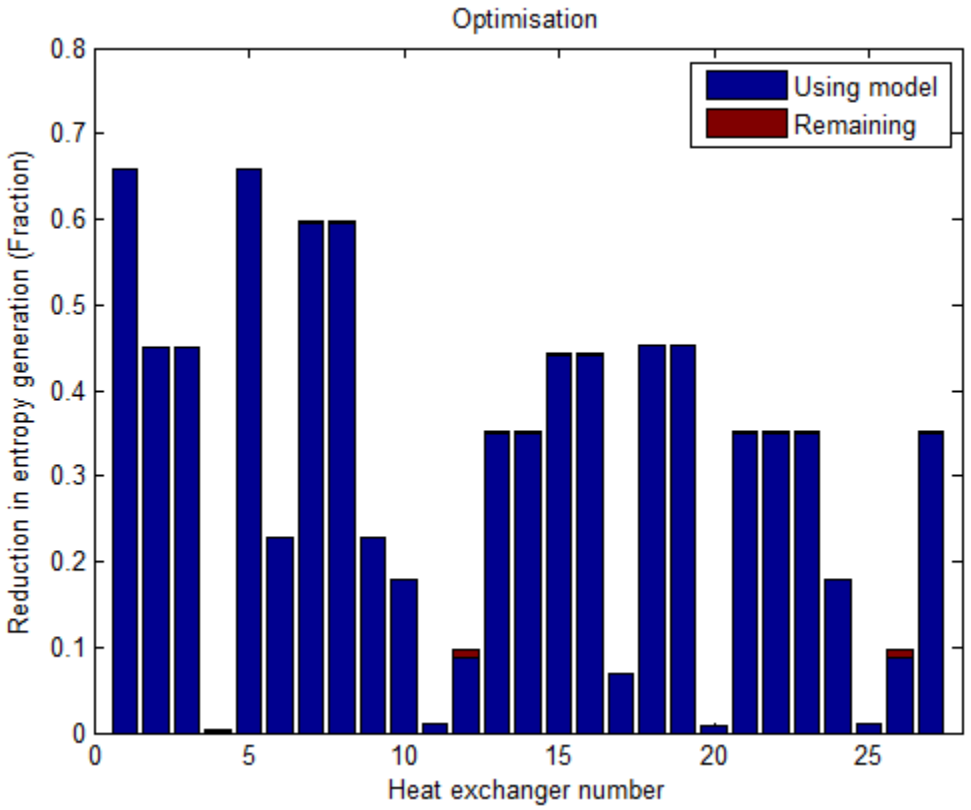

Figure 24: Optimisation

The heat exchangers in this sample set that could be optimised the most are the tube-fin heat exchangers. The shell-in-tube heat exchangers were optimised the least. All heat exchangers could be optimised using principles of entropy generation minimisation, with the optimisation ranging from 2% up to 64%. We can also see that the model created can be used to optimise the process, by resulting in the vast majority of reduction in entropy generation.

Chapter 7:

Conclusion

It was found that the main contributing factors that affected entropy generation in the set of heat exchangers were steam inlet temperature and secondly, tube-side diameter.

It was concluded that the intercept between the entropy generated due to fluid friction and operational heat transfer is good approximation of the minimum global entropy generated. The deviations between the intercept values and the global minimum ranged between 0.21 % and 21 % with an average deviation of 6.52%. Although the maximum values seem high it is very low compared to the maximums that is obtainable and as such can be considered to be good enough for a reasonable approximation.

It was seen that an increased inlet temperature resulted in most cases in less entropy generated for all the heat exchangers.

The majority of heat entropy was generated due to fluid friction, and the remainder was almost all due to the tube-side (steam) pressure drop, and lastly due to the shell-side (medium) pressure drop.

By using the principles of entropy generation minimization the entropy generated of each heat exchanger could be reduced by between 2% and 64%, with the tube-fin heat exchangers having the largest scope for improvement in the sample set used.

A model was also successfully derived for which the tube-side diameter could be solved implicitly. By adding a factor of 1.15 we could obtain a diameter that would result in entropy generation within 1% of the global minimum entropy generation.

Appendix A:

References

1. Gladyshev, G. P., *The second law of thermodynamics and the evolution of living systems*, Retrieved October 2, 2011, from Human Thermodynamics: http://www.humanthermodynamics.com/jht/second-law-systems-evolution.html.

2. Peyman, J., *Introduction to Heat Exchanger*, Retrieved August 6, 2013, from : Scope We: A Virtual Engineer, http://scopewe.com/introduction-to-heat-exchangers/.

3. Alibaba., *Toplife energy recource technology*, Retrieved August 6, 2013, from Alibaba: http://gzgele.en.alibaba.com/product/629439546-212250378/Aluminium_font_b_Tube-in-tube_b_font_Heat_Exchanger_Reycle_font_b_Core_b_font_.html.

4. Koen, B., *Heat Exchanger*, Retrieved August 6, 2013, from : The Full, http://www.thefullwiki.org/Heat_exchanger.

5. Truesdell, C. A., *The tragicomical history of thermodynamics* (1980), pp. 1822-1854, New York.

6. Clausius, R., *The mechanical theory of heat*, The mechanical theory of heat - with it's application to the steam engine and physical properties of bodies (1867) , pp. 353-400, London.

7. Cengel, Y. A., *Heat Transfer,* In Y. A. Cengel, A practical approach (2 ed.) (2005), pp. 667-716, McGraw-Hill.

8. Adetunji, O. (2009). *Introduction*. In O. Adetunji, Production Engineering (pp. 1-12). Pretoria: University of Pretoria.

9. International Organization for Standarization. (2010). ISO 9001 top one million mark.

10. BSI. (2012). *History of BSI group*. Retrieved October 3, 2012, from BSI: www.bsieducation.org/education.

11. Atkins, P. W. (1984). *The second law,* New York: Scientific American Library.

12 Bejan, A., Shape and structure in science and nature, *Natural form, questioning and theory,* Press syndicate of the University of Cambridge (2001), *pp. 1-11*,

13. Bejan, A., *Method of entropy generation minimisation, or modelling and optimisation based on combined heat transfer and thermodynamics*, Dept of Mechanical Engineering, Duke University, Durham, North Carolina 27708-0300, USA, Rev Ge'n Therm (1996) 35, pp. 637-646, Elsevier, Paris.

14. Chen, S., Liu, Z., Bao, S., Zheng, C., *Natural convection and entropy generation in a vertically concentric annular space*, International Journal of Thermal Sciences 49 (2010), pp. 2439-2452.

15. Kaluri, R., Basak, T., *Entropy generation due to natural convection in discretely heated porous square cavities*, Energy 36 (2011), pp. 5065-5080.

16. Caldas, M., Semiao, V., *Entropy generation through radiative transfer in participating media: analysis and numerical computation*, Journal of Quantitative Spectroscopy and Radiative Transfer 96 (2005), pp. 423–437.

17. Caldas, M., Viriato, S., *The effect of turbulence–radiation interaction on radiative entropy generation and heat transfer*, Journal of Quantitative Spectroscopy and Radiative Transfer 104 (2007), pp. 12–23.

18. Allouache, N., Chikh, S., Entropy *Generation in a Partly Porous Heat Exchanger*, European Symposium on Computer-Aided Process Engineering (2004) 14, pp. 139-144, Elsevier B.V.

19. Arivazhagan, M., Lokeswaran, S., *Entropy Generation Minimization of Shell-and-Tube Heat Exchanger with Porous Medium*, Experimental Techniques (2011), 1, pp. 1-9.

20. Guo, J., Cheng, L., Xu, M., *Optimization design of shell-and-tube heat exchanger by entropy generation minimization and genetic algorithm*, Applied Thermal Engineering 29 (2009) pp. 2954–2960.

21. Jankowski, T. A., *Minimizing entropy generation in internal flows by adjusting the shape of the cross-section*, International Journal of Heat and Mass Transfer 52 (2009), pp. 3439–3445.

22. Lerou, P., Veenstra, T.T., Burger, J.F., ter Brake, H.J.M., Rogalla, H., *Optimization of counterflow heat exchanger geometry through minimization of entropy generation*, Cryogenics 45 (2005), pp. 659–669.

23 Ogulata, R. T., Doba, F., *Experiments and entropy generation minimization analysis of a cross-flow heat*, International Journal of Heat Mass Transfer. Vol. 41, No. 2, pp. 373381, 1998.

24 Maheshkumar, P, Muraleedharan, C., *Minimization of entropy generation in flat heat pipe*, International Journal of Heat and Mass Transfer 54 (2011), pp. 645–648.

25 Silva, R.L., Garcia, E.C., *Temperature and entropy generation behaviour in rectangular ducts with 3-D heat transfer coupling (conduction and convection)*, International Communications in Heat and Mass Transfer 35 (2008), pp. 240–250.

26 Revellin, R., Lips, S., Khandekar, S., Bonjour, J., *Local entropy generation for saturated two-phase flow*, Energy 34 (2009), pp. 1113–1121.

27 Sahina, A.Z., Zubaira, Ahmed, S.M., Kahramanb, R., *Effect of fouling on operational cost in pipe flow due to entropy generation*, Energy Conversion & Management 41 (2000), pp. 1485-1496.

28 Sahiti, N., Krasniqi, F., Fejzullahu, X., Bunjaku, J., Muriqi, A., *Entropy generation minimization of a double-pipe pin fin heat exchanger*, Applied Thermal Engineering 28 (2008) 2337–2344.

29 Zimparov, V.D., da Silva, A.K., Bejan, A., *Constructal tree shape parallel flow heat exchangers, International journal of heat and mass transfer*, Volume 49, Issues 23-24, November 2006, pp. 4558-4566.

30 Raja, V., Basak, T., Das, S., *Thermal performance of a multi-block heat exchanger designed on the basis of Bejan's constructal theory*, International Journal of Heat and Mass Transfer 51 (2008), pp. 3582–3594.

31 Bello-Ochende, T., Olakoyejo, O.T., Meyer, J.P., Bejan, A., Lorente, S., Constructal flow orientation in conjugate cooling channels with internal heat generation, International Journal of Heat and Mass Transfer 57 (2013), pp. 241–249.

32 Olakoyejo, O.T., Bello-Ochende, T., Meyer, J.P., *Constructal conjugate cooling channels with internal heat generation*, International Journal of Heat and Mass Transfer 55 (2012), pp. 4385–4396.

33 Kim, Y., Lorente, S., Bejan, A., *Constructal multi-tube configuration for natural and forced convection in cross-flow*, International Journal of Heat and Mass Transfer 53 (2010), pp. 5121-5128.

34 Lorenzini, G., Alberto, L., Rocha, O., *Constructal design of T–Y assembly of fins for an optimized heat removal*, International Journal of Heat and Mass Transfer 52 (2009), pp. 1458-1463.

35 Amani, E., Nobari, M.R.H., *A numerical investigation of entropy generation in the entrance region of curved pipes at constant wall temperature*, Energy 36 (2011), pp. 4909-4918.

36 Luo, L., Fan, Y., Zhang, W., Yuan, X., Midoux, N., *Integration of constructal distributors to a mini cross-flow heat exchanger and their assembly configuration optimisation*, Chemical engineering science, Volume 62, Issue 13, July 2007, pp. 3205-3619.

37 Chen, L., Xie, Z., Sun, F., *Multiobjective constructal optimization of an insulating wall combining heat flow, strength and weight*, International Journal of Thermal Sciences 50 (2011), 1782-1789.

38 Vahdat, A., Amidpour, M., *Economic optimisation of shell-and-tube heat exchanger based on constructal theory* , Energy, Volume 36, Issue 2, February 2011, pp. 1087-1096.

39 Bello-Ochende, T.B., *Maximum flow access in heat exchangers, heat generating bodies and inanimate flow systems: Constructal law and the emergence of shapes and structures in thermo-fluid mechanics comment on "The emergence of design in pedestrian dynamics: Locomotion, self-organization, walking paths and constructal law" by Antonio F. Miguel*, Physics of Life Reviews 10 (2013), pp. 191–192.

40 Faizal, M., Ahmed, M.R., *Experimental studies on a corrugated plate heat exchanger for small temperature difference applications*, Experimental Thermal and Fluid Science 36 (2012), pp. 242–248.

41 Perry's Chemical Engineering Handbook (7 ed.), *Chapter 4 – Thermodynamics*, pp. 508-542, McGraw-Hill.

42 Greef, Z., Skinner, W., Practical application of energy balance in piping systems in piping system design (1 ed.) (2000), pp. 24-38, University of Pretoria.

Appendix B:

Nomenclature

Latin symbols

A	Area	m^2
C	Heat capacity	*W/K*
C_p	Specific heat capacity	*W/kgK*
D	Diameter	-
f'	Friction factor	-
h	Convection heat transfer coefficient	*W/K*
hx	Heat exchanger	-
k	Conduction heat transfer coefficient	*W/mK*
L	Length	*m*
m	Mass flow rate	*kg/s*
n	Number of tubes	-

Nu	Nusselt number	-
P	Pressure	Pa
Pr	Prandtl number	-
Q	Heat transfer	*W*
R	Resistance	K/Wm^2
R	Gas constant	*J/kgK*
Re	Reynolds number	-
S	Entropy	*W/K*
T	Temperature	*K*
U	Overall heat transfer coefficient	Wm^2/K
U	Work done	*W*
V	Volume	m^3
v	Speed	*m/s*

Greek symbols

β	Volume change factor	(-)
Δ	Change	(-)
μ	Viscosity	*kgm/s*
Σ	Summation	-
ε	Effectiveness	-
ε_{tubes}	Roughness of tubes	-

ρ	Density	kg/m^3

Subscripts

c	Cold fluid/surface
eff	Effective
gen	Generated
h	Hot fluid/surface
HT	Heat transfer
i	In
o	Out

Appendix C:

Matlab code

```
% Marnus Koorts
% M. Eng (Mechanical Engineering)
% Entropy Generation Minimisation
% 2013

function normal

clc
clear all

%Nomenclature
    %Tf     = Film Temperature (oC)
    %s      = Steam
    %m      = Medium (Acid, Water, Alkali, Air)
    %h      = Hot
    %c      = Cold
    %ind    = Indicator
    %p      = Pressure (kPa)
    %v      = Viscosity (m2/s)
    %V      = Volumetric Speed (m3/s)
    %Vv     = Speed (m/s)
    %Pr     = Prandtl Number (Pr)
    %S      = Entropy Generation (W)
    %C      = Heat Capacity (W/K)
    %f      = Friction Factor (-)
    %CR     = Capacity Ratio (-)
    %R      = Universal Gas Constant (J/kgK)
    %Nu     = Nusselt Number (-)
    %Re     = Reynolds Number (-)
    %Eff    = Effectiveness (1-E)
```

```
%Loading Data
load Cp
load Input
load MolarMass
load p
load Pr
load v
load k
load Validation_lit

%Pre allocation
        Sgen_temp_tot = zeros(1, 27)                    ;
        Sgen_fric_s   = zeros(1, 27)                    ;
        Sgen_fric_m   = zeros(1, 27)                    ;
        Sgen_tot      = zeros(1, 27)                    ;
        Xfact_s       = zeros(1,27)                     ;
        Xfact_m       = zeros(1,27)                     ;


for n = 1:27;
%General Constants
    %Input Variables
        Ms          =Input(n,8)                         ;
        Mm          =Input(n,9)                         ;
        Ts_i        =Input(n,10)                        ;
        Ts_o        =Input(n,11)                        ;
        Tm_i        =Input(n,12)                        ;
        Tm_o        =Input(n,13)                        ;
        Tf_s        =(Ts_i+Ts_o)/2-273                  ;
        Tf_m        =(Tm_i+Tm_o)/2-273                  ;
        Pss         =Input(n,14)                        ;
        Pts         =Input(n,15)                        ;
        Dss         =Input(n,3)                         ;
        Dts         =Input(n,28)                        ;

    %Dimensional Constants
        t           =0.002                              ;
        nr          =Input(n,21)                        ;
        L           =Input(n,4)                         ;
        Etubes      =0.046/1000                         ;

   %Lookup table indicators
        Tf_s_ind    =round(Tf_s)                        ;
        Tf_m_ind    =round(Tf_m)                        ;
        Ti_m_ind    =round(Tm_i-273)                    ;
        To_m_ind    =round(Tm_o-273)                    ;

    %Temperature dependant variables
        ps_f        =p(Tf_s_ind,3)                      ;
        pm_f        =p(Tf_m_ind,Input(n,17))            ;
        k_s         =k(Tf_s_ind,3)                      ;
        k_m         =k(Tf_m_ind,Input(n,17))            ;
        k_t         =k(Tf_s_ind,19)                     ;
        v_s         =v(Tf_s_ind,3)                      ;
```

```
        v_m         =v(Tf_m_ind,Input(n,17))            ;
        Pr_s        =Pr(Tf_s_ind,3)                     ;
        Pr_m        =Pr(Tf_m_ind,Input(n,17))           ;
        Cp_s        =Cp(Tf_s_ind,3)*1000                ;
        Cp_m        =Cp(Tf_m_ind,Input(n,17))*1000      ;
        Ch          =Cp_s*Ms                            ;
        Cc          =Cp_m*Mm                            ;
        Cmin        =min(Ch,Cc)                         ;
        R           =461.5                              ;


    for xxx=1:3
    %Loop inserted to increase the accuracy
        Dts_eff     =sqrt(nr*(Dts/2)^2)*2               ;
        Leff        =L*nr                               ;

    %Flow Rates
        Va_s        =Ms/p(Tf_s_ind,3)                   ;
        Vi_m        =Mm/p(Ti_m_ind,Input(n,17))         ;
        Vo_m        =Mm/p(To_m_ind,Input(n,17))         ;
        Va_m        =Mm/p(Tf_m_ind,Input(n,17))         ;
        Vva_s       =Va_s/(pi*(Dts_eff/2)^2)            ;
        Vva_m       =Va_m/(pi()*(Dss/2)^2)              ;

    %Heat transfer
        Q_max       =Cmin*(Ts_i-Tm_i)                   ;
        Q_act       =Mm*Cp_m*(Tm_o-Tm_i)                ;
        UA          =Q_act/(Ts_i-Tm_i)                  ;
        Eff         =Q_act/Q_max                        ;
        Ts_o        =Ts_i-Q_act/(Ms*Cp_s)               ;

        Re_s        =Vva_s*ps_f*Dts*nr/v_s              ;
        Re_m        =Vva_m*pm_f*Dss/v_m                 ;
        if  Re_s    >4000
            Nu_s    =0.037*Re_s^0.8*Pr_s^(1/3)          ;
            Nu_m    =0.037*Re_m^0.8*Pr_m^(1/3)          ;
            f_s     =((-1.8*log((Etubes/Dts/3.7)^1.11+6.9/Re_s))^(-1))^2;
            f_m     =((-1.8*log((Etubes/Dts/3.7)^1.11+6.9/Re_m))^(-1))^2;
            else
            Nu_s    =0.664*Re_s^0.5*Pr_s^(1/3)          ;
            Nu_m    =0.664*Re_m^0.5*Pr_m^(1/3)          ;
            f_s     =64/Re_s                            ;
            f_m     =64/Re_m                            ;
        end
        h_s         =k_s*Nu_s/Dts                       ;
        h_m         =k_m*Nu_m/(Dts+2*t)                 ;
        R_i         =1/(h_s*2*pi()*(Dts/2)*Leff)        ;
        R_w         =log((Dts+2*t)/Dts)/(2*pi()*k_t*Leff);
        R_o         =1/(h_m*2*pi()*(Dts+2*t)/2*Leff)    ;
        U           =R_i+R_w+R_o                        ;
        nr
=UA*(1/(h_s*2*pi()*Dts/2*L)+log((Dts+2*t)/Dts)/(2*pi()*k_t*L)+1/(h_m*2*pi()*(
Dts+2*t)/2*L));
    end
```

```
%Entropy Generation due to heat transfer
        Sgen_temp_s     =Ch*log(Ts_o/Ts_i)              ;
        Sgen_temp_m     =Cc*log(Tm_o/Tm_i)              ;
        Sgen_temp_tot(n)=(Sgen_temp_s+Sgen_temp_m)      ;

%Entropy Generation due to fluid friction
        Pts_o               =Pts-f_s*L*nr*ps_f*Vva_s^2/(2*Dts_eff);
        Pss_o               =Pss-f_m*L*pm_f*Vva_m^2/(2*Dss);
        Sgen_fric_s(n)      =-R*Ms*log((Pts_o)/Pts)      ;
        if Input(n,17)<3
        Sgen_fric_m(n)      =-R*Mm*log((Pss_o)/Pss)      ;
        else
        Sgen_fric_m(n)      =Va_m*Mm*f_m*L*pm_f*Vva_m^2/(2*Dss*(Tf_m+273));

        end
        Sgen_fric_tot       =(Sgen_fric_s+Sgen_fric_m)   ;

%Total Entropy Generation due to fluid friction
        Sgen_tot(n)     =Sgen_temp_tot(n)+Sgen_fric_tot(n);
        Sgen_tot(imag(Sgen_tot) ~= 0) = NaN             ;


%Xfact
        Xfact_s(n)      =Ms*Cp_s*(Ts_i-Ts_o)            ;
        Xfact_m(n)      =Mm*Cp_m*(Tm_o-Tm_i)            ;

end
```

Appendix D:

Figures

D.1 Effect of steam temperature and tube diameter on a number of variables

In this section a brief overview is given on the effect of varying the inlet steam temperature and tube-side diameter (Figure 26 to Figure 31). Due to the number of figures per page, the legend below is given to allow for more space.

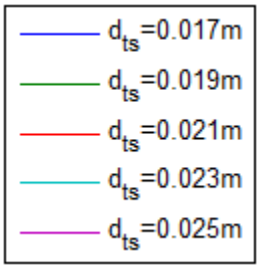

Figure 25: Legend

The section is split into three sections, section D.1.1. covers the effect of the abovementioned variables on tube-in-tube heat exchangers, section D.1.2. on tube-fin heat exchangers and section D.1.3. on shell-and-tube heat exchangers.

D.1.1 Tube-in-tube (Heat Exchanger 1)

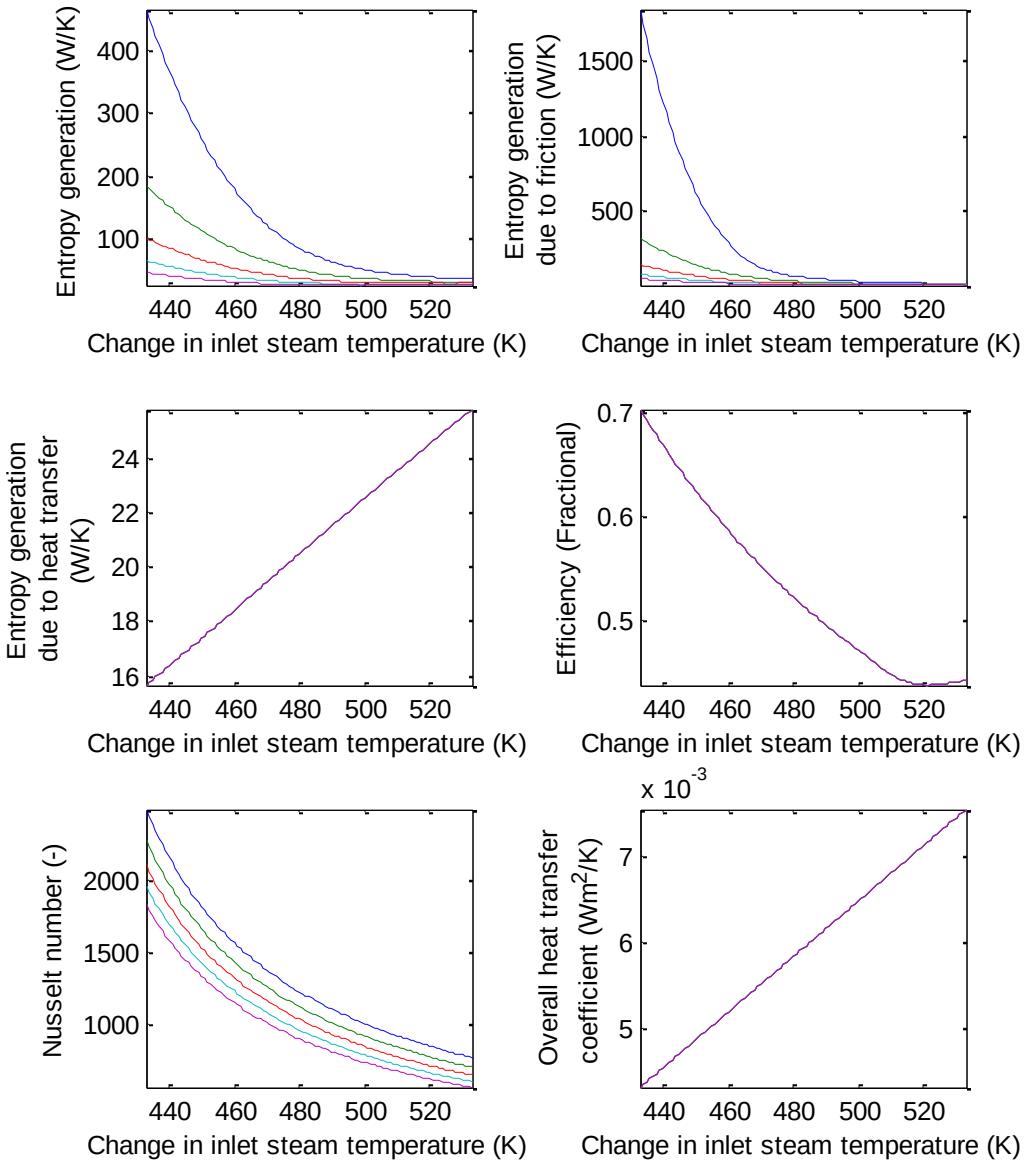

Figure 26: The effect of varying steam inlet temperatures and tube diameters on entropy, entropy generation due to friction, entropy generation due to heat transfer, efficiency, Nusselt number and the overall heat transfer coefficient for a tube-in-tube heat exchanger (Heat Exchanger 1)

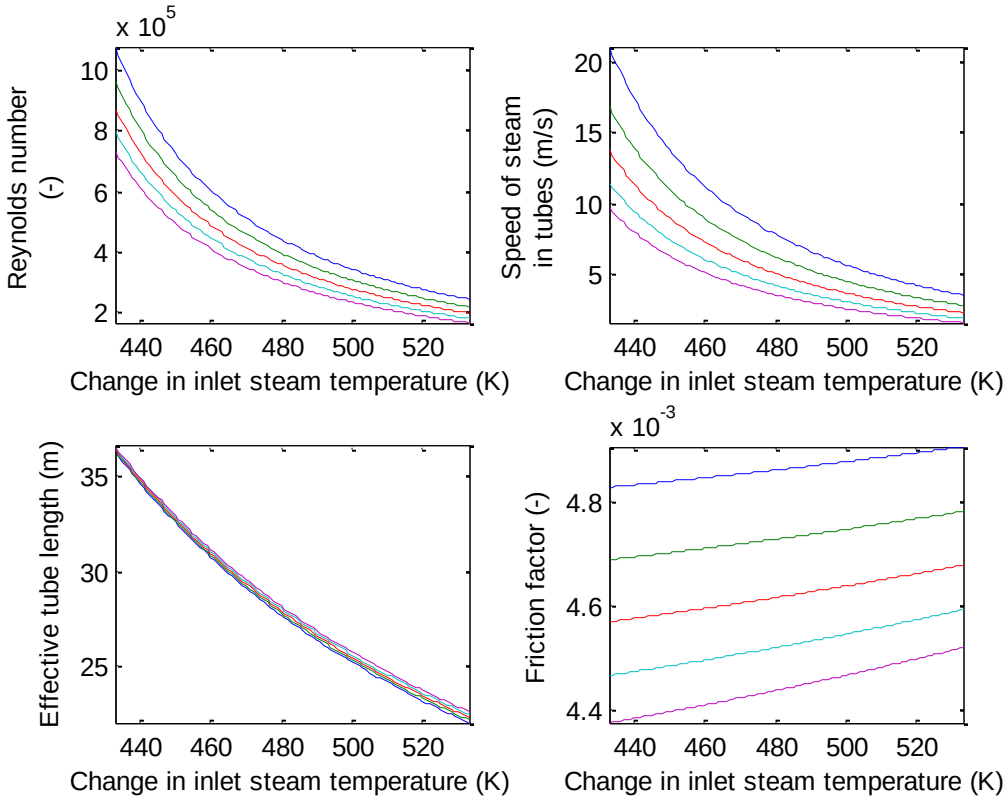

Figure 27: The effect of varying steam inlet temperatures and tube diameters on the Reynolds number, speed of steam, effective tube length and friction factor for a tube-in-tube heat exchanger (Heat Exchanger 1)

D.1.2 tube-fin (Heat Exchanger 2)

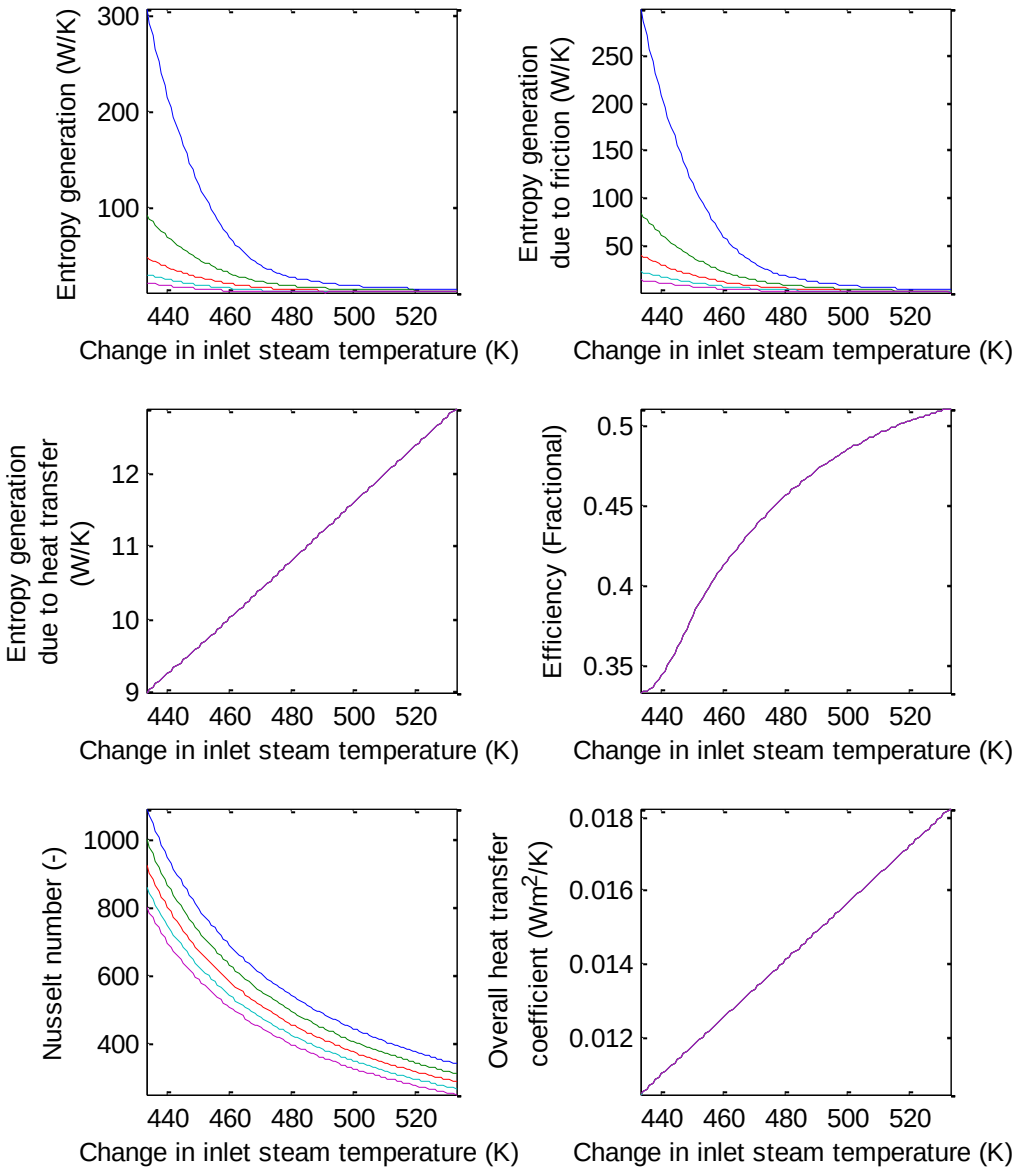

Figure 28: The effect of varying steam inlet temperatures and tube diameters on entropy, entropy generation due to friction, entropy generation due to heat transfer, efficiency, Nusselt number and the overall heat transfer coefficient for a tube-fin heat exchanger (Heat Exchanger 2)

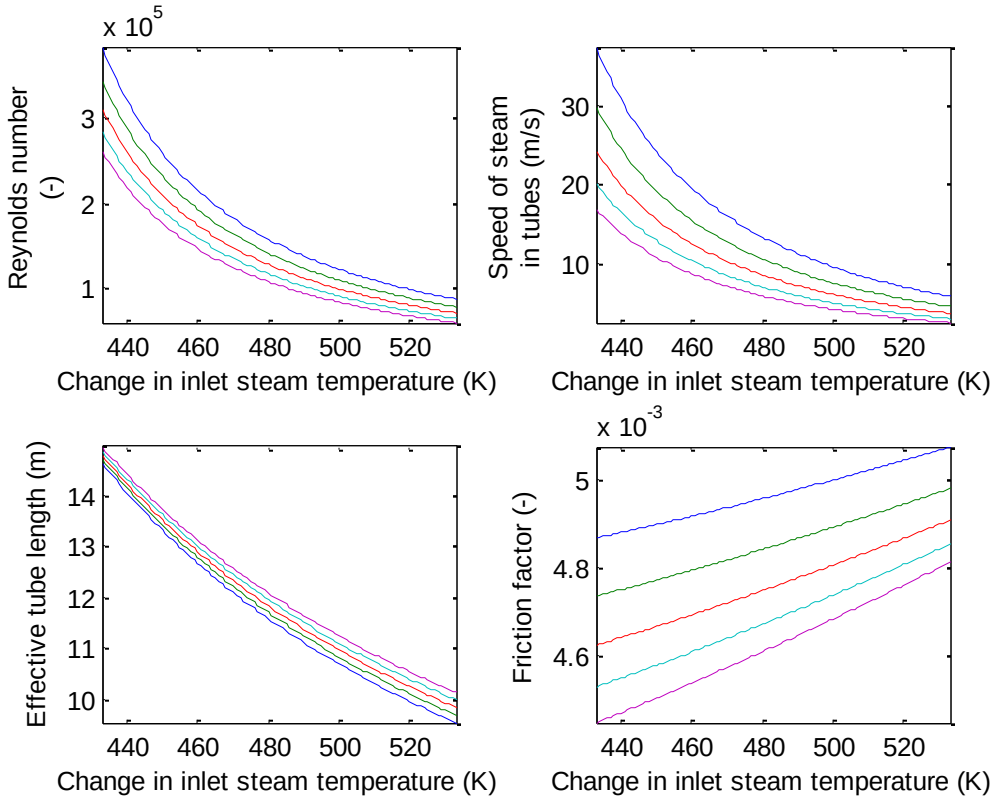

Figure 29: The effect of varying steam inlet temperatures and tube diameters on the Reynolds number, speed of steam, effective tube length and friction factor for a tube-fin heat exchanger (Heat Exchanger 2)

D.1.3 Shell-and-tube (Heat Exchanger 11)

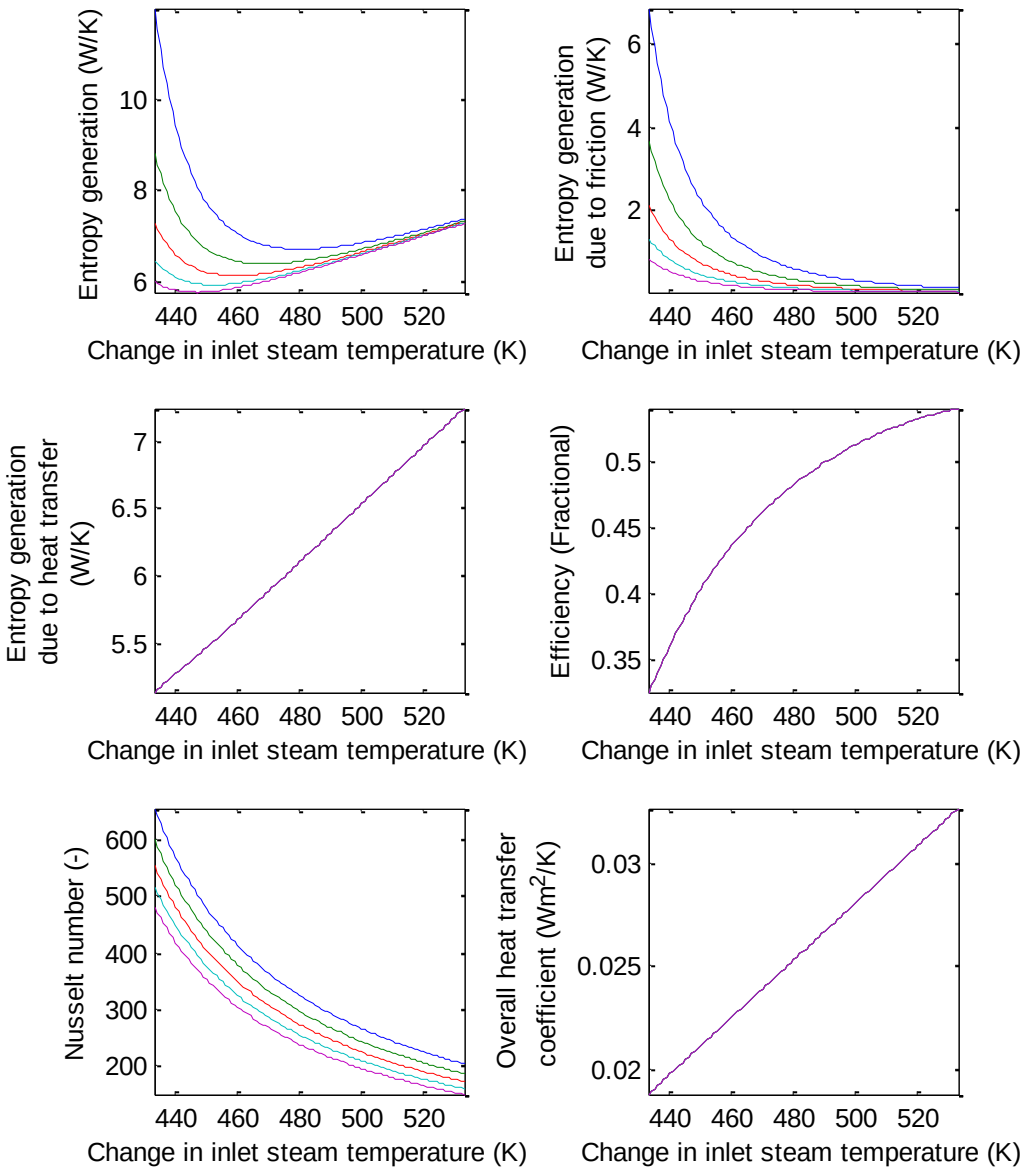

Figure 30: The effect of varying steam inlet temperatures and tube diameters on entropy, entropy generation due to friction, entropy generation due to heat transfer, efficiency, Nusselt number and the overall heat transfer coefficient for a hell-and-tube heat exchanger (Heat Exchanger 11)

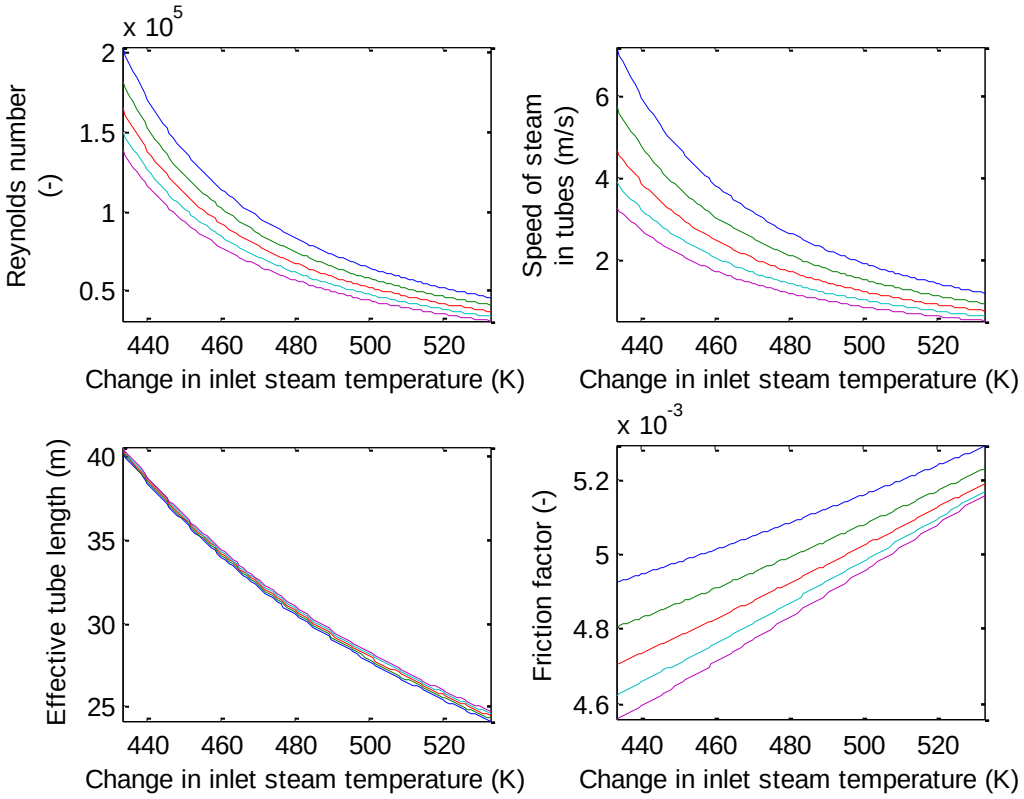

Figure 31: The effect of varying steam inlet temperatures and tube diameters on the Reynolds number, speed of steam, effective tube length and friction factor for a shell-and-tube heat exchanger (Heat Exchanger 11)

D.2Effect of all heat exchangers (HX1-27) on variables while varying mass flow rate

Figure 32 to Figure 33 show the effect of all the heat exchangers on a number of variables are modelled while varying the mass flow rate. All the data modelling this section use a 0.04 m tube-side diameter and only show information in the turbulent flow region (which is assumed to be at Reynolds numbers above 10000). Due to the large amount of data on each graph, the heat exchangers are colour coded as follows:

- Tube-fin - Red
- Tube-in-tube - Green
- Shell-and-tube - Blue

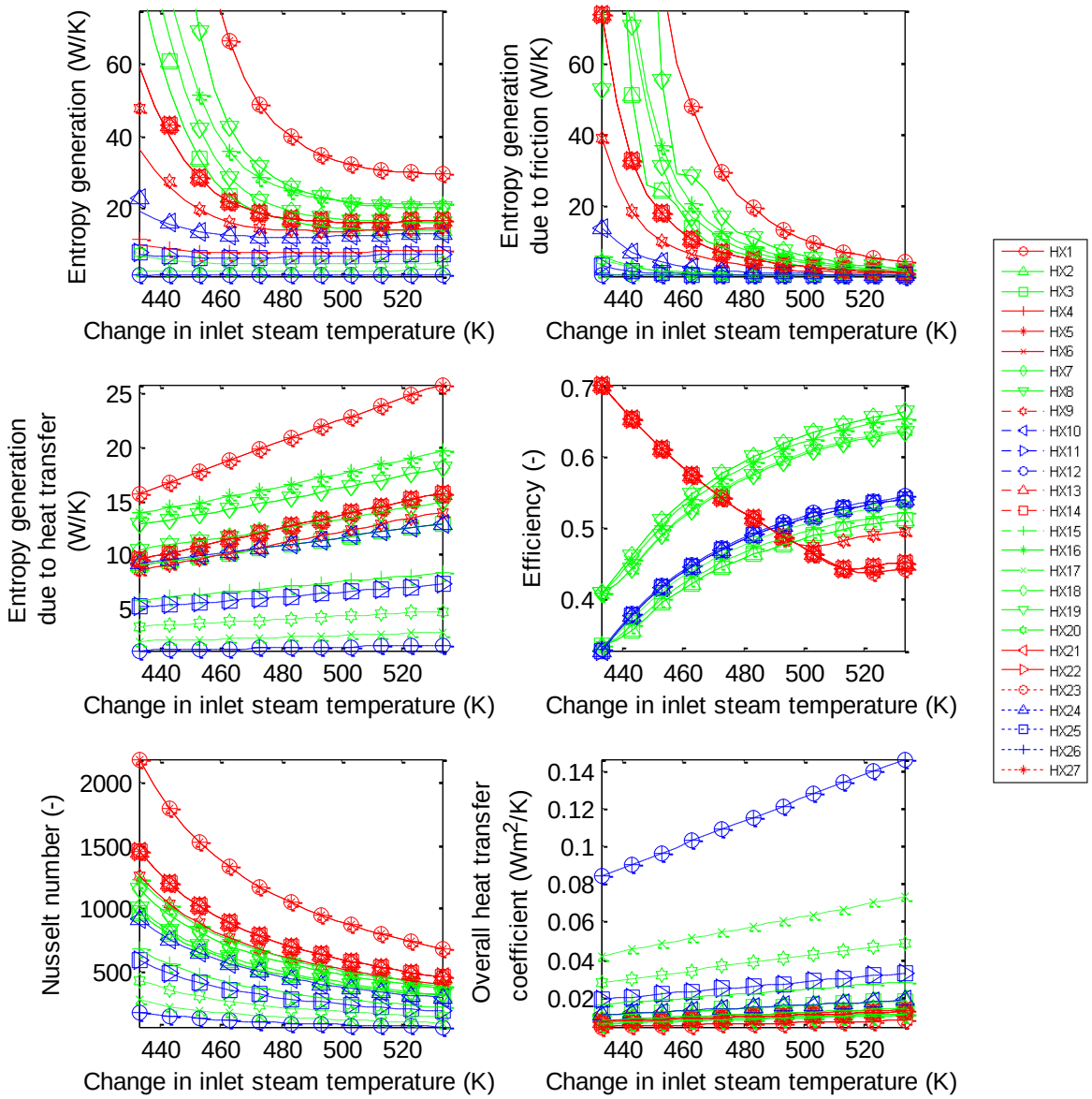

Figure 32: The effect of varying steam inlet temperatures on entropy, entropy generation due to friction, entropy generation due to heat transfer, efficiency, Nusselt number and the overall heat transfer coefficient for all the heat exchangers

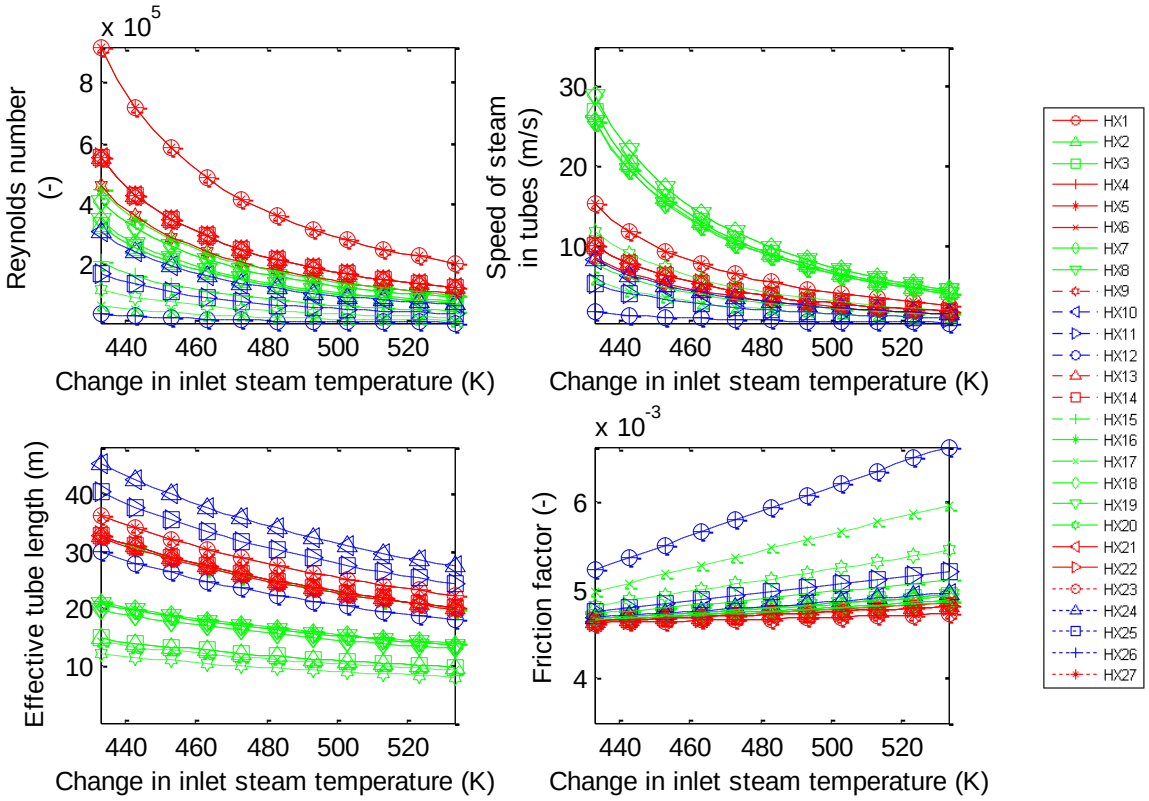

Figure 33: The effect of varying steam inlet temperatures on Reynolds number, speed of steam, effective tube length and friction factor for all the heat exchangers

D.3 Effect of only three heat exchangers

Due to the complexity of Figure 32 to Figure 33, one of each heat exchanger (1 tube-fin, 1 shell-and-tube and 1 tube-in-tube heat exchanger) with more or less similar specifications (+- 1000 kW, 0.04 m tube-side diameter, inlet steam temperature) is modelled against the other in order to see how differently they react to various variables in Figure 34 to Figure 35.

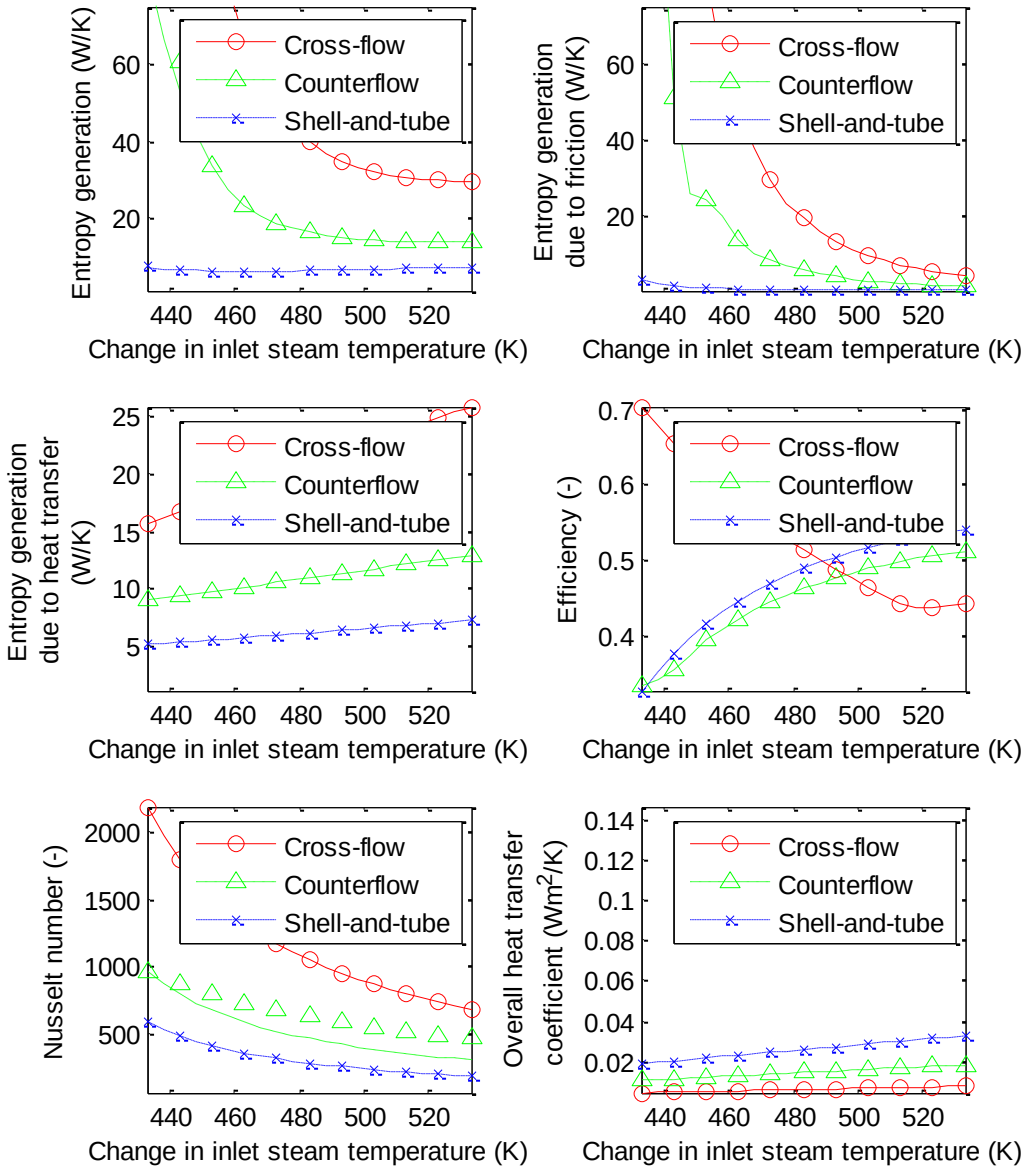

Figure 34: The effect of varying steam inlet temperatures for a tube-fin heat exchanger (Heat Exchanger 1), tube-in-tube heat exchanger (Heat Exchanger 5) and shell-and-tube heat exchanger (Heat Exchanger 11) on entropy generation, entropy generation due to friction, entropy generation due to heat transfer, efficiency, Nusselt number and the overall heat transfer coefficient for all the heat exchangers

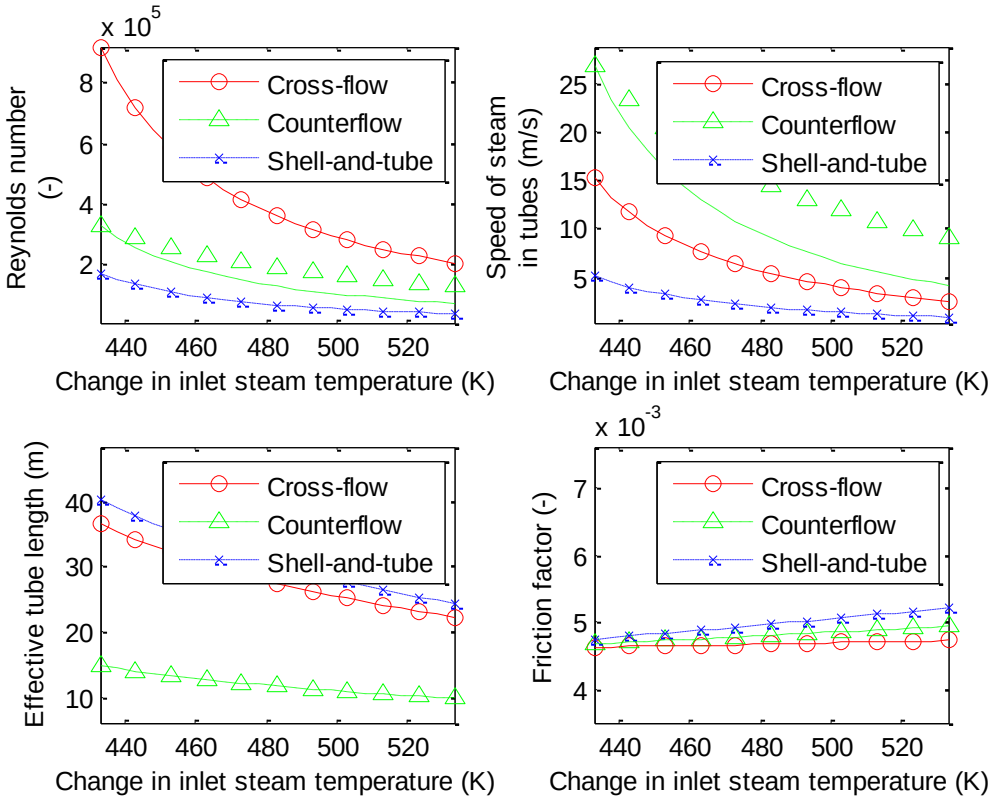

Figure 35: The effect of varying steam inlet temperatures for a tube-fin heat exchanger (Heat Exchanger 1), tube-in-tube heat exchanger (Heat Exchanger 5) and shell-and-tube heat exchanger (Heat Exchanger 11) on Reynolds number, speed of steam, effective tube length and friction factor for all the heat exchangers

D.4 Effect fluid friction and heat transfer on entropy generation

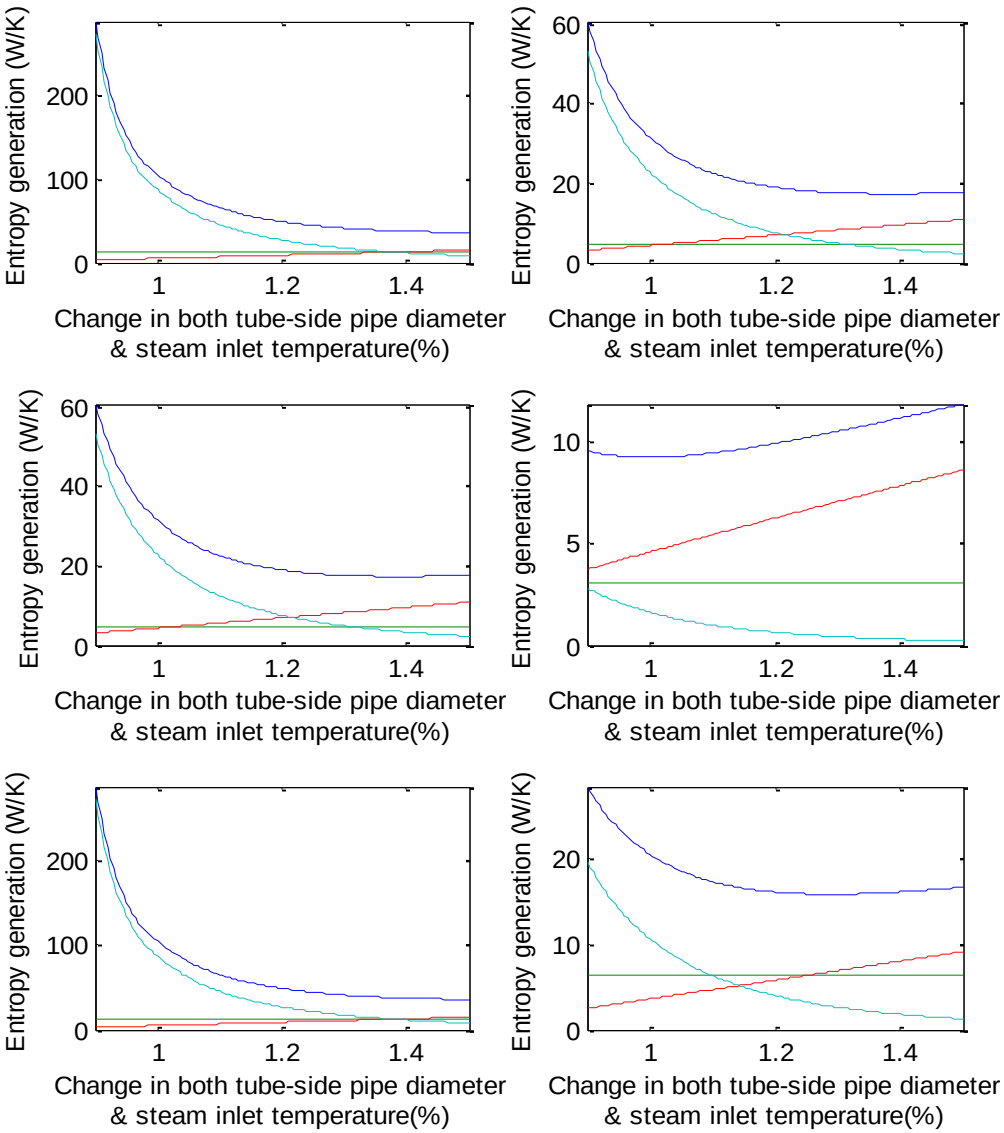

Figure 36: Effect of fluid friction and heat transfer on entropy generation for heat exchanger 1-6 by varying tube-side pipe diameter

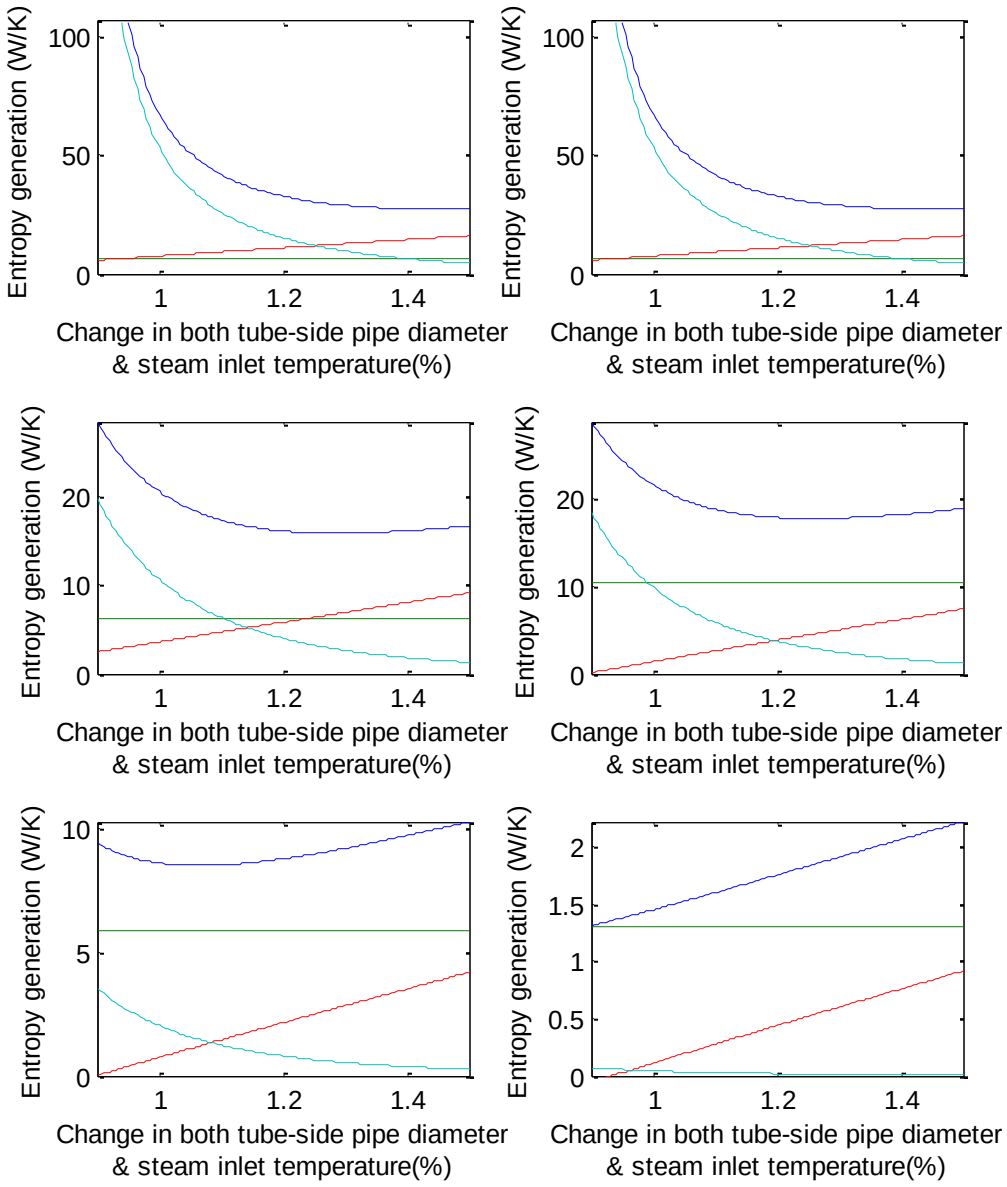

Figure 37: Effect of fluid friction and heat transfer on entropy generation for heat exchanger 7-12 by varying tube-side pipe diameter

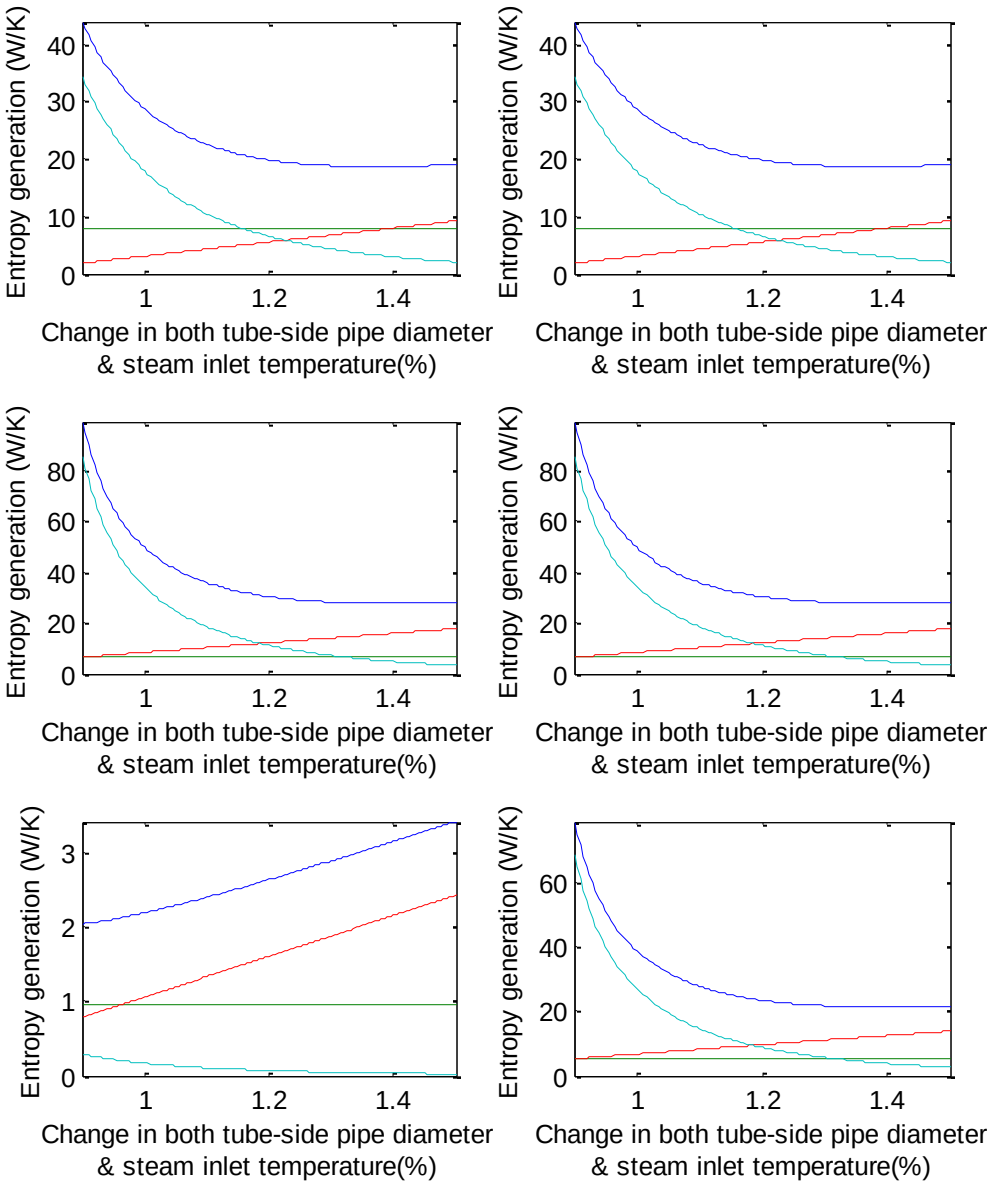

Figure 38: Effect of fluid friction and heat transfer on entropy generation for heat exchanger 13-18 by varying tube-side pipe diameter

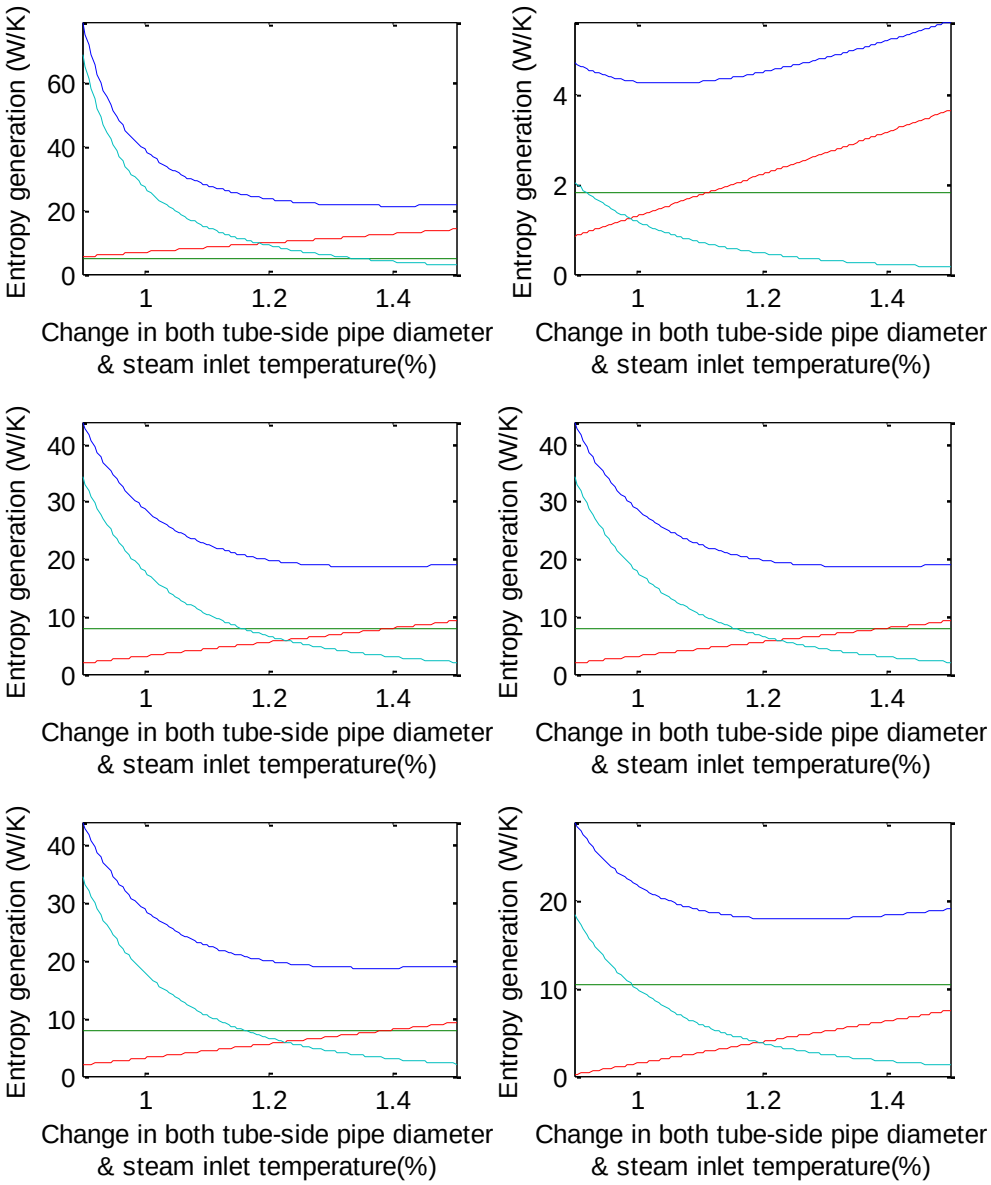

Figure 39: Effect of fluid friction and heat transfer on entropy generation for heat exchanger 19-24 by varying tube-side pipe diameter

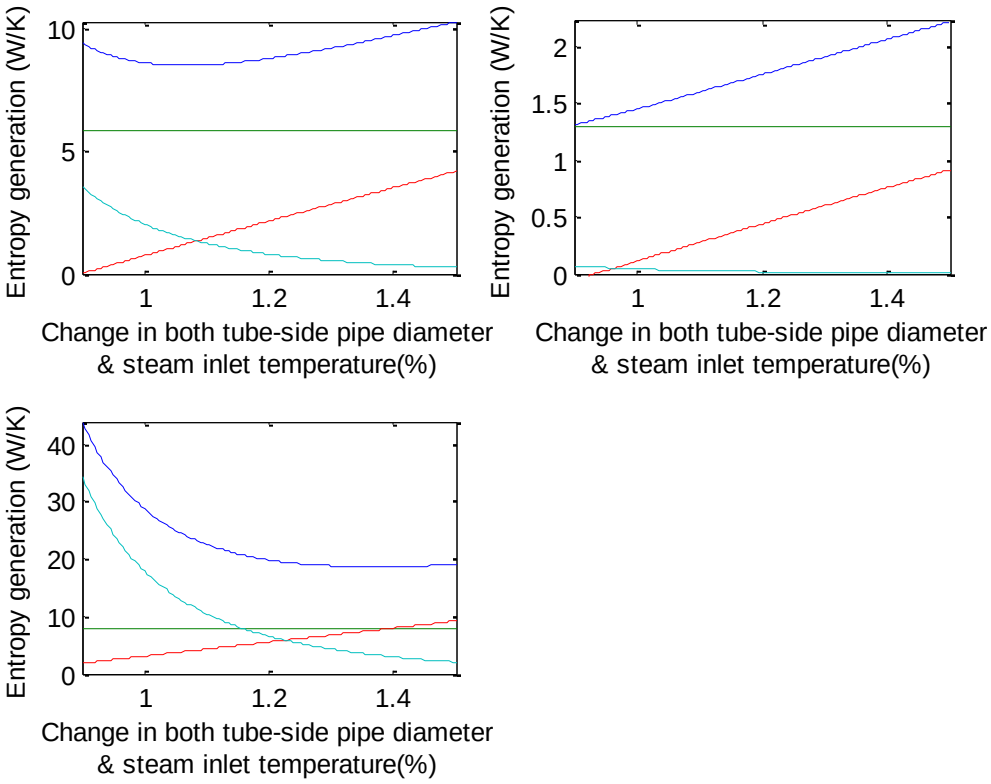

Figure 40: Effect of fluid friction and heat transfer on entropy generation for heat exchanger 25-27 by varying tube-side pipe diameter

Appendix E: Entropy equations

Table 9: Entropy generation equations (1)

Entropy generation equations					
Nr	Applicable Area	Sub-division	Equations	Author	Year
1	Tube/ Pipe/ Duct	Cable In Conduit	$S_{gen} = \frac{\varepsilon}{(1-\varepsilon)^{1.2}} + \frac{0.0069(1-\varepsilon)^{1.2}}{\varepsilon^{3.2}} + \frac{11.54\times10^{-8}}{R_{surface}} + 13.2R_{surface} + \frac{\frac{129\times6676}{0.5}\ln\frac{T_{cs}}{4.2} + 4\times10^{-10}\left[\frac{2500}{\frac{\pi}{4}(0.5\times10^{-3})^2}\right]^2}{\left[n_{Cu} + \frac{3.5}{4.5}(27-n_{Cu})\right]^2 T_{CS}}$	Sangkwon	1999
2		Hollow/unit length	$S_{gen} = \frac{q^2}{\pi k T^2 Nu} + \frac{32m^3 f}{\pi^2\rho^2 T D^5}$	Bejan	1998
3		Entrance - Curved Pipe	$S_{gen} = 2\int_{r=0}^{r=1}\int_{\phi=0}^{\phi=\pi}\int_{\theta=0}^{\theta=\theta_e} S_{P,T,gen} r dr B d\phi \frac{d\theta}{\delta}$	Amani and Nobari	2011

Table 10: Entropy generation equations (2)

Entropy generation equations					
Nr	Area	Sub-division	Equations	Author	Year
4	Tube/ Pipe/ Duct	Plate type	$S_{gen} = 2\int_{r=0}^{r=1}\int_{\Phi=0}^{\Phi=\pi}\int_{\theta=0}^{\theta=\theta_\theta} S_{P,T,gen} r dr B d\Phi \frac{d\theta}{\delta}$	Ko	2006
5		Plate-fin type	$S_{gen} = \sum_{k_z=1}^{M_z}\sum_{k_y=1}^{M_y}\sum_{k_x=1}^{M_x}\left[mc_p \ln\left(\frac{T_{ex}}{T_{in}}\right) - mRln\left(1-\frac{\Delta p}{p_{in}}\right)\right]_{k_x,k_y,k_z}$	Zhang, Yang, and Zhou	2010
6		Symmetrical and uniform heated vertical Pipe	$S_{gen} = \int_{r=0}^{\frac{L}{b}}\int_0^1 \left\{\frac{1}{T^{*2}}\left[\left(\frac{dT^*}{dX}\right)^2 + \left(\frac{dT^*}{dY}\right)^2\right] + \frac{PrEc}{T^{*2}}\left(\frac{dU}{dY}\right)^2\right\} dXdY$	Andreozzi, Auletta, and Manca	2006
7		Flat heat pipe	$S_{gen} = \frac{Q^2 R_{eff}}{[T_L(T_L + QR_{eff})]} + \frac{12\mu_v V l_{eff} Q}{t_v^2 \rho_v T h_{fg}} + \frac{8\mu_l Q^2 l_{eff}}{\rho_l \varepsilon t_v w r_c^2 T h_{fg}^2}$	Maheshkumar and Muraleedharan	2011
8		Ducts with specified cross-sectional area	$\dot{S}_{gen} = \frac{\dot{q}'^2}{\chi C_h k T^2 \mathrm{Pr}^\beta} Re^{-\alpha} + \frac{1}{128}\frac{\chi^3 C_f \mu^5}{\rho^2 T \dot{m}^2} Re^{5-\gamma}$	Jankowski	1999
9		Effect of fouling	$\dot{S}_{gen} = \dot{m} C_p \left(\ln\left(\frac{1-\tau e^{-4t\lambda}}{1-\tau}\right) - \tau\left(1-e^{-4t\lambda}\right) + \frac{1}{8}\frac{f\tau Ec}{St}\ln\left(\frac{e^{4t\lambda}-\tau}{1-\tau}\right)\right)$	Sahin, Zubair, Al-Garni, and Kahraman	2000
10		Ducts with fixed cross-sectional area	$\dot{S}_{gen} = \frac{\dot{q}'^2 A \mu^2}{4C_h \dot{m}^2 k T^2 \mathrm{Pr}^\beta} Re^{2-\alpha} + \frac{1}{2}\frac{C_f \dot{m}^4}{\rho^2 A^3 \mu T} Re^{-(\gamma+1)}$	Jankowski	1999
11	Heat Exchanger	General	$S_{gen} = \int_A \int_\delta J_q \frac{d}{dx}\left(\frac{1}{T}\right) dx dA$	Balkan	2005

Table 11: Entropy generation equations (3)

Entropy generation equations					
Nr	Area	Sub-division	Equations	Author	Year
12		Rotary Drier	$S_{gen} = m_s(f_e S_{s\,out} - f_i(f_e - f_i)S_{s\,in})$	Peinado et al.	2010
14		tube-fin	$S_{gen} = C\left[\frac{0.477(\Delta T^*)^2}{St^{0.4}A_{opt}^{*0.4}G_{opt}^{*0.4}} + \frac{R}{C_p} f A^* G_{opt}^{*3}\right]$	Ogulata, and Doba	1998
15		Tube-in-tube	$\dot{S}_{gen} = \left\{\frac{t_{eff,I}}{2\lambda_m O}\frac{(\dot{m}c_{p,h})^2}{T_h T_m}\left(\frac{dT_h}{dl}\right)^2 + t_{eff,II}\frac{(m\dot{c}_{p,l})^2}{T_m T_l}\left(\frac{dT_I}{dl}\right)^2 + \frac{\dot{m}}{\rho T}\frac{C}{2}\mu\frac{v_m}{D_h^2}\right\} dl$	Lerou, Veenstra, Burger, Ter Brake, and Rogalla	2005
16		Shell-and-tube	$\dot{S}_{gen} = (\dot{m}c_p)_1 \ln\frac{T_1^0}{T_1^i} + (\dot{m}c_p)_2 \ln\frac{T_2^0}{T_2^i} + \frac{\Delta P_1}{\rho_1}\dot{m}_1 \ln\frac{\left(\frac{T_1^0}{T_1^i}\right)}{T_1^0 - T_1^i} + \frac{\Delta P_2}{\rho_2}\dot{m}_2 \ln\frac{\left(\frac{T_2^0}{T_2^i}\right)}{T_2^0 - T_2^i}$	Arivazhagan and Lokeswaran	2011
17			$S_{gen} = \left[\frac{T_{h,lm} - T_{c,lm}}{T_{h,lm}T_{c,lm}}\right] + \left[\frac{\Delta P}{\rho} m \frac{\ln\left(\frac{T_0}{T_i}\right)}{T_0 - T_i}\right] + \left[\sum (mC_p)_j \ln\frac{T_0}{T_{j,i}}\right]$	Guo, Chengand Xu	2009
18		Double pipe fin heat exchanger	$S_{gen} = (mc_p)_a \ln\frac{T_{a,out}}{T_{a,in}} - m_a R_a \ln\frac{p_{a,out}}{p_{a,in}} + (mc_p)_w \ln\frac{T_{w,out}}{T_{w,in}}$	Sahiti, Krasniqi, Fejzullahu, Bunjaku, and Muriqi	2008
19		Double pipe fin heat exchanger	$S_{gen} = (mc_p)_a \ln\left[1 + \varepsilon\left(\frac{T_{w,in}}{T_{a,in}} - 1\right)\right] - m_a R_a \ln\frac{p_0}{p_0 + \Delta p} + (mc_p)_w \ln\left[1 - \frac{(mc_p)_a}{(mc_p)_w}\varepsilon\left(1 - \frac{T_{a,in}}{T_{w,in}}\right)\right]$	Sahiti, Krasniqi, Fejzullahu, Bunjaku, and Muriqi	2008

Table 12: Entropy generation equations (4)

Entropy generation equations					
Nr	Area	Sub-division	Equations	Author	Year
20	Heat Exchangers	Double pipe fin heat exchanger	$S_{gen} = (mc_p)_a \ln\frac{T_{a,out}}{T_{a,in}} - m_a R_a \ln\frac{p_{a,out}}{p_{a,in}} + (mc_p)_w \ln\frac{T_{w,out}}{T_{w,in}}$	Sahiti, Krasniqi, Fejzullahu, Bunjaku, and Muriqi	2008
21			$S_{gen} = (mc_p)_a \ln\left[1+\varepsilon\left(\frac{T_{w,in}}{T_{a,in}}-1\right)\right] - m_a R_a \ln\frac{p_0}{p_0+\Delta p} + (mc_p)_w \ln\left[1-\frac{(mc_p)_a}{(mc_p)_w}\varepsilon\left(1-\frac{T_{a,in}}{T_{w,in}}\right)\right]$	Sahiti, Krasniqi, Fejzullahu, Bunjaku, and Muriqi	2008
22		General	$S_{gen} = \int_A \int_\delta J_q \frac{d}{dx}\left(\frac{1}{T}\right) dxdA$	Balkan	2005
23		Rotary drier	$S_{gen} = m_s(f_e S_{s\,out} - f_i(f_e - f_i)S_{s\,in})$	Peinado, de Vega, Garcia-Hernando, and Marugan-Cruz	2010
24	Refrigeration	Refrigerator - heat leak	$S_{gen} = \frac{A}{L}\left[k^{\frac{1}{2}} \ln\left(\frac{T_H}{T_L}\right)\right]^2$	Bejan	1998
25		Refrigerator - absorber	$S_{gen} = \left[\frac{h_g^{sol}(P_{evap},T_{abs},X_{ws})}{T_{abs}} - s_g^{sol}(P_{evap},T_{abs},X_{ws})\right] m_{vwe} + \left[\frac{h_g(P_{abs},T_{evap}) - h_g(P_{abs},T_{abs})}{T_{abs}} - s_g(P_{abs},T_{evap}) + s_g(p_{abs},T_{abs}\right] m_{wve} - \left[\frac{U_{abs}A_{abs}}{N}(T_{cwin} - T_{abs})\left(\frac{1}{T_{cwin}} - \frac{1}{T_{abs}}\right)\right] + \left[\frac{1}{T_{abs}}\mu(P_{evap},T_{abs},X_{ws})m_{ws}\right] + \left[\frac{m_{cw}\left(h_f(T_{cwin}) - h_f(T_{cwo})\right)}{T_{avg}} - \left(S_f(T_{cwin}) - S_f(T_{cwo})\right)\right]$	Myat, Thu, Kim, Chakraborty, Chun, and Ng	2011

Table 13: Entropy generation equations (5)

Entropy generation equations					
Nr	Area	Sub-division	Equations	Author	Year
26	Refrigeration	Refrigerator - generator	$S_{gen} = -\left[\frac{h_g^{sol}(P_e, T_{gen}, X_{ss})}{T_{abs}} - s_g^{sol}(P_c, T_{gen}, X_{ss})\right] m_{wvc} - \left[\frac{h_g(P_c, T_c) - h_g(P_c, T_{gen})}{T_{gen}} - s_g(P_c, T_{cond}) + s_g(p_c, T_{grn}\right] m_{wvc} + \left[\frac{U_{gen}A_{gen}}{N}(T_{hwin} - T_{gen})\left(\frac{1}{T_{hwin}} - \frac{1}{T_{gen}}\right)\right] + \left[\frac{1}{T_{gen}}\mu(P_c, T_{gen}, X_{ss})m_{ss}\right] + \left[\frac{m_{hw}\left(h_f(T_{hwin}) - h_f(T_{hwo})\right)}{T_{avg}} - \left(S_f(T_{hwin}) - S_f(T_{hwo})\right)\right]$	Myat, Thu, Kim, Chakraborty, Chun, and Ng	2011
27		Refrigerator - condenser	$S_{gen} = \left[\frac{h_g(P_c, T_{gen})}{T_{cond}} - s_g(P_c, T_{gen})\right] m_{wvc} - \left[\frac{U_{cond}A_{cond}}{N}(T_{cwin} - T_{cond})\left(\frac{1}{T_{cwin}} - \frac{1}{T_{cond}}\right)\right] + \left[\frac{m_{hw}\left(h_f(T_{cwin}) - h_f(T_{cwo})\right)}{T_{avg}} - \left(S_f(T_{cwin}) - S_f(T_{cwo})\right)\right]$	Myat, Thu, Kim, Chakraborty, Chun, and Ng	2011
28		Refrigerator - evapourator	$S_{gen} = -\left[\frac{h_f(T_{cond}) - h_f(T_{evap})}{T_{evap}} - s_f(T_{cond}) + s_f(T_{evap}\right] m_{wvc} - \left[\frac{U_{evap}A_{evap}}{N}(T_{chiwin} - T_{evap})\left(\frac{1}{T_{chiwin}} - \frac{1}{T_{evap}}\right)\right] + \left[\frac{h_g(T_{evap}, T_{evap}) - h_f(T_{evap})}{T_{evap}} - s_f(T_{evap}) + s_g(P_{evap}, T_{abs})\right] m_{wve} + \left[\frac{m_{chiw}\left(h_f(T_{chiwin}) - h_f(T_{chiwo})\right)}{T_{avg}} - \left(S_f(T_{chiwin}) - S_f(T_{chiwo})\right)\right]$	Myat, Thu, Kim, Chakraborty, Chun, and Ng	2011
29		Gas-hydrate cool storage system	$S_{gen} = S_{gen\ temperature\ configuration} + S_{gen\ phase\ change\ raet\ configuration}$	Bi, Guo, Zhang, Chen, and Sun	2010

Table 14: Entropy generation equations (6)

Entropy generation equations					
Nr	Area	Sub-division	Equations	Author	Year
30	Flow	External body with heat transfer and drag	$S_{gen} = \frac{Q_B(T_B - T_\infty)}{T_B T_\infty} + \frac{F_D U_\infty}{T_\infty}$	Bejan	1998
31	Electronics	Universal heat sink	$S_{gen} = \frac{(T_c - T_a)}{\psi_c T_a} + \frac{(T_s - T_h)}{\psi_h T_s}$	Yazawa and Shakouri	2011
32		Rotating disk	$S_{gen} = V\left\{\frac{k}{T_0^2}\left(\frac{dT}{dz}\right)^2 + \frac{\mu}{T_0}\left\{2\left[\left(\frac{du}{dr}\right)^2 + \frac{1}{r^2}u^2 + \left(\frac{dw}{dz}\right)^2\right] + \left(\frac{dv}{dz}\right)^2 + \left[r\frac{d}{dr}\left(\frac{v}{r}\right)^2\right]\right\} + \frac{\sigma B_0^2}{T_0}(u^2 + v^2)\right\}$	Arikoglu, Ozkol, andKomurgoz	2008
33		Heat sink	$\dot{S}_{gen} = \frac{\phi^2 R_{sink}}{T_\infty^2} + \frac{A_{tube}}{T_\infty}\frac{\frac{1}{2}\rho U_{in}^3 L}{D_h} f$	Jian-hui, Chun-xin, and Li-na	2009
34		Microchannel	$S_{gen} = \frac{a^2}{k}\left\{\begin{array}{c}\frac{1}{\theta_f^2}\left[\left(\frac{d\theta_f}{dx}\right)^2 + \left(\frac{d\theta_f}{dy}\right)^2\right] + \frac{\gamma_1}{d\theta_{w1}^2}\left(\frac{d\theta_{w1}}{dy}\right)^2 + \frac{\gamma_2}{d\theta_{w2}^2}\left(\frac{d\theta_{w2}}{dy}\right)^2 \\ + \frac{1}{\theta_f}\left(\frac{du}{dy}\right)^2 \\ + \frac{M^2}{\theta_f}(u-k)^2 + \frac{1}{\theta_{w1}}\left(\frac{M^2K^2c_1}{\delta_1}\right) + \frac{1}{\theta_{w2}}\left(\frac{M^2K^2c_2}{\delta_2}\right)\end{array}\right\}$	Zhao,and Liu as well as Yang, Furukawa, and Torii	2010 as well as 2008
35			$S_{gen} = V\left\{\frac{k}{T^2}(\nabla T)^2 + \frac{\mu}{T}\left\{2\left[\left(\frac{du}{dx}\right)^2 + \left(\frac{dv}{dy}\right)^2\right] + \left(\frac{dv}{dy} + \frac{du}{dx}\right)^2\right\} + \frac{Q_j}{T}\right\}$	Hung	2008
36			$S_{gen} = \frac{k}{T^2}\left[\left(\frac{dT}{dx}\right)^2 + \left(\frac{dT}{dr}\right)^2\right] + \frac{\eta}{T}\left\|\frac{du}{dr}\right\|^{n+1}$	Singh, Anoop, Sundararajan, and Das	2010
37			$S'_{gen} = \mu^{0.25}\left(C_{1t}\frac{\mu^{0.15}}{T^2 k^{0.6} C_p^{0.4}} + \frac{C_{2t}}{T\rho^2}\right)$	Ibáñez, and Cuevas	2010
38	Forced Convec-tion	Mixed	$S_{gen} = 2qH\left[\frac{1}{T_{ave}} - \frac{t}{T_\infty}\right] + 2\frac{\mu_\infty}{T_\infty}\int_0^H \mu \left.\frac{d\mu}{dx}\right\|_{x=\frac{d}{2}} dy$	Balaji, Hölling, and Herwig	2007

Table 15: Entropy generation equations (7)

Entropy generation equations					
Nr	Area	Sub-division	Equations	Author	Year
39	Natural Convection	Porous media	$S_{gen} = \int_{A_i}^{A_o}\left\{\left[\frac{d}{dX}\left(\sum_{k=1}^{N}\theta_k\Phi_k\right)\right]^2+\left[\frac{d}{dY}\left(\sum_{k=1}^{N}\theta_k\Phi_k\right)\right]^2\right\}dA + \Phi\int_{A_i}^{A_o}\left\{\begin{array}{c}\left[\left(\sum_{k=1}^{N}U_k\Phi_k\right)\right]^2+\left[\left(\sum_{k=1}^{N}V_k\Phi_k\right)\right] \\ +Da\left(2\left[\frac{d}{dX}\left(\sum_{k=1}^{N}U_k\Phi_k\right)\right]^2+2\left[\frac{d}{dY}\left(\sum_{k=1}^{N}V_k\Phi_k\right)\right]^2\right) \\ +\frac{d}{dY}\left(\sum_{k=1}^{N}U_k\Phi_k\right)+\frac{d}{dX}\left(\sum_{k=1}^{N}V_k\Phi_k\right)^2\end{array}\right\}dA$	Kaluri and Basak	2011
40		Global asymmetric cooling	$S_{gen} = \frac{a^2}{k_f}\left\{\frac{Bi_1(2+Bi_2)}{2+Bi_2 24\theta_{af}(Bi_1+Bi_2+Bi_1Bi_2)}+\frac{Bi_2(2+Bi_1)}{2+Bi_1 24\theta_{af}(Bi_1+Bi_2+Bi_1Bi_2)}\right\}$	Ibanez, Cuevas, and Lopez de Haro	2003
38	Motors	Jet engine	$\dot{S}_{gen} = \int_V\left[\frac{k_{eff}}{T^2}(\nabla T)^2+\frac{\mu_{eff}}{T}\left\{2\left[\left(\frac{du_x}{dx}\right)^2+\left(\frac{du_y}{dy}\right)^2+\left(\frac{du_x}{dx}+\frac{du_y}{dx}\right)\right]\right\}+ \int_0^{\infty}\int_{4\pi}\left[-\left(\kappa_{a,\lambda}+\kappa_{s,\lambda}\right)\frac{I_\lambda(r,s)}{T_\lambda(r,s)}+\kappa_{a,\lambda}\frac{I_{b,\lambda}(r)}{T_\lambda(r,s)}+\frac{\kappa_{s,\lambda}}{4\pi}\int_{4\pi}\frac{I_\lambda(r,s')}{T_\lambda(r,s)}\Phi(s',s)d\Omega'+ \frac{\kappa_{a,\lambda}}{T(r)}\left[I_\lambda(r,s)-I_{b,\lambda}(r)\right]\right]d\Omega d\lambda\Big]dV$	Chu,and Liu	2009
39		Jet engine with oscillation	$\bar{S}_{gen} = \frac{I_3+\alpha^2 I_2+(2\pi S)^2}{I_2^{3/2}}\left[1-\left(\frac{I_1}{4\alpha\bar{x}}\right)^{1/2}\right]$	Cervantes and Solorio	2002
40		Solid-gas reactor	$\dot{S}_{gen} = \frac{(\dot{q}_{tot}V_{tot})^2\varepsilon_i^{-\frac{1}{2}}(1-\varepsilon_i)^{\frac{5}{2}}}{3W\lambda_p T_0^2}\times\left[(1+\eta)^{\frac{1}{2}}\left(\tilde{\lambda}_i+\tilde{k}_i\eta\right)^{\frac{1}{2}}\right]$	Azoumah, Neveu, and Mazet	2006
41	Radiation	Natural	$S_{gen} = \left\{-k_{e,\eta}\frac{G_\eta}{T_{EX,\eta}}+k_{a,\eta}\frac{4\pi I_{b,\eta}}{T_{EM,\eta}}+k_{s,\eta}\frac{G_\eta}{T_{SC,\eta}}-k_{a,\eta}\frac{(4\pi I_{b,\eta}-G_\eta)}{T_M}\right\}dVd\eta$	Caldas, and Semiao	2005
42		Forced	$\bar{S}_{gen} = -\bar{k}_{a,\eta}\left\{\bar{I}_{b,\eta}\int_{4\pi}\overline{\left(\frac{1}{T_\eta(\vec{s})}\right)}d\Omega-\int_{4\pi}\overline{\left(\frac{\bar{I}_\eta(\vec{s})}{T_\eta(\vec{s})}\right)}d\Omega+\overline{G_\eta}\,\overline{\left(\frac{1}{T}\right)}-4\pi\overline{\left(\frac{\bar{I}_{b,\eta}}{T}\right)}\right\}dVd\eta$	Caldas, and Semiao	2007

Table 16: Entropy generation equations (8)

Entropy generation equations					
Nr	Area	Sub-division	Equations	Author	Year
43	Radiation	Through semitransparent Medium	$S_{gen} = dVd\lambda \int_{4\pi}\left[-\left(\kappa_{a,\lambda}+\kappa_{s,\lambda}\right)\frac{I_\lambda(r,s)}{T_\lambda(r,s)}+\kappa_{a,\lambda}\frac{I_{b,\lambda}(T_M(r))}{T_\lambda(r,s)}+\frac{\kappa_{s,\lambda}}{4\pi}\int_{4\pi}\frac{I_\lambda(r,s')}{T_\lambda(r,s)}\phi(s',s)d\Omega'\right]d\Omega+\frac{\kappa_{a,\lambda}dVd\lambda}{T_M(r)}\int_{4\pi}\left[I_\lambda(r,s)-I_{b,\boldsymbol{\lambda}}(T_M(r))\right]d\Omega$	Liu, and Chu	2007
44		With forced conduction between parallel plates	$S_{gen}=\frac{\lambda(T)}{T^2}\left[\left(\frac{dT}{dx}\right)^2+\left(\frac{dT}{dy}\right)^2\right]\frac{\mu}{T}\left(\frac{du}{dy}\right)^2-\sum_{bands}\int_{4\pi}\sum_{i=1}^{4}\left[w^i k_v^i\left(I_v^b(T)-I_v^i(\vec{\Omega})\right)\times\left(\frac{1}{T}-\frac{1}{T_v^i(\vec{\Omega})}\right)\right]d\Omega\Delta V$	Ben Nejma, Mazgar, Abdallah, and Charrada	2008
45	Chemical	Gas absorption	$S_{gen}=\frac{4\gamma v_{z,max}^2}{T\delta_L}+c_{AO}Rv_{z,max}\left(x\left[\frac{x\left[1-\left(\frac{x}{\delta_L}\right)^2\right]}{z\sqrt{\left(\frac{D_{AB}}{v_{z,\max}}\right)\pi z}}\right]\exp\left(-\frac{v_{z,max}x^2}{4D_{AB}z}\right)\right)+\frac{RD_{AB}}{c_{AO}}\frac{\left(\left(\frac{c_{AO}}{\sqrt{\left(\frac{D_{AB}}{v_{z,max}}\right)\pi z}}\right)\exp\left(-\frac{v_{z,max}x^2}{4D_{AB}z}\right)\right)^2}{\left[1-\operatorname{erf}\left(\frac{x}{\sqrt{\left(\frac{4D_{AB}}{v_{z,max}}\right)z}}\right)\right]}$	Chermiti, Hidouri, and Brahim	2011
46		Propylene glycol production	$S_{gen}=-FM_{po}\left(\sum\theta_i C_{p_i}\right)\left[\left(\frac{T-T^e}{T}\right)+\ln\left(\frac{T^e}{T}\right)\right]+FM_{po}\left(\frac{\tau k_0\exp(-E/RT)}{1+\tau k_0\exp(-E/RT)}\right)\left(\left(-\frac{\Delta G_{R,r}}{T_r}\right)+\Delta H_R\frac{(T-T_r)}{TT_r}\right)$	Manzi, Vianna, and Bispo	2009